12-2014

Steps Toward a Net-Zero Campus with Renewable Energy Resources

Andrew Clarke
Clemson University, adclark@g.clemson.edu

Follow this and additional works at: https://tigerprints.clemson.edu/all_dissertations

Part of the Electrical and Computer Engineering Commons

Recommended Citation

STEPS TOWARD A NET-ZERO CAMPUS WITH RENEWABLE ENERGY
RESOURCES

A Dissertation
Presented to
the Graduate School of
Clemson University

In Partial Fulfillment
of the Requirements for the Degree
Doctor of Philosophy
Electrical Engineering

by
Andrew Donald Clarke
December 2014

Accepted by:
Dr. Elham Makram, Committee Chair
Dr. Keith Corzine
Dr. Richard Groff
Dr. Pierluigi Pisu

ABSTRACT

With the increasing attention and support behind plug in hybrid electric vehicles, research must be conducted to examine the impacts of vehicles on electric distribution and transmission systems. This research aims first to model the behavior of vehicle battery chargers during system disturbances and mitigate any impacts. A distribution test system example is modeled and several different vehicle charger topologies are added. Faults are applied to the distribution system with vehicle chargers connected and the results are examined. Based on these results, a control strategy to mitigate their negative impacts is suggested. Photovoltaic panels are then added to the system and the study is repeated.

Several services that plug in hybrid electric vehicles are capable of providing to the electric system are presented in order to allow electric vehicles to be seen as an asset to electric systems rather than a burden. These services are particularly focused on an electric system such as might be found on a college campus, which in this case is represented by the Clemson University electric distribution system. The first service presented is dynamic phase balancing of a distribution system using vehicle charging. Distribution systems typically face problems with unbalance. At most large car parks, a three phase electric supply is expected even though current standardized chargers are single phase. By monitoring system unbalance and choosing which phase a vehicle is allowed to charge from, unbalance between phases is reduced in a distribution system. The second service presented is a decentralized vehicle to campus control algorithm based on time of use rates. Using time of use electricity prices, discharging vehicle

batteries during high prices and recharging at low prices is explored. Battery degradation as well as limits placed by required vehicle range availability are included in the decision on whether to charge or discharge. Electric utilities will also benefit from a reduction of load at peak times if vehicles discharge back to the campus. A comparison with stationary battery energy storage is included.

DEDICATION

To my wife and my parents. Thank you for your unwavering love and support through

this journey.

ACKNOWLEDGMENTS

TABLE OF CONTENTS

Page

Table of Contents (Continued)

LIST OF TABLES

LIST OF FIGURES

List of Figures (Continued)

List of Figures (Continued)

List of Figures (Continued)

List of Figures (Continued)

NOMENCLATURE

AER	All Electric Range
$Cost_B$	Battery Cost
$Cost_{BL}$	Baseline Cost for Off Peak PHEV Charging
$Cost_C$	Cost to Charge Stationary Battery
$Cost_E$	Cost of Energy Exchange during V2C
Cyc_R	Rated Cycle Life of Battery
E_B	Rated Capacity of Battery
E_C	Energy Supplied to PHEV for Charging
E_D	Energy Discharged through V2C
E_H	Energy Used to Drive PHEV from Work to Home
E_W	Energy Used to Drive PHEV from Home to Work
HEV	Hybrid Electric Vehicle
ICE	Internal Combustion Engine
I_{Peak}	Peak Current Phasor
P	Real Power
$P_{Estimate_{Phase}}$	Estimated Phase Power without PHEV Charging Power
$P_{EstimateNew_{Phase}}$	Estimated Phase Power including Charging Power of PHEVs with Assigned Phase
$PHEV$	Plug In Hybrid Electric Vehicle
$P_{PHEV}(x)$	Individual PHEV Charging Power
$P_{Measured_{Phase}}$	Measured Phase Power including PHEV Charging Power
Q	Reactive Power
$Rate_{Off}$	Off Peak Electricity Price
$Rate_{On}$	On Peak Electricity Price
Sav_{SB}	Savings from Stationary Battery
Sav_{V2C}	Savings from V2C
SOC	State of Charge
TOU	Time-of-use
$V2C$	Vehicle to Campus
$V2G$	Vehicle to Grid
V_{Peak}	Peak Voltage Phasor

CHAPTER ONE

INTRODUCTION

PHEV Benefits

With the threats of increasing gas prices and more strict regulations on greenhouse gas emissions, hybrid electric vehicles (HEVs) are becoming a realistic alternative to traditional vehicles propelled solely by internal combustion engines (ICEs). According to [1], over 1 million HEVs were sold worldwide by the end of 2007.

According to [1], the IEEE places the following three criteria on a HEV in order for it to be classified as a plug in hybrid electric vehicle (PHEV): The vehicle battery must have a capacity of at least 4kWh and be capable of propelling the vehicle; The vehicle must be capable of having its batteries recharged by connecting to the electric utility grid; The vehicle must have an all-electric range (AER) of at least 10 miles.

While HEVs offer increased fuel efficiency compared to traditional ICE vehicles, a PHEV offers an additional increase in fuel efficiency and decrease in greenhouse gas emissions over a traditional HEV. Table 1 shows an average emission of CO_2 gas based on vehicle type [1]. According to [2], batteries "…offering an effective electric range of 20 miles (32.2km) will yield over 45% reduction in petroleum consumption."

Table 1

Average CO_2 Emission per Mile

Vehicle Type	CO_2 Emissions/Mile Driven
Conventional	1.192 pounds CO_2/mile
Hybrid	0.577 pounds CO_2/mile
Plug-In Hybrid	0.385 pounds CO_2/mile

ICEs are typically between 15% and 30% efficient. Electric drives are a significantly better option than internal combustion engines in speed varying situations. According to [2], 25% of greenhouse gases emitted by the transportation sector could be eliminated by a 30% penetration of PHEVs. The location of PHEV penetration will determine the impact that it has on the existing electric utility grid [3]. According to [4], "PEVs will likely exhibit a large degree of temporal and spatial diversity." Table 2 shows an estimate of PHEV penetration from [3].

Unfortunately for PHEV technology, it is still more expensive than traditional vehicle technology. The savings on gas consumption currently do not always outweigh the increased cost of batteries in PHEVs [1]. According to [5], a PHEV can be more expensive if the average distance driven per day is less than 22 miles. However, there are certain tax incentives available to help ease the burden of the increased cost. Batteries used in PHEVs are usually NiMH or Li-Ion technologies [2].

Table 2
Estimated PHEV Penetration

Market Penetration	PEV per Customer			
	0	1	2	3
2%	96.85%	3.12%	0.03%	0.00%
4%	93.77%	6.09%	0.14%	0.00%
8%	87.82%	11.63%	0.54%	0.01%

PHEV Charging

With the increasing PHEV penetration comes an increased need for PHEV charging locations and charging power. One possibility for PHEV charging would be using a solar powered charging station in parallel with the existing electric grid [1].

Charging PHEVs will create the possibility of overloading the existing electric utility grid infrastructure. If charging is uncontrolled, this possibility sharply increases. Nighttime charging can be beneficial to the grid but if the vehicle charging is shifted by a few hours, serious concerns may arise [5]. Smart chargers can help to prevent a large number of vehicles charging at inopportune times. The reason that nighttime charging can be beneficial to the grid is that base load generation increases and allows for a flatter load profile. Only a small amount of power must be generated by non-base load generators [2]. In a study conducted by [2], at 50% PHEV penetration, 80% of the electricity required for charging came from the bottom 2/3 of the load profile with no new generation required. The study goes on to say that the current electric utility grid infrastructure could supply power to meet 70% of the charging needs of passenger vehicles in the US if each vehicle travels an average of 33 miles per day. This level of penetration could decrease gas consumption by 85 billion gallons per year and decrease greenhouse gas emissions by 27% [2].

Another way to further manage PHEV charging is to require the vehicle operator to enter information about the intended driving distance and the minimum allowable charge that must be retained in the batteries [6]. According to [7], the majority of vehicles will be charged either while at home or at work. The batteries will need to be fully charged overnight to be ready for a daytime commute. This will require that most vehicles will charge at home from 21:00 to 06:00. In a study summarized in [7], using uncoordinated charging, batteries were charged at a constant 4kWh. This type of charging placed a large strain on the electric utility grid infrastructure by increasing

power losses and introducing large voltage variations. With coordinated charging however, requiring the vehicle operator to input what time their vehicle must be fully charged, calculation of the optimal charging profile is possible. The coordinated charging showed less voltage variations and decreased power losses over the study using uncoordinated charging. In order to coordinate the charging though, the load profile must be known or calculated using stochastic programming. If the load profile is calculated, losses will increase over the known load profile case [7]. Some other ways utilities will have the ability to coordinate charging will be to control pricing for charging energy or to directly control what vehicles can charge at a certain time [3].

As noted previously, the primary concern for the electric utility infrastructure is overloading. According to [8], "As a rough rule of thumb, unless charging cycles are controlled, every two PEVs charging simultaneously at home could increase peak demand as much as adding one new home to the neighborhood." Most PHEVs will be charged at work, home, shopping centers, or specific charging stations should they be available [8]. For charging to be available at any of these locations, circuitry will need to be available for customers to connect their vehicles. It is estimated by [4] that 22% of PHEV drivers would return home from work and desire to begin charging of their vehicles between the hours of 5pm and 6pm. Also according to [4], "One important characteristic of PEVs relative to other loads is that the charging can be deferred." Requiring vehicles to defer charging until after a certain time will help to decrease overloading during peak times but may present a problem for the electric utilities if all vehicles are permitted to begin charging at the same time due to the expected load spike.

Adding the load of PHEV charging will also change prices of power at certain times. According to [9], nighttime charging will be cheaper for customers of a utility that regulates charging of PHEVs, further increasing the appeal for using deferred charging. A study conducted by [4] examined the effect that PHEVs had on an electric utility grid distribution system. The study found that a large percentage of distribution transformers were likely to become overloaded with the connection of PHEVs. "In general, assets closest to the customer will be the most sensitive to overloading from early PEV adoption as they do not benefit as much from spatial diversity" [4]. A study by [10] assuming a 9% penetration level concluded that using a slow charging profile relieves many of these overloading cases however. The fast charging profile is what causes the overloading. It is also suggested that staggering charging loads could further reduce the potential for overloads. Generation capacity is not considered to be a significant limitation as long as PHEV charging is performed at off peak times and penetration levels are not considered to be high. According to [10], "...Existing electric power generation plants would be used at full capacity for most hours of the day to support up to 84% of the nation's cars, pickup trucks and SUVs for a daily drive of 33 miles on average."

Customers will also have to account for charging in the driving cycle. In general, customers would prefer a fast charging cycle rather than a slow charging cycle [3]. Also, according to [11], batteries that can handle a fast charging cycle are not necessarily the best option for use in powering PHEVs. Customers will also have to account for the fact that a vehicle cannot be driven while charging [11]. "Higher charging currents result in a shorter charging time and greater vehicle usage availability, but a higher charging current

will also result in heat dissipation in the battery during charging, due to battery cell internal resistance" [11]. This heating in the batteries has the potential to cause damage and shorten battery life [11]. "Federal Highway Administration statistics shows … about 81% use their private vehicle to drive alone to work" [3]. Charging has the potential to cause problems during the first few years of PHEV adoption because the majority of charging stations available for PHEV charging are likely to be at vehicles' home locations. This means that because customers will not have vehicle charging readily accessible at work, the battery charge must last for a commute both to and from work [3].

Charging is available at three primary levels. Level 1 charges the vehicle on a 120V and 15A or 20A circuit. This level of charging allows for a power transfer of 1.44kW to a vehicle. The problem with this level of charging is that it is extremely slow to fully charge a battery. Level 2 charges the PHEV on a 240V and 40A circuit. This level of charging allows for a power transfer of 9.6kW to a vehicle. While this level of charging is faster than level 1, it is also more expensive due to the requirement of a new charging circuit that has to be installed. The final level of charging, which is level 3, charges vehicles on a 480V three phase circuit. This allows for a transfer of 60kW to 120kW. This level of charging is the fastest, but also the most expensive. A new charging circuit is required for this level. Also, the charger for this level cannot be built into the vehicle like it can in other levels due to the size [11]. Level 1 charging is expected to require a charging time of between 8 and 14 hours, depending on the starting charge level. Level 2 charging decreases this charging time to between 4 and 6 hours [8].

In addition to providing details on the three levels of charging, [11] also offers the suggestion that rather than charging batteries in the vehicle, the batteries could also be replaced with fully recharged batteries whenever the charge is depleted. The final method of charging explored by [11] is the use of inductive power transfer loops placed in the roadways. Inductive power transfer works without making a physical connection between the power source and the vehicle. To accomplish this, high frequency signals are used in order to reduce power losses during transfer. This allows for vehicles to charge while stopped at traffic lights or while sitting in traffic [11].

<p style="text-align:center;">Vehicle to Grid</p>

Vehicle to grid (V2G) technology works by taking power from vehicles during peak loading times and delivering it to the electric grid [1]. V2G, "… involves connecting PHEVs to the grid while idle, and tapping into their on-board battery packs as sources of stored energy to provide a number of grid services" [2]. The use of this technology is expected to increase the stability, reliability, cost-effectiveness, and efficiency of the grid. According to [5], electric system outages cost consumers more than $79 billion per year. V2G technology has the potential to help lessen the strain on available generation during peak times as well as lessen the need to construct additional generation units. The current, non-flat daily load profile requires certain types of generation units, which are generally smaller, more expensive, and less efficient, to be run intermittently in addition to the constant base load generation units. Using PHEVs in V2G, the load profile can be flattened out significantly. This is accomplished by filling the trough with charging loads and providing power back to the electric grid during peak

loading times. This would ultimately lead to higher system efficiency and lower costs. Using this technology, PHEVs act as mobile electricity storage units, storing energy produced during off peak loading and providing energy during peak loading. Due to this, V2G technology also presents the opportunity to store power from distributed, renewable resources for use later by an electric utility [5]. Renewable resources, including wind, solar, and bio-fuel could also benefit from the previously mentioned technology [6]. A study performed in [5] showed even with a PHEV penetration level of 50%, new generation would not be required for the Midwest. Another study explained in [5] showed that with as little as 10% PHEV penetration, up to 25% of the installed generation capacity could be replaced in the most areas of the United States.

Operating using V2G technology, PHEVs have the potential to supply the existing electric utility grid with real power in addition to positive or negative reactive power. Using this capability will allow PHEVs to operate as a voltage controller and stabilizer for the grid. This will help to increase the overall robustness of the grid [12]. According to [9], because of this, "It was most profitable to run the PHEVs for ancillary services, such as regulation and spinning reserves, which are controlled by Independent Service Operators."

A major concern with this technology is that in order to utilize it in a meaningful way, a significant number of PHEVs must be connected to the electric grid at any given time. PHEVs are expected to remain connected to the grid at almost all times other than when they are being driven according to [5]. A study shows that a PHEV connection availability of 92% during rush hour, the time when the largest number of vehicles are

disconnected from the grid for driving, is expected. The average vehicle is parked, which for PHEVs would also mean connected to the electric grid, 90% of its life [2]. Another major concern with using PHEVs with the V2G technology is the potential for faults on the electric utility grid. If a sustained fault occurs and is not cleared in a short enough time period, the batteries in PHEVs may be damaged by the high current drawn by a fault. The high current drawn causes cells to overheat and leads to the potential for rupturing of the batteries [12].

Vehicle owners and electric utilities both have the ability to make money using V2G. According to [5], a vehicle owner could make anywhere between $184 and $3285 per year by allowing electric utilities to utilize V2G technology using the PHEV. These profits could be partially offset by the probable decrease in the battery life of the PHEV due to repeated charging and discharging cycles [2]. In order for this to become viable, metering of electricity flow and communication between the electric grid and PHEVs is typically required. Instead of using PHEVs to decrease the required generation providing power to meet loading demands at a given time, [2] suggests that this technology may also be utilized to provide the electric grid with spinning reserves and regulation. The circuitry used for level 1 charging, which is 120V at 15A, allows for up to 2kW of reverse power flow from a PHEV to the electric grid. The circuitry used for level 2 charging increases this limit to 10kW [2].

A study described in [6] examined the viability of this technology using a test system. The four items included in this study were a PHEV, renewable generation resources, an electric grid, and residential loads. The common bus for this system was

DC. For storage in the PHEV, super-capacitors and batteries were used in combination.
The only loads considered in the study were the battery charging and the residential
loads. When more power is generated than is needed to sustain the residential loads, the
PHEV is charged. When there is not enough generation to power the load however, the
storage in the PHEV is drained. For PHEV charging, the user entered charging
preferences into an online database that could be updated at any time. Another source of
storage in this study was a stationary battery bank that was part of the residential loads.
According to [6], the addition of the storage capacity to the electric utility grid "Provided
better local load leveling."

<div align="center">Energy Storage</div>

Several types of energy storage technology are used throughout the world. These
include pumped hydro, compressed air, super capacitors, flywheels, various types of
batteries, flow batteries, super conducting magnetic energy storage, and hydrogen. Of
these types of storage, some are suitable for usage in PHEVs while some remain useful
for a grid but are not usable in PHEVs. Pumped hydro energy storage consists of two
reservoirs connected through a pump, which doubles as a generator. During periods of
excess generation, the unit acts as a pump and transfers water from the lower elevation
reservoir to the higher elevation reservoir. Whenever energy is needed, the unit acts as a
generator and water is released from the higher elevation reservoir through the generator.
Currently, pumped hydro energy storage has a worldwide capacity to generate 127GW of
power. Another type of storage which operates in a similar manner to pumped hydro is
compressed air energy storage. This type of energy storage works by using excess

energy to compress air. This compressed air is then released through a turbine to generate electricity when necessary. This type of storage is not widely used however, with a worldwide capacity of approximately 400MW [13]. A third type of energy storage available is super conducting magnetic energy storage, or SMES. SMES works by storing electric energy in a magnetic field. This type of storage requires that the super conducting wire be kept at an extremely low temperature in order to keep losses at an acceptable level. Energy is retrieved from the storage system when, "Switches tap the circulating current and release it to serve a load" [14]. The final type of energy storage that does not show promise as an option for PHEV energy storage that will be discussed here is flywheel energy storage. Using this type of storage, kinetic energy is stored in a rotating flywheel, usually made of composites or steel. Steel rotors operate at low speeds but have a high mass. Composite rotors operate at much higher speeds but are far lighter than steel rotors. In both cases, the rotor is kept in a vacuum and spins on bearings in order to minimize friction and losses. A large advantage to using flywheels for energy storage is that they are environmentally friendly and can be very closely placed. Flywheels can produce between 40kW and 1.6MW of power for 5 seconds to 2 minutes depending on the unit. This makes them useful for short term storage, but not as a long duration supply [14].

One energy storage technology that has the potential to be useful for powering PHEVs if a smaller structure is developed is the flow battery. A flow battery stores energy in an electrolyte solution that is then pumped through the battery when energy is needed. This provides an advantage over traditional batteries in that flow batteries have a

longer lifespan than traditional batteries due to the cycling of the electrolyte. The problem with flow batteries however, is the physical size. In order to have storage for enough electrolyte, a large tank must accompany the cell [15]. Another method of energy storage is hydrogen storage. Hydrogen has a higher enthalpy than gasoline, so it is a very good fuel source for a vehicle. There are five different methods of storage for hydrogen discussed in [16]. In order for hydrogen storage to be used however, the leak rate of the storage unit must be kept low or else long term storage will not be possible. When using the compressed gas storage method, an efficiency of 52.3% was found by [16]. If the efficiency could be improved, this technology could be successfully used in vehicles. A third technology that is usable in PHEVs is traditional batteries. There are four primary types of batteries in use. These are lead-acid, nickel-cadmium, nickel-metal hydride, and lithium-ion. Lead-acid batteries allow for a high rate of discharge, but are not environmentally friendly and have a low energy density. Nickel-cadmium batteries offer the advantage over lead acid batteries of a longer lifespan and higher energy density, but cost much more. Nickel-metal hydride batteries are very similar to nickel-cadmium batteries except they are environmentally friendly and have a higher capacity. The highest energy density of the traditional batteries is in lithium-ion batteries, but accompanying this high energy density is a higher cost and the requirement for complicated charging circuitry [17].

The type of energy storage that appears to be the most promising in combination with traditional batteries for PHEVs is the super capacitor. A super capacitor has a much larger capacity than a traditional capacitor and a power density that is at least 10 times

higher than traditional batteries. Using super capacitors also allows for very rapid charging and discharging. Super capacitors can be charged on the order of seconds while traditional batteries require a charge time on the order of hours. The life expectancy of super capacitors is also much higher than that of traditional batteries. The major limiting factors with super capacitors are energy density and cost. Compared to traditional batteries, super capacitors have a higher power density as previously mentioned, but a lower energy density. This leads to a discharge time on the order of seconds while traditional batteries are between the orders of minutes and hours. Super capacitors are also far more expensive than traditional batteries. This will yield a higher cost initially, but should be somewhat offset by the longer life expectancy [18].

<u>Unbalance Conditions [19]</u>

With the steadily increasing popularity of PHEVs, charging infrastructure is needed to allow owners the security of being able to recharge when it becomes necessary. PHEV owners are therefore expected to desire charging stations installed both at home as well as large car parks located at commercial buildings. In large commercial car parks, due to the number of PHEV chargers that will be present, it is expected that power will be fed from a three phase distribution system. As mentioned previously, AC PHEV chargers are typically divided into three levels. Currently available PHEV chargers fall into the classification of the standardized levels 1 and 2 [20]. Due to the higher energy transfer capability of level 2 chargers compared to level 1, which corresponds to a shorter charge time, it is expected PHEV owners will desire these chargers if available.

Many existing studies attempt to examine the effects of PHEVs on a distribution system. These studies focus primarily on transformer overheating, system overloading, and ancillary services that can be provided through vehicle to grid (V2G) [21]-[25]. However, existing studies fail to consider the problem of power unbalance in the distribution system. In distribution systems, balancing of power between phases is attempted by distributing single phase loads equally between the three phases. In a car park, it is expected that one third of the chargers will be connected to each phase in order to attempt balancing. With varying loads due to individual PHEV charging rates and intermittent loads from vehicles connecting and disconnecting, this becomes impossible using a static phase connection with single phase PHEV chargers. It is very likely that a PHEV car park will therefore exacerbate the unbalance conditions already present in most distribution systems by drawing uneven power from each phase.

These conditions may be harmful to the distribution system due to zero and negative sequence currents that flow in the system when unbalance is present. Unbalanced conditions lead to higher losses, higher temperatures in transformers and motors, diminished power transfer limits of devices, and the potential to inhibit correct protection device operation [26]-[27]. One goal of this work is to present an idea that can significantly decrease or eliminate unbalanced operation of a car park by balancing real power.

Future Advancements

PHEVs are still an up and coming technology. According to [2], the DRIVE Act will require vehicle manufacturers to make at least 50% of their vehicles flex fuel capable

by 2016. This will mean significantly more attention on PHEV technology in the coming years. Also according to [2], parallel and series drive component configurations are both still being researched by the U.S. Department of Energy to determine which will provide the better vehicle. Before PHEVs can be fully accepted as a viable replacement for conventional vehicle technology, battery capacity will have to be increased to allow for a longer all electric operation range [7]. According to [11], battery pack capacity will have to be further increased to accommodate travelling at high speeds due to an increase of power losses at high speeds. Also, before PHEVs reach a large penetration, power quality, losses, and overloading potential must be carefully studied. Finally, grid enhancements, if necessary, must be performed before PHEV penetration reaches an unacceptable level using current infrastructure [7].

CHAPTER TWO

MODELING

In order to examine the impacts of PHEVs on a distribution system, several charger models are developed [28]. The chargers modeled represent a single phase, 240V AC Level 2 charger, which is capable of supplying up to 6.6kW to a PHEV during charging [29]. The charger consists of an AC/DC converter followed by a DC/DC converter. The AC/DC converter draws power from the electric grid and supplies it to a DC link capacitor. The DC/DC converter then supplies the battery with the constant current or voltage required for charging a PHEV battery. For a PHEV battery that has a state of charge (SOC) less than 75%, constant current charging is used [30]. Due to the short simulation time of the fault simulations, the SOC of the battery is assumed constant over the duration of the simulations where the full charger models are used. Thus, constant current charging is used for the entire simulation. There are two primary types of control for the AC/DC stage of the PHEV charger. These are current control and voltage control [31]. In order to fully examine the effects of PHEVs on a distribution system, both control topologies are developed. Two types of filters were also used at the terminals of the chargers. One type, the L filter, consists of only an inductor in series with the mains line while the other, the LCL filter, consists of two inductors connected in series and a capacitor connected in shunt between them. An L filter allows for less components in the charger while an LCL filter provides slightly better performance in terms of harmonics. The filter component values are selected based on information in

16

[32]. Figures 1 and 2 show the two topologies of the PHEV chargers with L and LCL filters, respectively.
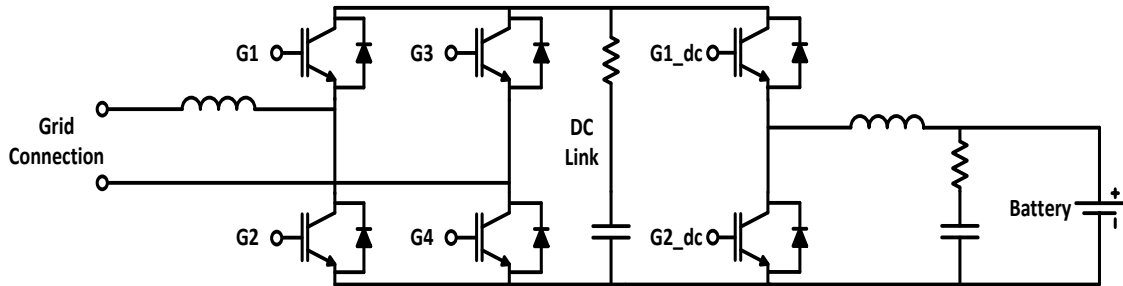
Fig. 1. Topology of PHEV Charger with L Filter
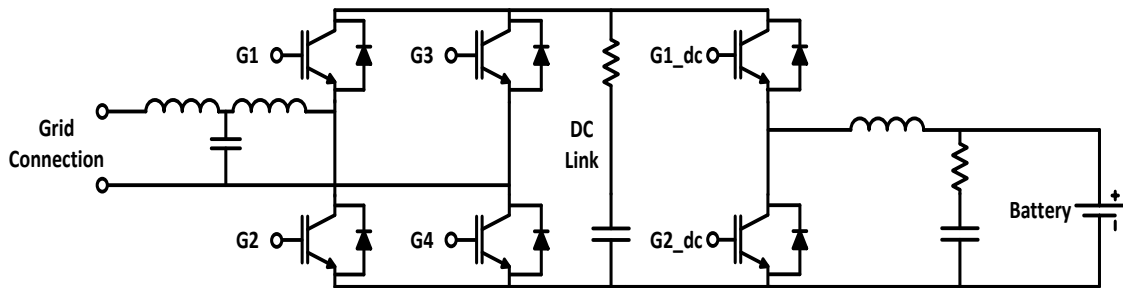
Fig. 2. Topology of PHEV Charger with LCL Filter

Current Controlled Charger

The physical components of the current controlled charger are based off of [30]. The control stages are based on [33-34] and are described in detail in [35]. In a current controlled charger, the AC/DC converter directly controls the current flowing from the grid to control real and reactive power. In this charger model, unity power factor operation is chosen, however other power factors are also possible. This is accomplished by first comparing the DC link voltage with its desired value, which is 500V, to generate

an error signal. This value is then normalized and passed through a PI controller. A saturation block is included in the charger in order to decrease settling time. A signal is also included that stops the integrator of the PI controller whenever the saturation limit is met and the error is still accumulating in that direction. Whenever the saturation limit is no longer hit, a reset signal is sent to all PI controllers in the control system. Next, the output of the first PI controller is multiplied by the grid voltage and then subtracted from the actual current flowing from the grid in order to generate a current error signal. Finally, it is passed through another PI controller and a comparator which implements sinusoidal pulse width modulation to generate gating signals for the AC/DC converter.

In order to generate the gating signal for the DC/DC converter, the desired battery current is compared with the actual battery current. This difference is run through a PI controller and then finally into a sinusoidal pulse width modulation block. Figures 3 and 4 show block diagrams of the control of the AC/DC converter stage and DC/DC converter stage, respectively.
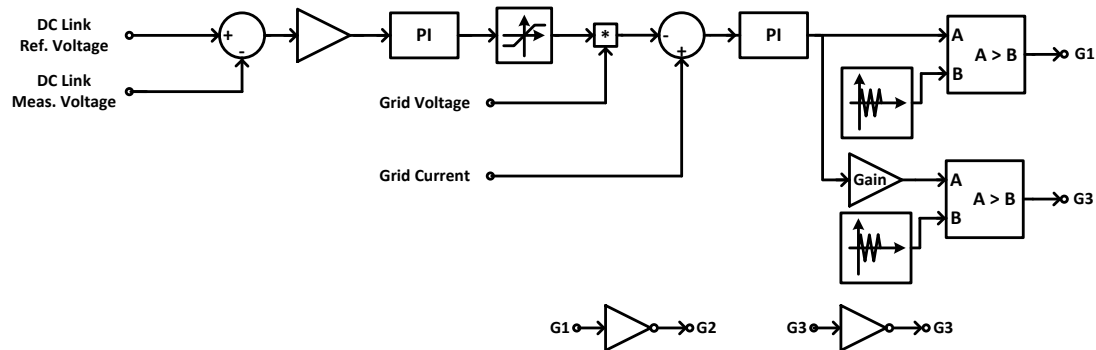

Fig. 3. Control of AC/DC Stage of Current Controlled PHEV Charger
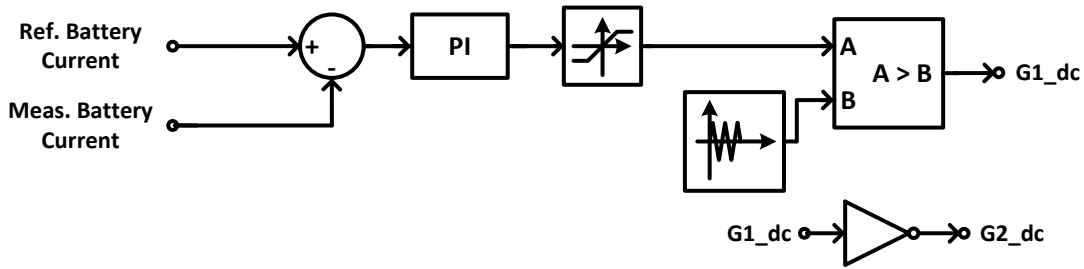
Fig. 4. Control of DC/DC Stage of PHEV Charger

Voltage Controlled Charger

In a voltage controlled charger, the AC/DC converter controls the current flowing from the grid by controlling the phase and magnitude difference between the grid voltage and the voltage on the inverter side of the filter using vector control. In order to determine this voltage difference, a decoupled controller is used. This decoupled controller calculates the desired voltages in the odq domain and then transforms them back to the abc domain. The control strategies utilized in this charger are adapted from [36] and presented in [37]. Because the charger modeled is single phase, a direct transformation cannot be used. A set of intermediate axes, named α and β, are first developed. These axes are generated using a technique known as a second order generalized integrator. These axes are then transformed to the d and q axes based on the grid angle, θ, which is obtained through a phase locked loop. Based on a set of input vectors, which represent the desired reactive power and dc link voltage, and the grid side voltage projected onto the d and q axes, the desired inverter side voltage, projected onto the d and q axes, is calculated. This is accomplished by using a phase locked loop to align the d axis with the grid voltage. Once the axes are aligned with the grid voltage, the current flowing into the charger terminals is also mapped to the d and q axes. Through

19

the transformation, the d axis current is aligned with the grid voltage, meaning it controls the real power drawn by the charger. The q axis current is rotated 90 degrees from the grid voltage, meaning it controls the reactive power drawn by the charger. Based on the difference between the desired DC link voltage of 500V and the actual DC link voltage, a reference value of d axis current is generated. Based on the difference between the actual and desired reactive power drawn by the charger, a reference value q axis current is generated. The error between the actual and reference d and q axis currents is then used to generate the desired d and q axis voltages. These voltages are then transformed back onto the α and β axes and finally fed into a 3 kHz sinusoidal pulse width modulation block to generate the gating signals for the AC/DC converter. Figures 5 and 6 show block diagrams of the d and q axis voltage controls, respectively. The gating signals for the DC/DC converter are generated in the same way as the current controlled charger.
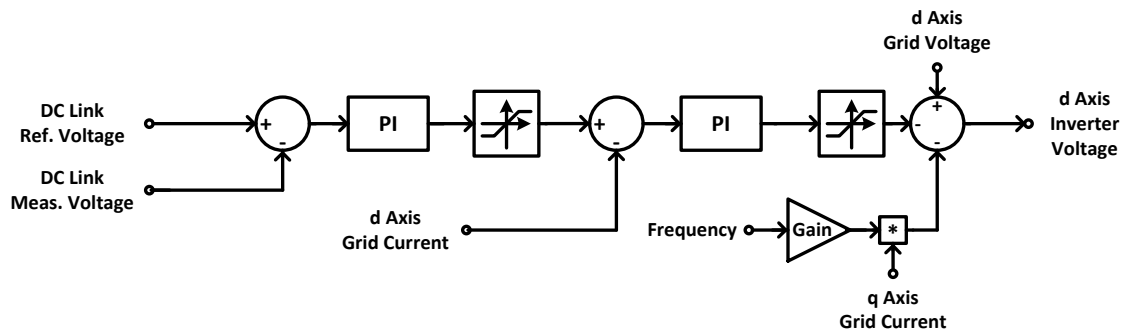
Fig. 5. Control of d Axis Voltage

20
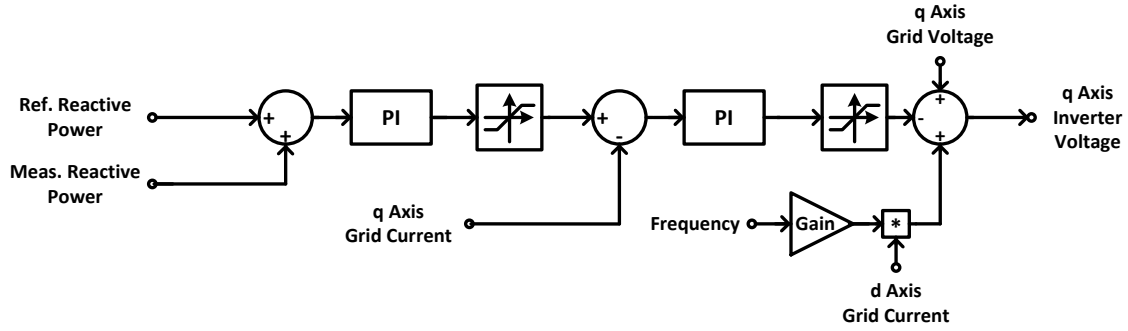
Fig. 6. Control of q Axis Voltage

Steady State Equivalent Charger [19]

It is shown in [35] that a single phase PEV charger can be developed that will accurately draw or supply a commanded real power based on this control methodology. Long term simulations with the full charger models are not possible due to computing requirements caused by high frequency switching. A controlled current source is therefore used to model each PEV charger in place of the full detailed model for long term simulations. The required current can be calculated based on Eq. 1 by using the measured voltage at the terminal of each PEV charger and the desired real and reactive powers. Based on the limits prescribed by standardized level 1 and 2 chargers, the real power is limited to a maximum of 7 kW per PEV [29].

$$I_{peak} = \frac{2(P + jQ)^*}{V_{peak}^*} \tag{1}$$

IEEE 13 Node Test Feeder

In order to determine the effect that the addition of PHEVs has on a distribution system during system disturbances, PHEVs were added to the IEEE 13 Node Test Feeder [38]. The IEEE 13 Node Test Feeder is an unbalanced, 4.16 kV distribution system. The

system consists of 5 three phase lines, 3 two phase lines, and 2 single phase lines. The system is fed from a 115 kV source that represents a transmission system. The total system load before PHEVs are added to the system is 3697 kVA.
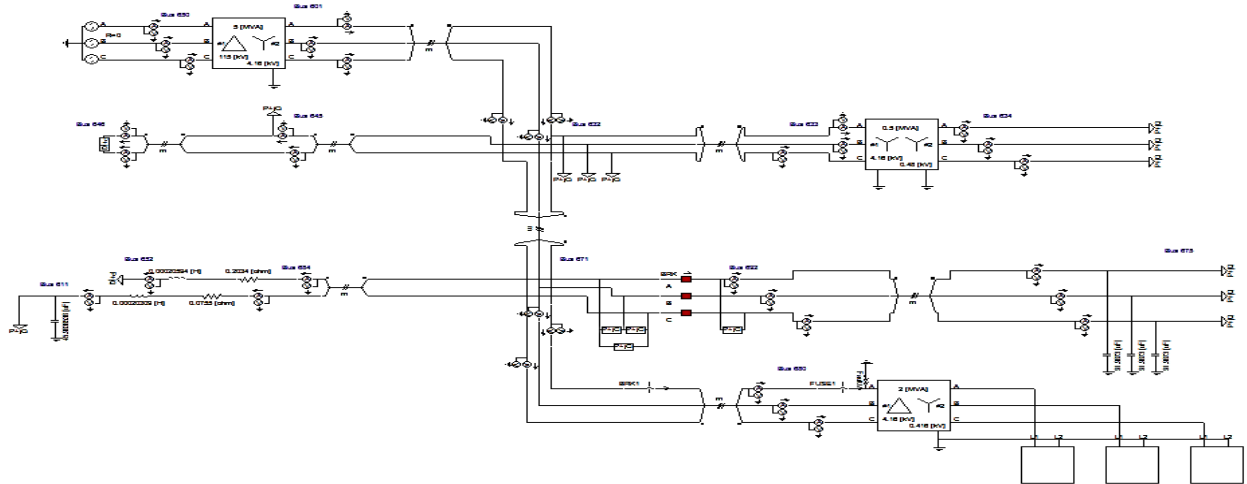
Fig. 7. IEEE 13 Node Test Feeder with PHEVs Added at Bus 680

Due to limitations of the PSCAD software used for simulation, a very small time step had to be used whenever the full model of the distribution lines found in [39] was used for simulation. This is primarily due to the very short length of the distribution lines in the system. The very small time step caused simulations to take an unreasonably long time to complete. In order to shorten the simulation time to a more reasonable length, all distribution line models were replaced with mutually coupled lines. The mutually coupled lines neglect line charging however due to the short line length, this was not expected to significantly impact results. In order to verify that modeling all distribution lines as mutually coupled lines produced similar results, the results from a single line to ground fault at bus 680 were compared. The results are shown in Fig. 8. It can be seen that apart from a small difference in magnitude, the results are almost identical.
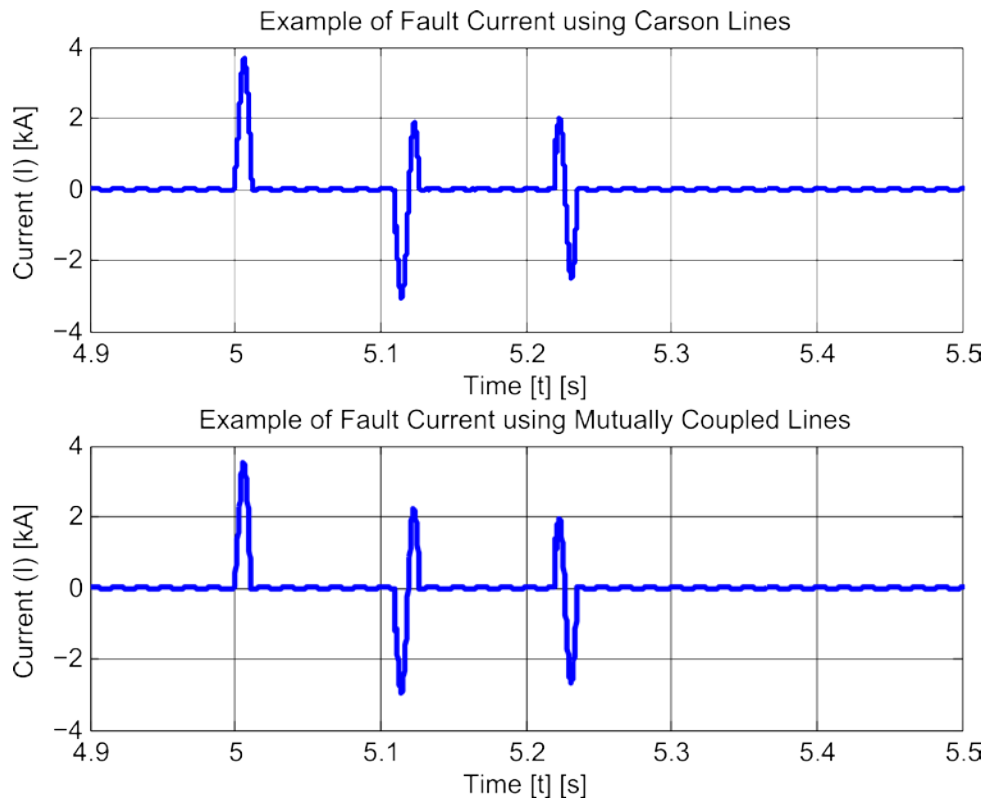
Fig. 8. Comparison of Fault Currents using Carson Lines and Mutually Coupled Lines

For the addition of PHEVs, a three phase delta-wye grounded transformer was added to bus 680. On the low voltage side of this transformer, which is rated at 416V, a total of 16 vehicle chargers were connect from line to neutral on each phase. Each charger draws 6.2 kW, making the total load added by the vehicle chargers 297.6 kW. This represents an addition of slightly more than 8.5% of the original system load. In order to isolate the effects of the addition of PHEVs from the addition of a large load at the same bus, a base case was set up with an equivalent constant power load connected in place of the vehicle chargers. For all scenarios, the base case with equivalent load was compared with the results of the simulations containing vehicle chargers. Protection devices were also added to the system in the form of a single phase recloser protecting

the upstream side of the line connecting buses 671 and 680. The recloser operates on the timings found in table 3. In order to clear a permanent fault, a fuse was added to the downstream side of the line connecting bus 671 to bus 680. For a permanent fault, the fuse blew at 5.83 seconds, which occurs before the recloser reaches lockout. Once the fuse blows, phase A of bus 680 is isolated from the rest of the system.

Table 3

Recloser Timings

Cycle Type	Open Time	Close Time
Fast	0.1 Second	0.01 Second
Slow	0.1 Second	0.5 Second

Clemson University Electric Distribution System [40]

For balancing and Vehicle to Campus (V2C) simulations, the Clemson University electric distribution system is modeled in SimPowerSystems, an add-on toolbox for MATLAB. A system diagram can be found in Fig. 9. Parameters used were provided by Clemson University Utility Services. Due to the large amount of data corresponding to a system this size, inclusion of all system parameters is not feasible. The system is a primarily three phase, 12.47kV distribution system connected by underground tape shielded cables. Carson's equations are used to calculate line parameters assuming a triangle configuration with a neutral in the center [41]-[43]. The system is fed by a connection to a 44kV transmission system. At peak load for 2013, the system was drawing 22.03MVA of three phase apparent power. Most buildings on campus are fed by three phase distribution transformers that step the voltage down to either 480V or 208V.

There are also two 15kW photovoltaic arrays and a 5.5MVA gas turbine used for peak load shaving.

For some studies, an unbalanced load is applied to the system. For these unbalanced simulations, the powers of all the loads connected to phase A are increased by 2%, the powers of all the loads connected to phase B are increased by 1%, and the powers of all the loads connected to phase C are decreased by 3%, all compared to balanced conditions. It is important to note however that these loads are connected on the secondary sides of the distribution transformers, some of which are Delta-Wye connected. This causes the unbalance in the system to appear on different feeders compared to the unbalance in the loads.
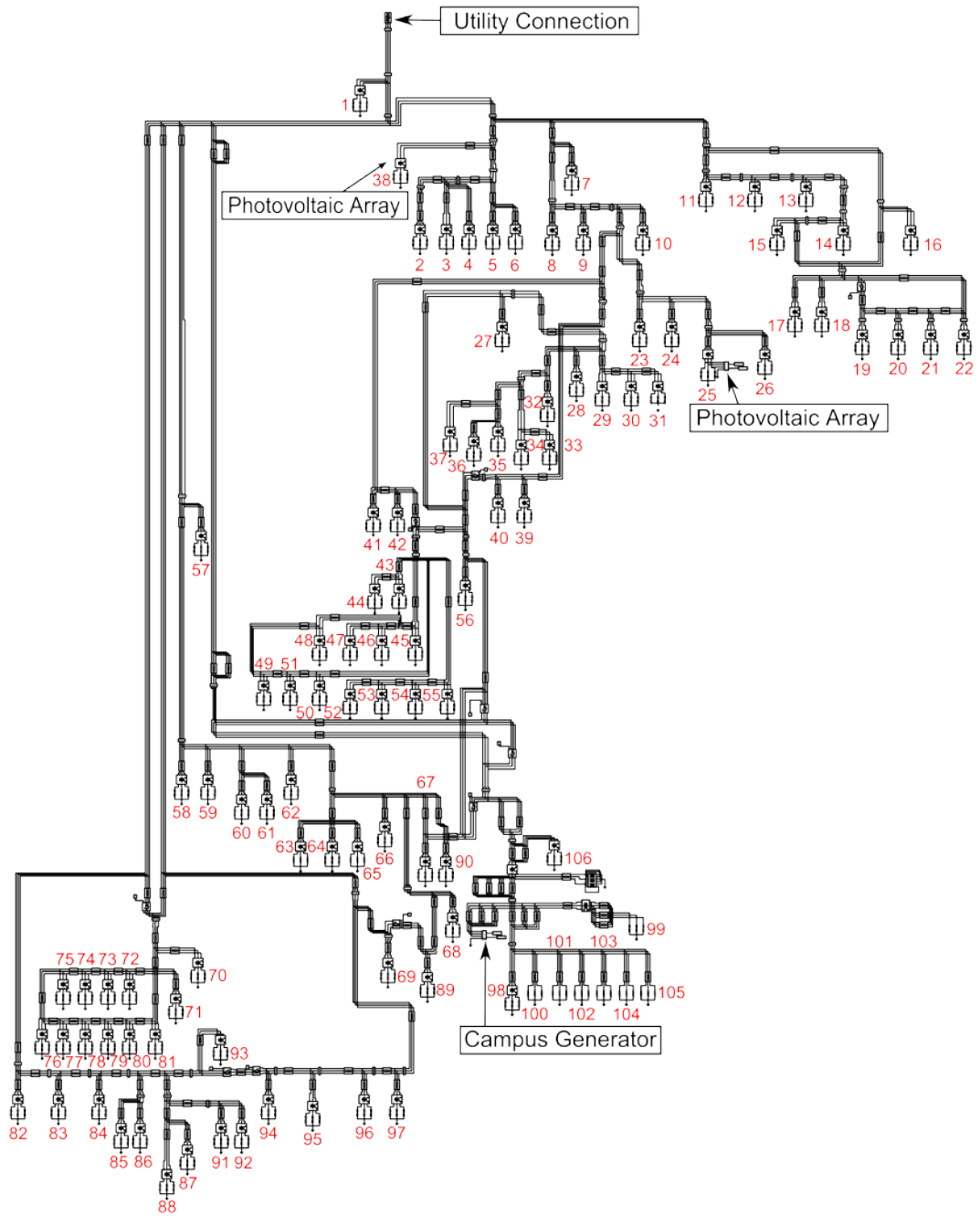
Fig. 9. Clemson University Electric Distribution System

Table 4

Clemson University Electric Distribution System Locations

Location	Description	Location	Description
1	4.16 kV System East	62	Lehotsky Hall
2	Strom Thurmond Institute	63	Rhodes Research Building
3-4	Brooks Center	64-65	Riggs Hall
5-6	East Chiller Facility	66	Lee Hall
7	Biosystems Research Complex	67	Stadium Suites
8	Godley-Snell Research Center	68	Rhodes Hall Annex
9	Band Practice Field	69	Poole Agricultural Building
10	Service and Support	70-81	Calhoun Courts
11-22	Lightsey Bridge Apartments	82	Redfern Health Center
23-24	Hinson CWP	83	Edwards Hall
25	Fluor Daniel	84	Schilletter Hall
26	Harris A. Smith Building	85	Vickery Hall
27	Jervey Athletic Center	86	Jordan Hall
28-31	Doug Kingsmore Stadium	87	Kinard Annex
32-34	Rugby Fields	88	Long Hall
35-36	Rowing Boathouses	89	Academic Success Center
37	Pump Station	90	Lee Hall Annex
38	Life Sciences Facility	91	Sikes Hall
39-41	Littlejohn Coliseum	92	Alumni Center
42	Intramural Fields	93	Manning Hall
43-55	Clemson Memorial Stadium	94	Byrnes Hall
56	Fike Recreation Center	95	President's Home
57	Hendrix Student Center	96	Smith Hall
58	Daniel Hall	97	Lever Hall
59	Barre Hall	98-105	Central Energy Facility
60-61	McAdams Hall	106	4.16 kV System West

CHAPTER THREE

FAULT ANALYSIS ON AN UNBALANCED DISTRIBUTION SYSTEM
IN THE PRESENCE OF PHEVS

Without Solar Generation [37]

A fault analysis was performed on a distribution system by applying a single line to ground fault on phase A at bus 680 of the IEEE 13 Node Test Feeder. The fault was applied at 5 seconds into the simulation in order to allow the system to reach steady state. In the case of a temporary fault, the fault was cleared from the system at 5.275 seconds, at which time the recloser is open. For the permanent fault, cases were run with the current controlled charger with L filter connected. In order to isolate the impacts of adding PHEV chargers to the distribution system from the impacts of adding a large load at the same location, the base case taken for comparison has a load connected at the location PHEVs are connected for other simulations. This load has a power equivalent to the PHEV charging power on each phase when chargers are connected. It was found that in the case of a permanent fault, the addition of PHEVs had little effect on the system compared to the base case with equivalent load due to the voltage remaining close to 0V until the fuse clears the fault. The permanent fault scenario is not further explored due to this.

In the case of temporary faults, it was found that certain types of PHEV chargers had a negative impact on the distribution system during the period after the fault clears from the system and the recloser remains open. For the voltage controlled charger with L filter, a high voltage, high frequency signal was fed back to phase A of bus 680 from the vehicles connected to phases A and C on the low voltage side of the transformer. For this

28

charger model, the peak magnitude of the voltage is more than twice the peak magnitude of the steady state voltage. The voltage waveform of bus 680 during the fault and fault recovery periods for both the base case with equivalent load and the case with voltage controlled chargers with L filters can be seen in Fig. 10.
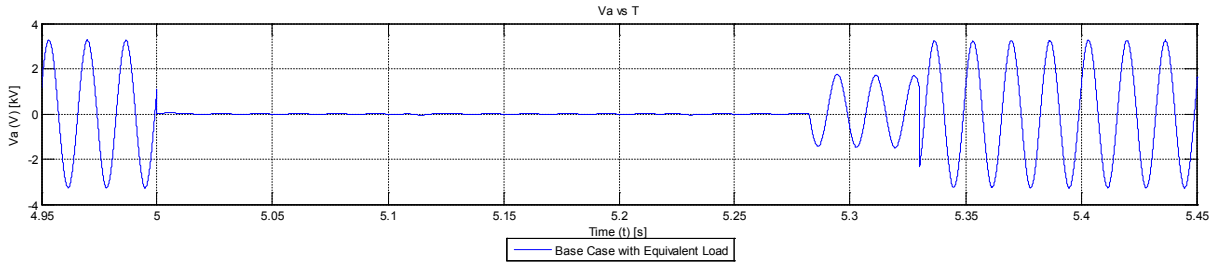

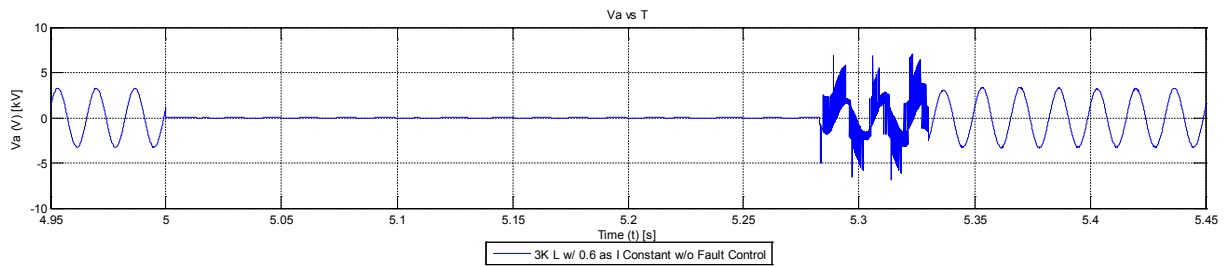Fig. 10(a). Base Case with Equivalent Load Bus 680 Phase A Voltage

Fig. 10(b). Voltage Controlled Charger with L Filter Bus 680 Phase A Voltage

A current transient was also seen on phase B at bus 680 after the recloser reconnects phase A to the system. This waveform can be seen in Fig. 11.

29

Fig. 11(a). Base Case with Equivalent Load Bus 680 Phase B Current
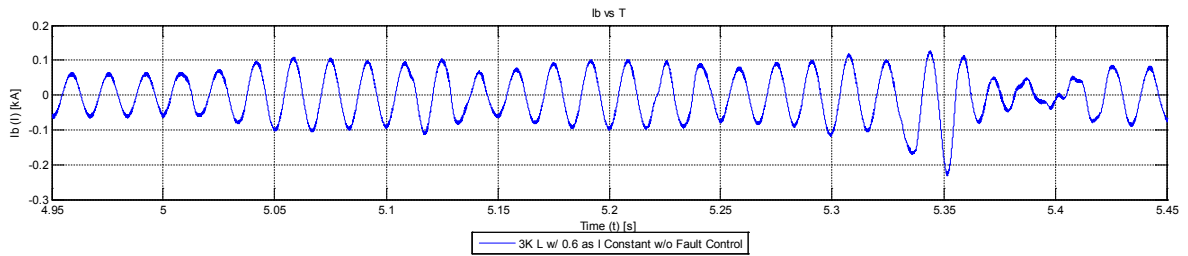
Fig. 11(b). Voltage Controlled Charger with L Filter Bus 680 Phase B Current

With the current controlled charger with L filter, a similar effect to that of the voltage controlled charger with L filter was observed. The primary difference between the two is that the current controlled charger with L filter maintains its peak value longer than the voltage controlled charger with L filter. The voltage waveform of phase A at bus 680 is shown in Fig. 12.

Fig. 12(a). Base Case with Equivalent Load Bus 680 Phase A Voltage

Fig. 12(b). Current Controlled Charger with L Filter Bus 680 Phase A Voltage

Unlike the voltage controlled chargers, the current controlled chargers show only a very small current transient that maintains a mostly sinusoidal shape. The current waveform of phase B at bus 680 with the current controlled charger with L filter connected can be seen in Fig. 13.
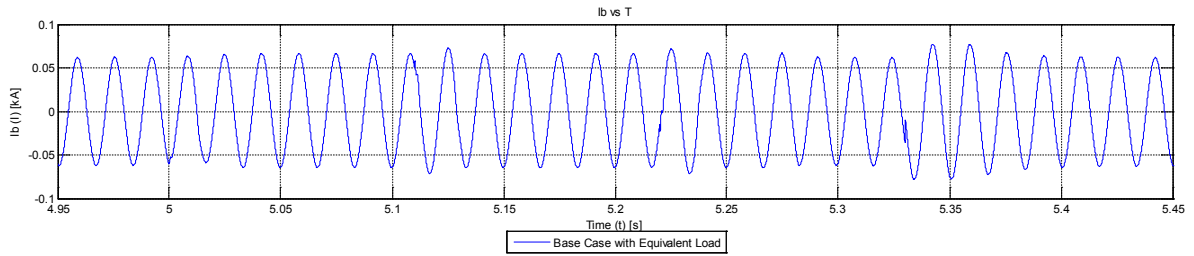
31

Fig. 13(a). Base Case with Equivalent Load Bus 680 Phase B Current
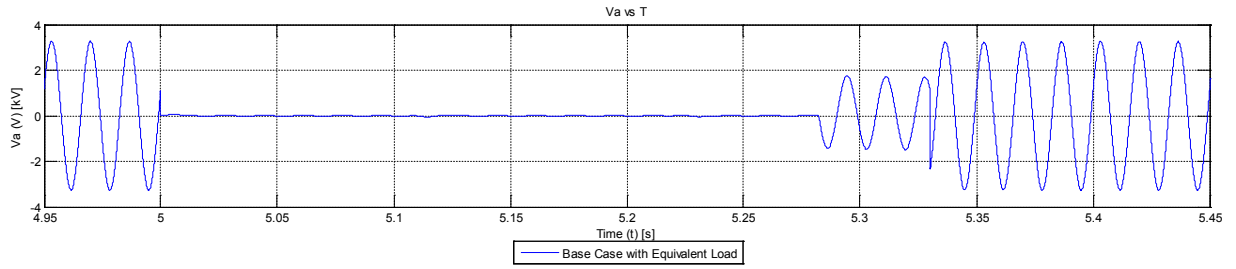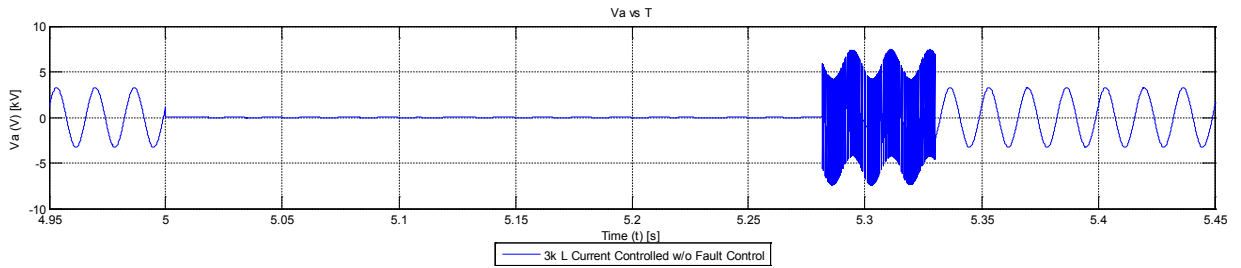

Fig. 13(b). Current Controlled Charger with L Filter Bus 680 Phase B Current

The voltage controlled charger with LCL filter shows a negative impact during the same period as the two chargers with L filters, however, the peak magnitude is much greater for this charger. With this charger, the peak magnitude is over 9 times the steady state value in the case of the voltage. The voltage waveform of phase A at bus 680 can be seen in Fig. 14. Note that in this figure, the scale of the lower plot is much larger in order to show the full distorted waveform. The steady state values of the base case with equivalent load and of the case with chargers connected are almost the same. The current transient seen with this charger model was very similar to that of the voltage controlled charger with L filter and can be seen in Fig. 15.

Fig. 14(a). Base Case with Equivalent Load Bus 680 Phase A Voltage

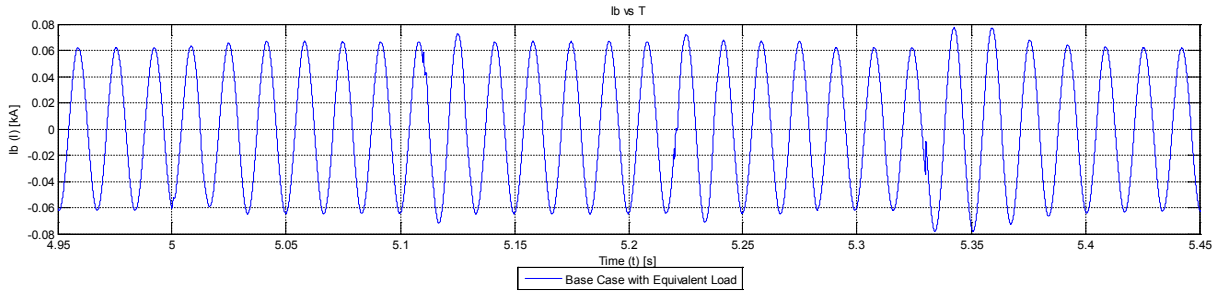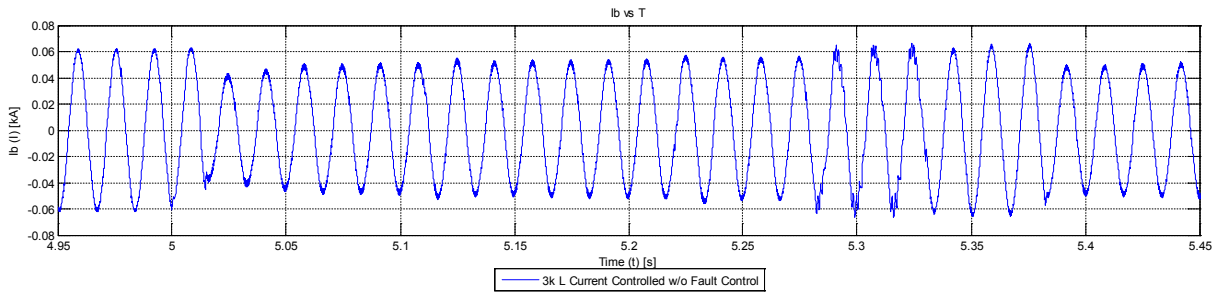Fig. 14(b). Voltage Controlled Charger with LCL Filter Bus 680 Phase A Voltage

Fig. 15(a). Base Case with Equivalent Load Bus 680 Phase B Current

Fig. 15(b). Voltage Controlled Charger with LCL Filter Bus 680 Phase B Current

Unlike the other three charger models, the current controlled charger with LCL filter did not show a negative impact on the distribution system during fault recovery. The voltage of phase A at bus 680 is shown in Fig. 16. The current transient seen from

the current controlled charger with L filter is very similar to the other current controlled charger in that the current remains mostly sinusoidal with only a very small increase in magnitude compared to steady state. The current waveform of phase B at bus 680 is shown in Fig. 17.
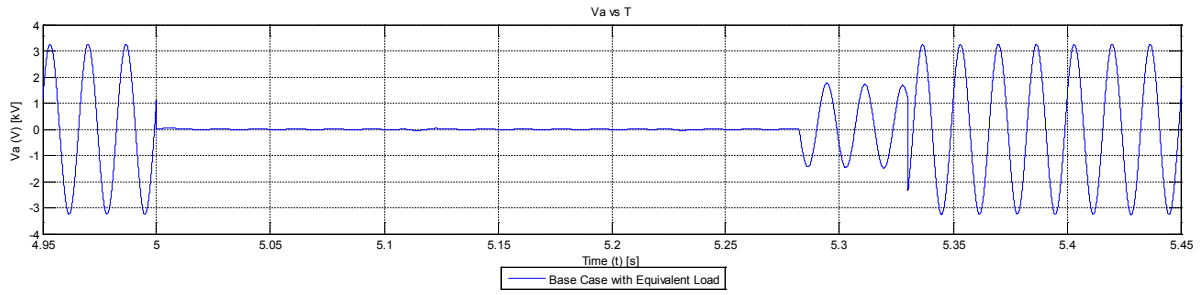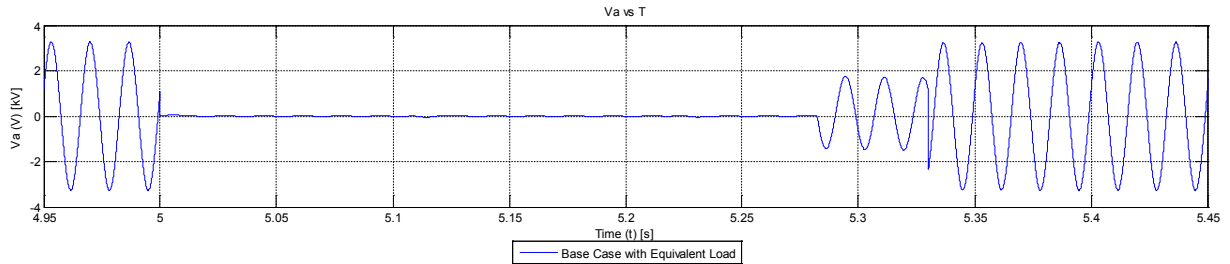

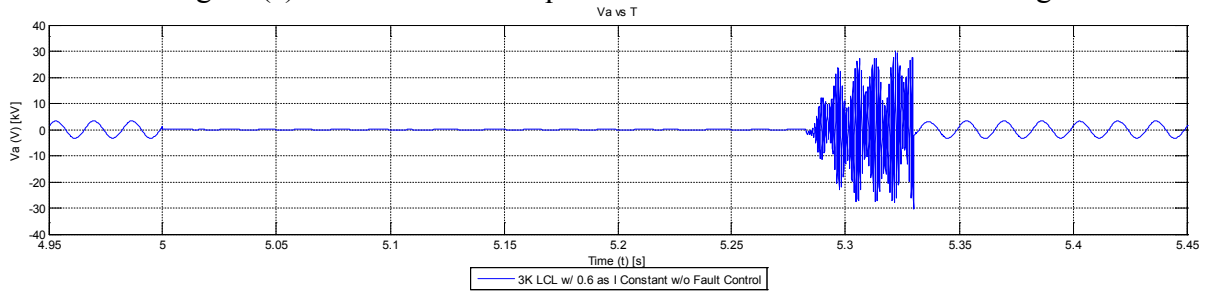Fig. 16(a). Base Case with Equivalent Load Bus 680 Phase A Voltage
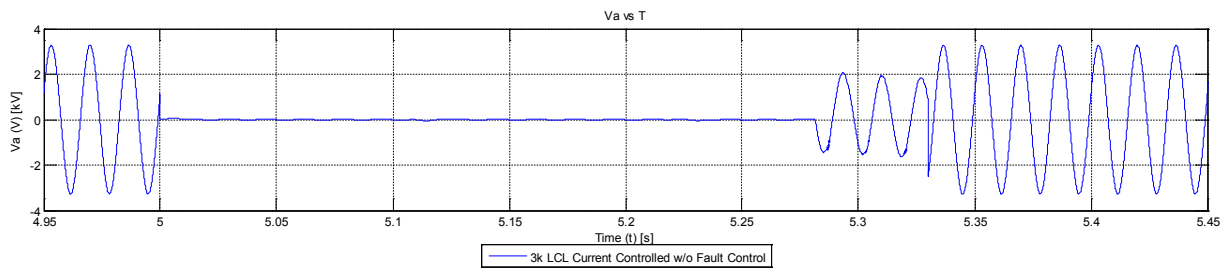
Fig. 16(b). Current Controlled Charger with LCL Filter Bus 680 Phase A Voltage
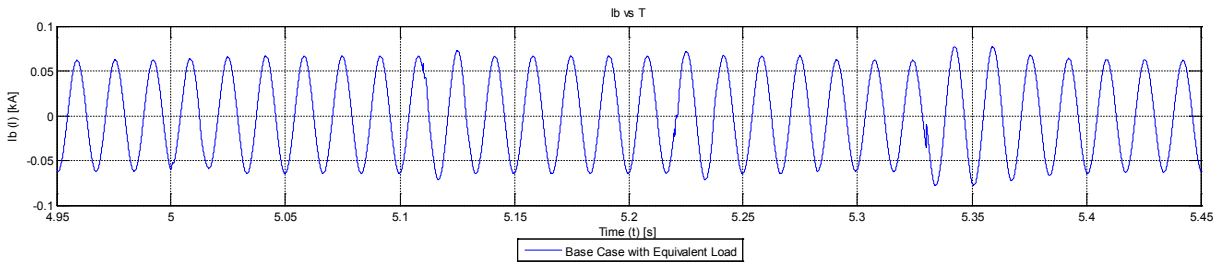
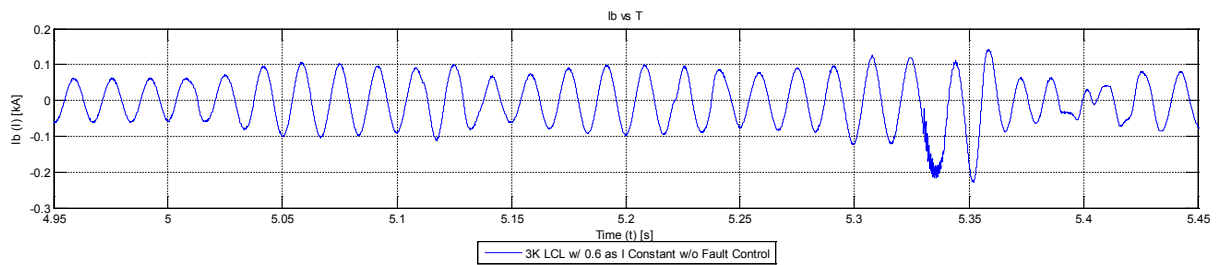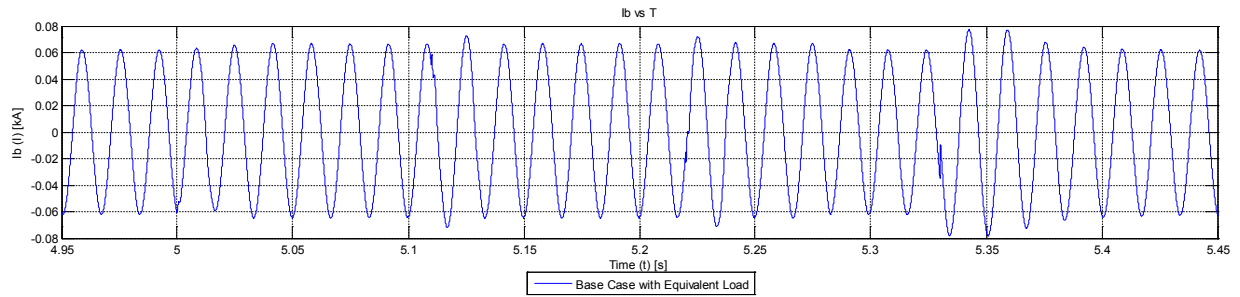Fig. 17(a). Base Case with Equivalent Load Bus 680 Phase B Current
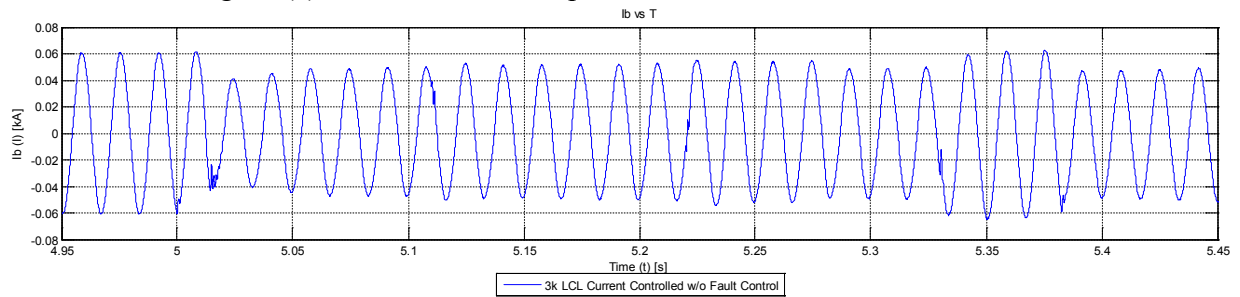
Fig. 17(b). Current Controlled Charger with LCL Filter Bus 680 Phase B Current

Based on the results seen with all chargers except the current controlled with LCL filter model, it was desired to mitigate the negative impacts on the distribution system during fault recovery. This was accomplished by monitoring the terminal voltage at the point at which the charger is connected. Whenever the line to neutral voltage drops below 200V, all switching in the vehicles was stopped and the switches were left in the open position. This voltage was chosen because it was well below normal voltage drop limits in a distribution system, based on the nominal charger line to neutral terminal voltage of 240V. The circuit shown in Fig. 18 has the switches removed to show the charger configuration whenever the terminal voltage drops below 200V. Once the terminal voltage recovers to a normal value, switching is no longer blocked and the charger is allowed to resume normal operation.
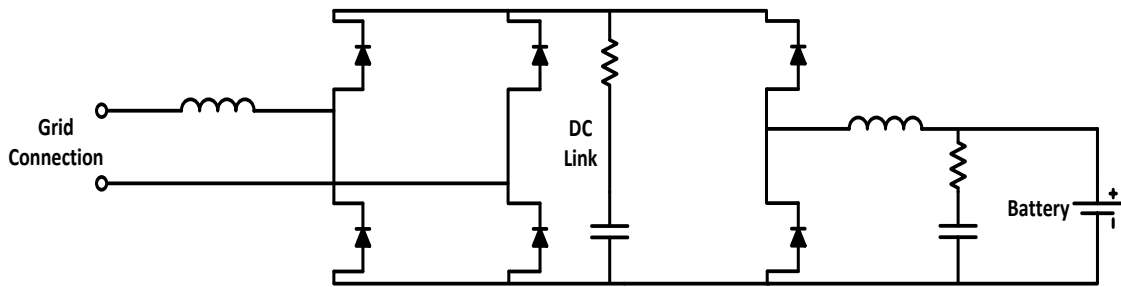
Fig. 18. Charger Circuit When Terminal Voltage Drops Below 200V

With the fault control logic included, the results of connecting the voltage controlled charger with LCL filter to the distribution system during a fault and fault recovery are shown in Fig. 19 and Fig. 20. This case was chosen due to it having the worst negative impacts on the distribution system without fault control included. As can be seen in the figures, the high frequency high voltage is no longer present during fault recovery. Also, the current transient seen after the recloser reconnects the system to phase A of bus 680 is smaller in magnitude and remains mostly sinusoidal instead of having the large amount of distortion seen without fault control included in the charger.

Fig. 19(a). Voltage Controlled Charger with LCL Filter Bus 680 Phase A Voltage without Fault Control Logic

Fig. 19(b). Voltage Controlled Charger with LCL Filter Bus 680 Phase A Voltage with Fault Control Logic

Fig. 20(a). Voltage Controlled Charger with LCL Filter Bus 680 Phase B Current without Fault Control Logic

Fig. 20(b). Voltage Controlled Charger with LCL Filter Bus 680 Phase B Current with Fault Control Logic

37

With Solar Generation

It was found that while PHEV chargers had a negative impact on the distribution system during fault recovery, as soon as the distribution grid was reconnected to bus 680, all transients ceased very quickly. This fast recovery is believed to be due in large part to the transmission system being represented as an infinite source. In order to examine the effects on a system where all of the power is not drawn from a single infinite source, a large penetration of solar, which is capable of supplying approximately 60% of the base system load, is added to the system. The photovoltaic array panel and converter design were provided by the makers of PSCAD and are detailed in [44]. Solar arrays are connected in pairs at the following buses: 601, 633, 671, 675, and 680. Similar studies to those run without solar connected to the system are completed and the results are compared with both a base case containing solar and an equivalent load connected in place of chargers as well as the case including chargers with no solar.

In this case, the photovoltaic arrays support the voltage during fault recovery and allow the vehicles to attempt to track that voltage. This can be seen in Fig. 21 which shows both base cases with a constant power load equivalent to the power drawn by the vehicles. Fig. 21(a) shows the system without solar and Fig. 21(b) shows the system with solar.
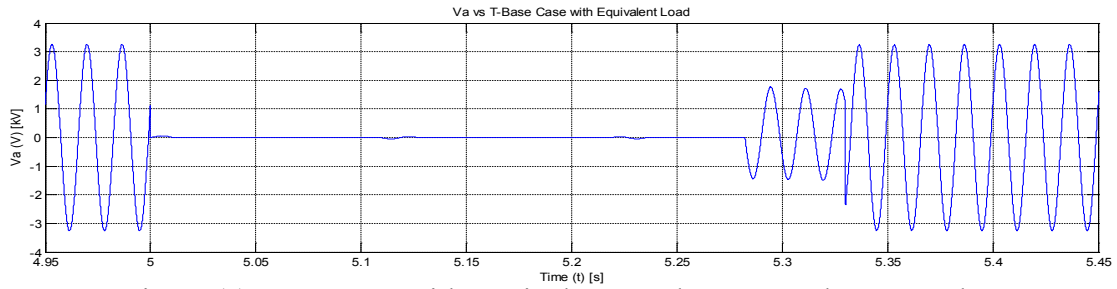
Fig. 21(a). Base Case with Equivalent Load Bus 680 Phase A Voltage
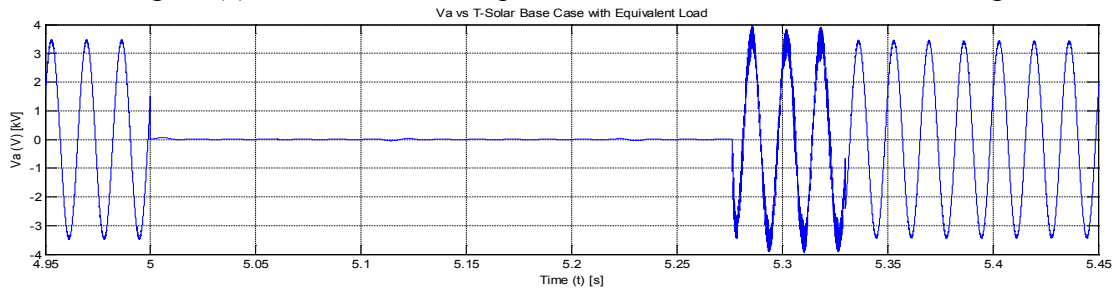
Fig. 21(b). Base Case with Equivalent Load including Solar Bus 680 Phase A Voltage

The negative impacts seen are less due to the voltage support provided by the solar. The voltage support also means that the previously described fault control logic must include a delay to be effective. The switching is not allowed to resume until the terminal voltage has been above the threshold for at least 0.1 seconds. This time was chosen based on it being as long as the longest open time of the recloser, ensuring that the vehicles will not resume switching while the recloser is open. Results are shown in Fig. 22(a-e). Fault control logic is again able to mitigate most of the negative effects, however, due to the voltage support provided by the photovoltaic panels, the vehicles still negatively impact the system during fault recovery. With fault control, the peak voltage is reduced from approximately 3.5 times the steady state peak value to less than 2 times the steady state peak value.
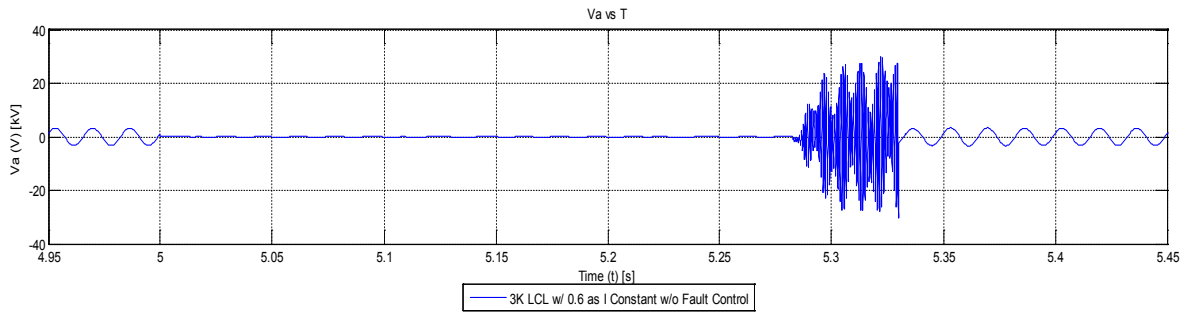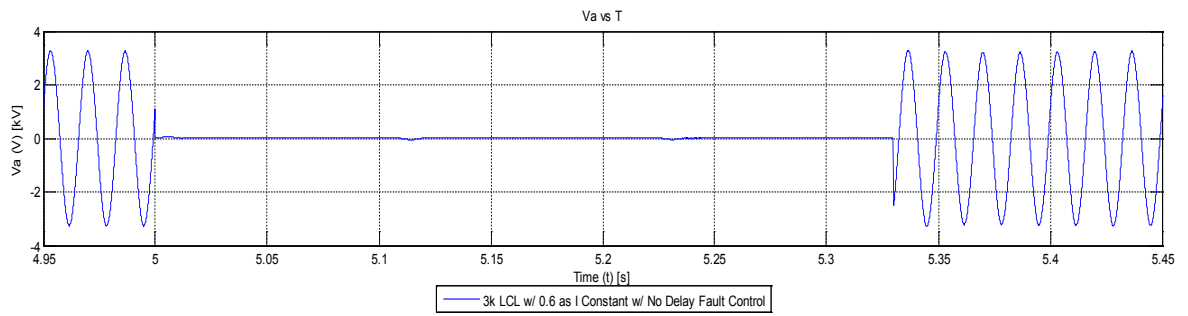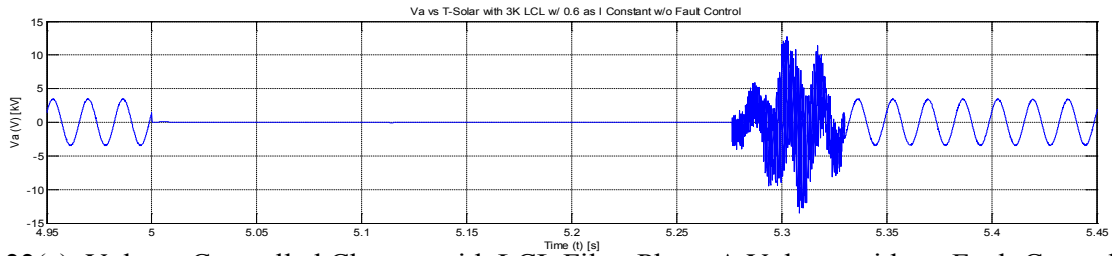
Fig. 22(a). Voltage Controlled Charger with LCL Filter Phase A Voltage without Fault Control Logic

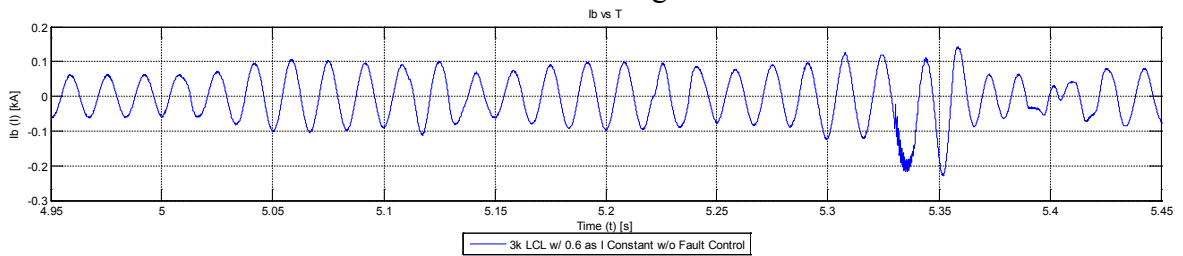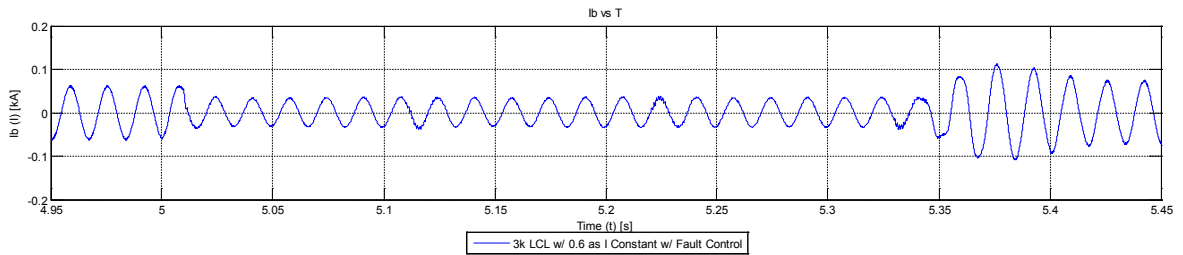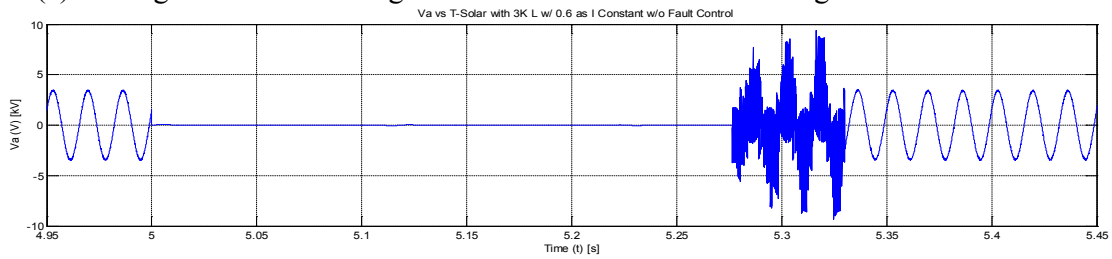Fig. 22(b). Voltage Controlled Charger with L Filter Phase A Voltage without Fault
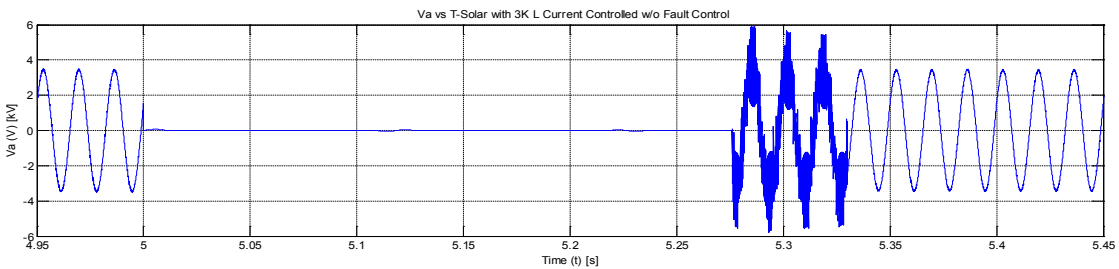
Control Logic

Fig. 22(c). Current Controlled Charger with L Filter Phase A Voltage without Fault Control Logic
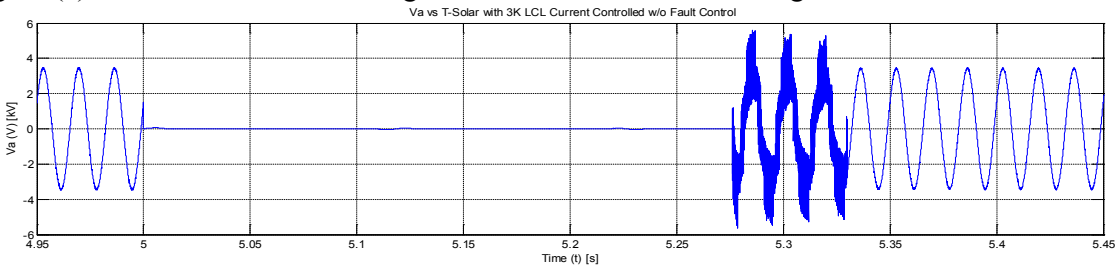
Fig. 22(d). Current Controlled Charger with LCL Filter Phase A Voltage without

Fault Control Logic
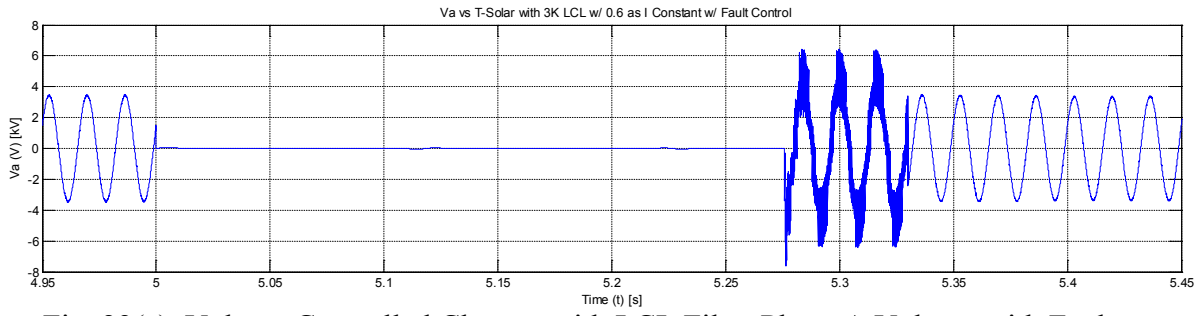
Fig. 22(e). Voltage Controlled Charger with LCL Filter Phase A Voltage with Fault

Control Logic

CHAPTER FOUR

AN INNOVATIVE APPROACH IN BALANCING REAL POWER USING PHEVS

Balancing Real Power in a Feeder [40]

The goal of this idea is to automatically change the phase that PHEV chargers are connected to based on measured power flows in the system. Some vehicle chargers that are drawing power will be switched to the less heavily loaded of the three phases and some vehicle chargers that are supplying power will be switched to more heavily loaded phases. The effect of this is shifting some power away from heavily loaded phases. This in turn increases power on lightly loaded phases in order to balance the three phases as necessary. Because PHEV charging rates are not altered using this idea, PHEV charging is allowed to continue in almost the same way as with a static phase connection. The impact on PHEV owners is therefore expected to be unnoticeable, while the overall car park is expected to have less impact on the distribution system than an equivalent car park without phase balancing present.

In order to be successful, each PHEV must have the ability to switch between all three phases. This is accomplished by adding a switching element between the terminals of the PHEV charger and the distribution grid. In this study, single phase breakers are used, however, power electronic solid state switches or any other switch that allows disconnection from one phase and connection to another could also be used for this purpose. To illustrate the feasibility of this idea, a sample heuristic algorithm that requires minimal computations is developed and used to control the phase each PHEV charger is connected to.

To accomplish this, the algorithm works by taking in information from each charger about how much real power it is drawing and responding with what phase each PHEV charger should be connected to. It also requires an input of the unbalanced real power measured where the balancing occurs. In order to be successful, the PHEVs must draw their power from where the algorithm will balance power.

An approximation of the real power that would flow through each phase without the connection of PHEVs is calculated using Eq. 2. The real power measured from the system is required by the algorithm. The real power consumed by each charger and memory of which phase each PHEV charger is connected to from the previous time step are also required. By neglecting the feeder losses caused by the addition of the PHEV to a phase, Eq. 2 can be used. However, the losses caused by the addition of a PHEV to a phase are anticipated to be much smaller than the power drawn by the PHEV charger.

$$P_{Estimate_{Phase}} = P_{Measured_{Phase}} - \sum_{x \in Phase} P_{PHEV}(x) \qquad (2)$$

The estimated values of real powers for each phase without PHEVs connected are compared with the values from the previous calculation. If the estimated real power has not changed by a certain percentage and no PHEVs have been connected or disconnected since the last placement, the algorithm exits and waits for the specified time before starting over. If the estimated real power has changed or a PHEV has been connected or disconnected since the last placement, the algorithm is allowed to continue and the PHEVs are then sorted into a list based on the absolute value of the power consumed or supplied by each charger, with the largest listed first. Starting with the first power in the sorted list, the real power of the PHEV charger associated with it is checked to determine

if it is drawing real power, supplying real power, or neither. If the PHEV charger is drawing real power, it is assigned a connection to the phase with the minimum estimated real power. This will cause an increase in the observed real power load on that phase. If the PHEV charger is supplying real power, it is assigned a connection to the phase with the maximum estimated real power. This will cause a decrease in the observed real power load on that phase. If the PHEV charger is neither drawing nor supplying real power, it is disconnected from the system. Based on the assigned phase connection, the estimated real power is recalculated using Eq. 3.

$$P_{EstimateNew_{Phase}} = P_{Estimate_{Phase}} + \sum_{x \in Phase} P_{PHEV}(x) \tag{3}$$

This assignment will continue until all PHEVs in the sorted list are placed. The switching elements connected to the PHEV chargers are then commanded to automatically switch without user interaction. As a result, this algorithm will exit and wait for the specified time before starting over. The time before the next calculation is based on a tradeoff. By increasing the time before the next calculation, wear on the switching elements will be reduced. By decreasing the time before the next calculation, the accuracy will be increased and PHEVs will be allowed to begin charging faster after connection to a charger. Due to the automatic switching used, the vehicles will continue to charge or discharge even if they are commanded to change phases multiple times during connection. In this case, the switching elements are represented through three single phase breakers added at the terminals of each PHEV charger, which allows each individual PHEV charger to be automatically connected to any of the three phases based

on the commanded phase. Switches consisting of power electronics could also be used in place of breakers. Fig. 23 shows a flowchart of this algorithm.
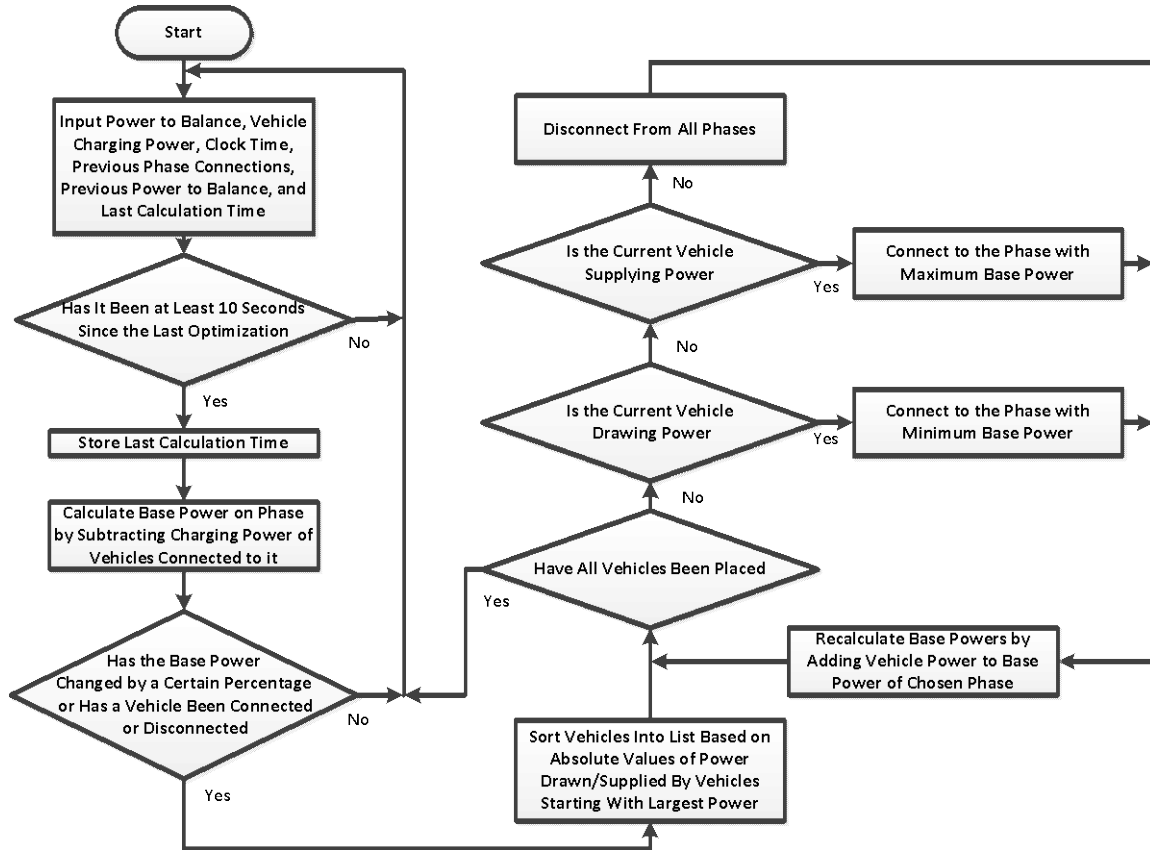
Fig. 23. Feeder Real Power Balancing Algorithm

Using the Clemson University electric distribution system, the real power balancing algorithm is applied. A PHEV car park is added to the campus system simulation at one of the major parking lots on campus. A total of up to 30 PHEV charging stations are connected to the system in the car park at a given time, based on the power drawn by each PHEV and the algorithm described in this paper. The car park is connected to the system using a Wye Grounded-Wye Grounded three phase transformer. This transformer type is chosen because the balancing algorithm described in this paper

45

intentionally unbalances the PHEV load on the secondary of this transformer in order to balance the real power flowing elsewhere in the system. Using a Wye Grounded-Wye Grounded three phase transformer allows the unbalanced power on one phase of the secondary to not influence another phase on the primary side of the transformer.

The real power measured that the algorithm will attempt to balance is flowing into the bus where the car park is connected. This bus feeds both the car park as well as other downstream loads, which are the original source of unbalance in the feeder. Fig. 24 shows the real power flowing into the bus both before and after the balancing algorithm is applied. For the first half of the time shown, the balancing algorithm is not applied and PHEVs are connected according to Table 5. After the first half of the time shown, the balancing algorithm is applied and PHEVs are assigned to phases in such a way as to balance the real power flowing into the bus. As can be seen in Fig. 24, applying the real power balancing algorithm to the car park almost perfectly balances the real power flowing into the bus. This balancing is accomplished by switching vehicles from the heavily loaded phases, A and B, to the lightly loaded phase, C. Table 6 shows the powers for each phase and maximum percent difference both before and after balancing occurs, as measured at the car park bus. This in turn has the effect of pushing the entire system towards a more balanced operation, as can be seen in Fig. 25. At this bus, the load on the two heavily loaded phases, A and B, is again reduced and the load on the lightly loaded phase, C, is increased by approximately the same amount of the reductions of the other two phases. Table 7 shows the powers for each phase and maximum percent difference both before and after balancing occurs, as measured at the utility feed.

Table 5. Initial PHEV Phase Connections

PHEV Number	Connected Phase
1,4,7,10,13,16,19,22,25,28	A
2,5,8,11,14,17,20,23,26,29	B
3,6,9,12,15,18,21,24,27,30	C

Table 6. Results of Real Power Balancing Algorithm – Car Park Bus.

Case	Phase A Power	Phase B Power	Phase C Power	Maximum Percent Difference
Before Balancing	709.5 kW	728.2 kW	667.1 kW	8.758 %
After Balancing	701.4 kW	701.3 kW	702.2 kW	0.128 %

Table 7. Results of Real Power Balancing Algorithm – Utility Feed.

Case	Phase A Power	Phase B Power	Phase C Power	Maximum Percent Difference
Before Balancing	5.18 MW	5.23 MW	4.84 MW	7.711 %
After Balancing	5.17 MW	5.20 MW	4.87 MW	6.593 %

During normal operation of distribution systems, many loads may vary frequently. In order to be practical for real world applications, the algorithm must be able to adapt to load variations. The algorithm's ability to keep up with these variations can be seen in Fig. 26. In this figure, the first half of the time shown is the same power as is shown in the second half of Fig. 24. During this period, the real power balancing algorithm has been applied. At halfway through the time shown, the load is instantaneously changed. At this point, the balancing algorithm keeps the PHEVs connected to the same phases as

before the load change for 10 seconds. This is the time between balancing calculations selected for this algorithm. Therefore, this represents the longest time between a system change and recalculation to assign a new phase configuration. After this point, the balancing algorithm runs again and the phase assignments of the PHEVs are switched in order to better balance the system. It should be noted that this figure is the results of two simulations plotted one after the other due to limitations on changing load values in SimPowerSystems during a simulation. However, the initial values for PHEV phase connections and powers in the second simulation are taken from the results of the first simulation.
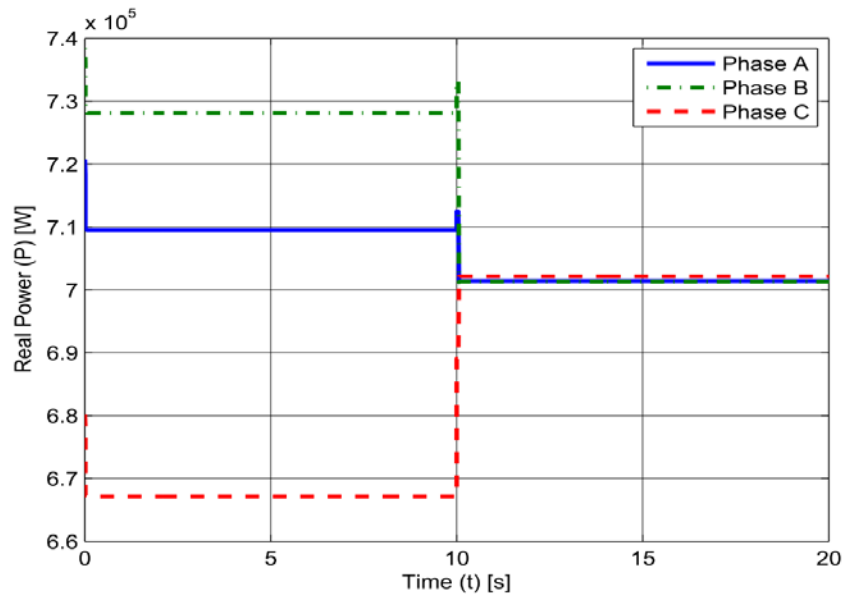

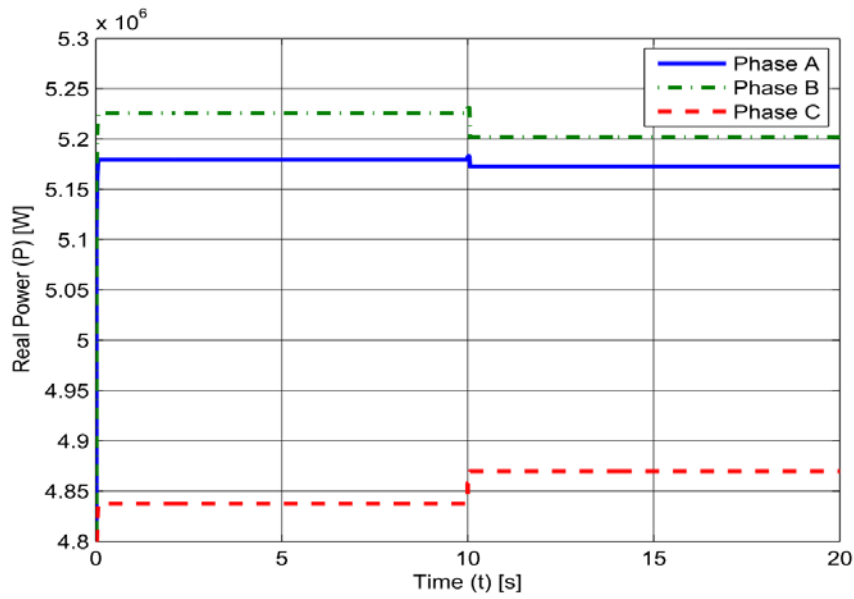Fig. 24. Results of Feeder Real Power Balancing Algorithm – Car Park Bus

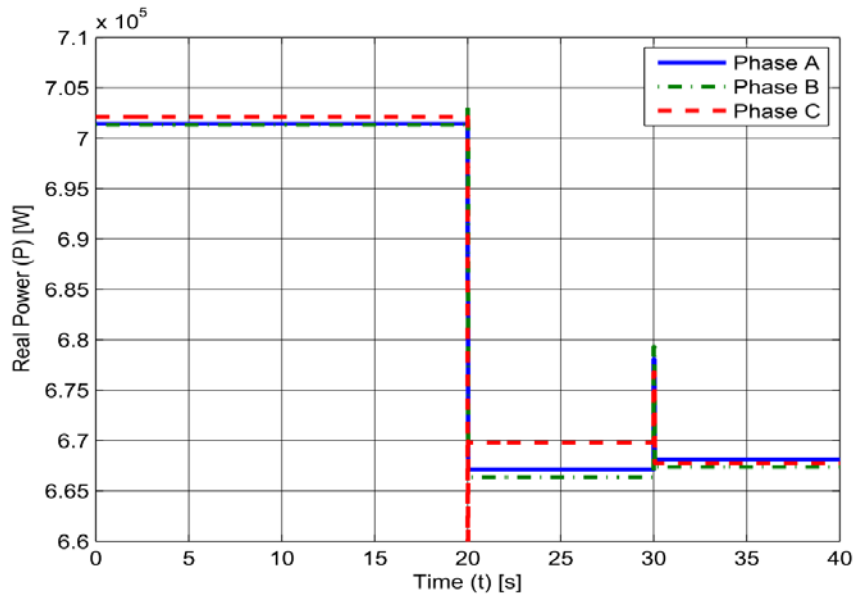Fig. 25. Results of Feeder Real Power Balancing Algorithm – Utility Feed

Fig. 26. Results of Feeder Real Power Balancing Algorithm Under Changing Load – Car

Park Bus

49

Balancing PHEV Car Park Real Power [19]

The goal of this section is to present the idea of moving PHEV chargers between phases automatically to balance a car park instead of a feeder and show the viability of using such a scheme in a realistic example of a car park. This algorithm works in much the same way as the algorithm for feeder balancing with a few differences. The algorithm works by first receiving data on how much power each PHEV charger is currently drawing or supplying. It then checks to see if a predefined time has passed since the last placement of vehicles. For this study, the time between assignments was again chosen as 10 seconds.

After this time delay has passed since the last calculation, the algorithm checks if any vehicles have been connected or disconnected or if any vehicle charging rates have changed since the last calculation. If none of these have happened, the calculation time is stored and the algorithm exits and waits for the time delay again before resuming. No PHEV chargers are moved between phases in this scenario. If at least one of these has happened however, the algorithm continues calculating a new assignment. The PHEV charger powers are first sorted into a list from largest to smallest by absolute value. Unlike the feeder balancing algorithm, the initial power on each phase is considered to be 0 W. The list is then stepped through one entry at a time, starting with the first PHEV charger in the list, which corresponds to the PHEV charger with the maximum absolute value of power. The PHEV charger is checked to see if it is drawing or supplying power. If it is drawing power, it will be assigned to the phase drawing the minimum power. If it is supplying power, it will be assigned to the phase drawing the maximum power. If it is

doing neither, it will be assigned to disconnect from all three phases. If two phases or more phases are drawing the same power, the priority of the equal phases, is phase A, phase B, and finally phase C. The new power on each phase is recalculated at each step using Eq. 4 based on the assignment, which is developed by replacing $P_{Estimate_{Phase}}$ with 0W in Eq. 3 because the only power flowing into the car park is for PHEV charging. The assignment continues until all PHEV chargers have been assigned a phase or commanded to disconnect. After all assignments are complete, the switching commands are sent and the PHEV chargers automatically switch to the assigned phase. A graphical representation of this algorithm can be found in Fig. 27.

$$P_{EstimateNew_{Phase}} = \sum_{x \in Phase} P_{PHEV}(x) \qquad (4)$$
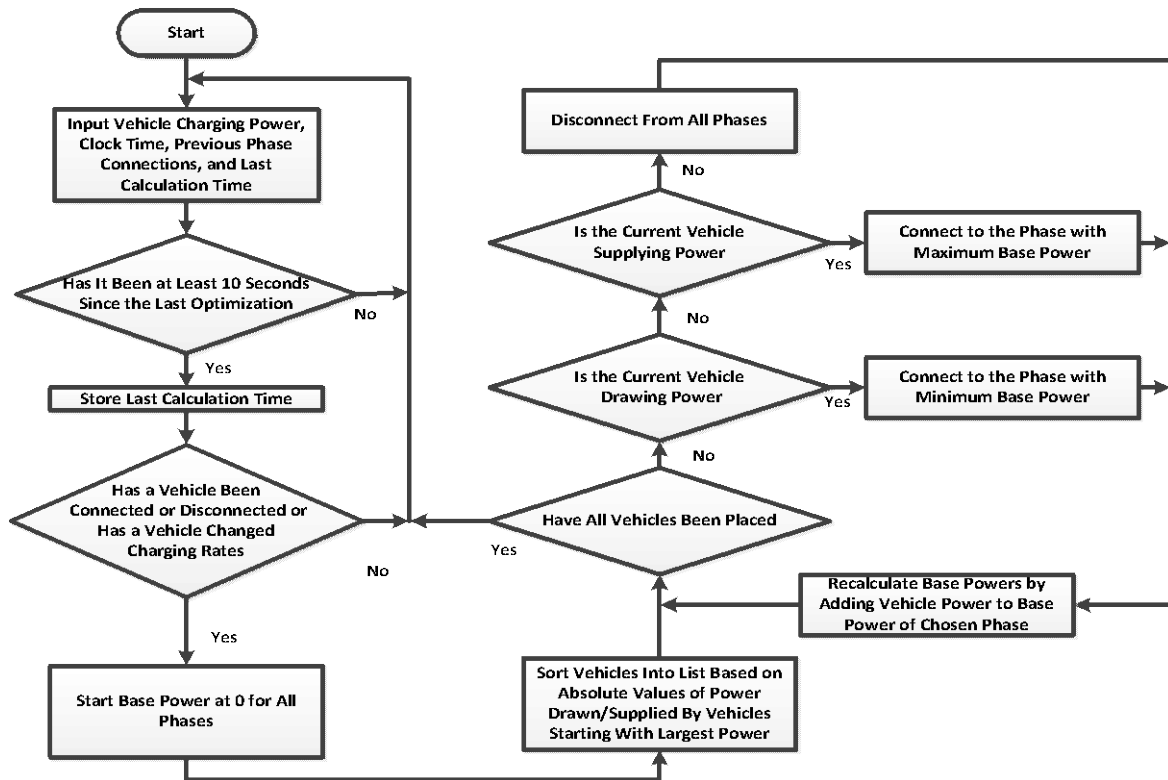
Fig. 27. Self-Balancing Car Park Algorithm

To test the sample algorithm, it is applied to a simulated car park containing 300 level 2 PHEV chargers and different scenarios are tested to show its operation and the feasibility of this idea. For the first half of all scenarios, balancing using PHEVs does not occur and represents a traditional car park with static phase connections. One third of all chargers are connected to each phase. Balancing is then allowed using PHEVs and the new powers drawn from each phase are shown. The first scenario represents the most extreme case possible. It is extremely unlikely to occur, however it is possible. In this case, a total of 100 PHEVs are each connected to a charger and all PHEVs are considered to have parked at a charger connected to phase A while drawing the maximum power of 7 kW. This makes the power drawn from phase A 700kW while the powers drawn from

52

phases B and C are 0W. Figure 28 shows that before PHEV balancing occurs, the power drawn by the car park is extremely unbalanced and will likely have negative effects on the distribution system supplying power to it. After PHEV balancing occurs however, the power drawn by the car park very close to balanced. This is because vehicles are switched from phase A to phases B and C. It should be noted that the power on phase A remains slightly higher than phases B and C because after all phases have an equal number of PHEV chargers assigned to them, there is still one remaining to be assigned and based on the priority described earlier, it is placed on phase A. Also, the power for phases B and C is the same so the lines overlap in this figure.
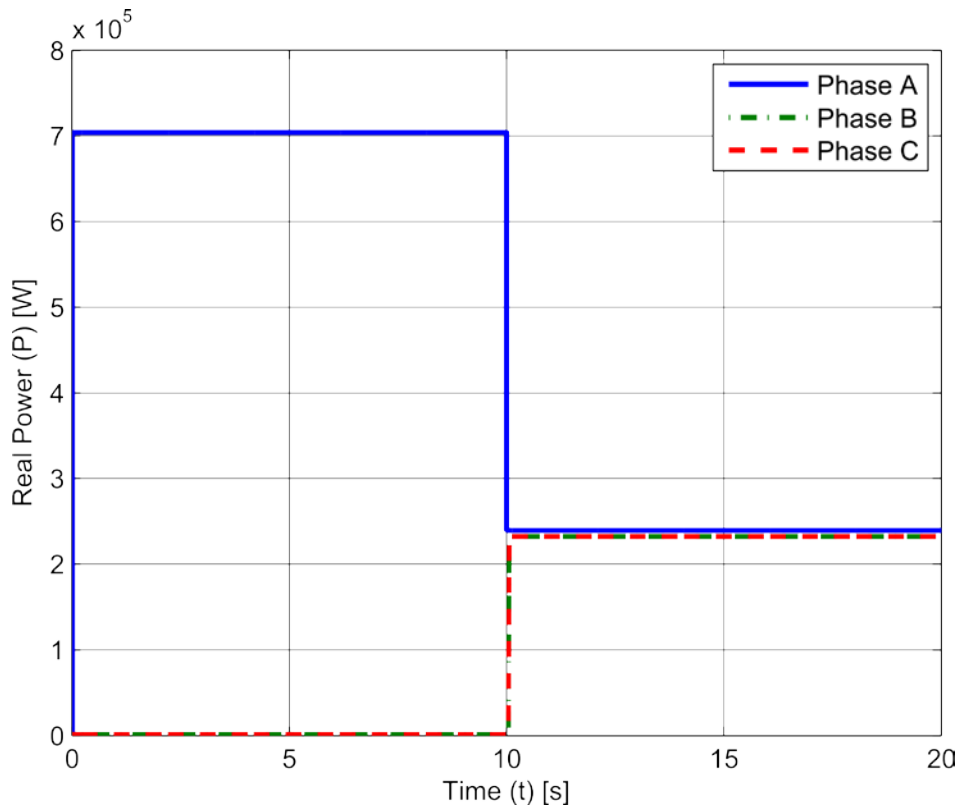
Fig. 28. Self-Balancing Car Park – Results from First Scenario

Another scenario is conducted in which all 300 PHEV charger powers are chosen using a pseudorandom function in MATLAB. In this case, the initial period before balancing begins shows the powers of the three phases are closer to balanced. However, unbalance still exists. After the initial 10 seconds of unbalance conditions, PHEVs are used for balancing and the power between phases becomes closely matched. Figure 29 shows the results. It should be noted that there is a transient seen during the switching, as would be expected based on the instantaneous changes of the simple switching devices and current sources used for testing the algorithm. However, because it is not of interest for showing the feasibility of this idea, the full magnitude is not shown.

Fig. 29. Self-Balancing Car Park – Results from Second Scenario

In order to be practical in a real world car park, the self-balancing car park must be able to keep up with reconfiguration of the PHEV load in the car park. As PHEVs are plugged in or unplugged from chargers, the power drawn from the chargers will change. When this happens, the PHEV chargers th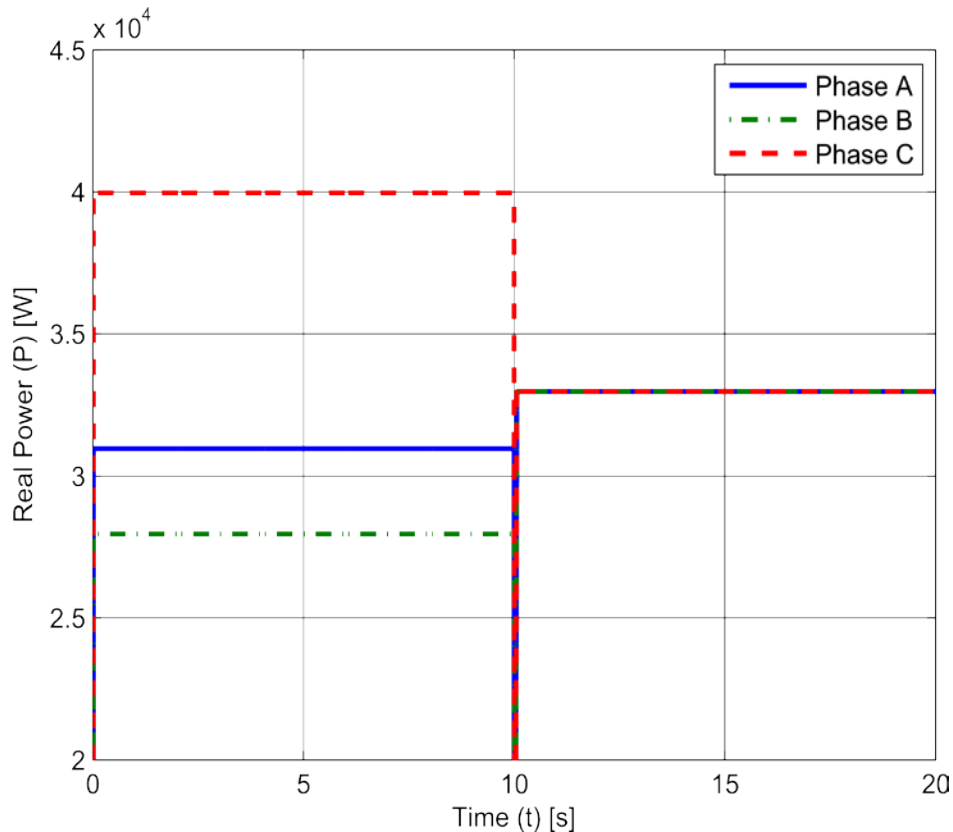at are drawing power must be reconfigured to rebalance the power drawn by the car park. A third scenario is conducted where PHEV charger powers are changed half way through the simulation. Figure 30 shows the results of a changing load. The first 20 seconds of Fig. 30 is the same as shown in Fig. 29. At 20.05 seconds, all PHEV charger powers are again assigned using a pseudorandom function in MATLAB. The phase each PHEV charger is connected to is not changed until 30 seconds, however, due to the 10 second delay between assignments. During this short period, new PHEVs that are connected to the system will not begin to charge because the charger was previously disconnected from all phases. At 30 seconds, the balancing algorithm runs again and the assignments are updated. The powers of the three phases again approach balanced conditions.
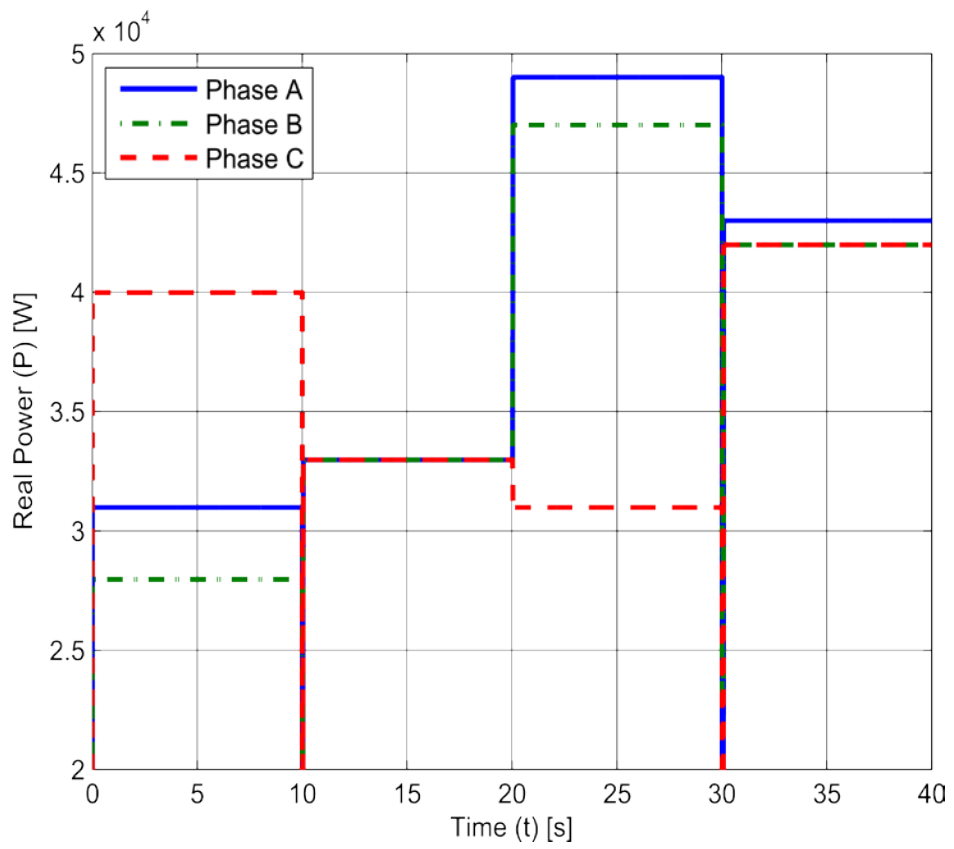
Fig. 30. Self-Balancing Car Park – Results from Third Scenario

CHAPTER FIVE

DECENTRALIZED VEHICLE TO CAMPUS

Vehicle to Building [45]

One method of implementing a V2G scheme involves using time-of-use (TOU) rates. TOU rates charge more for energy used during peak usage periods than for energy used during off peak usage periods [46]. Using TOU rates in a V2G scheme, a PHEV owner would charge the vehicle battery during off peak pricing periods and discharge the battery back to the electric grid during peak pricing periods.

V2G schemes typically require a communication network to be installed to allow utilities to communicate with PHEV chargers. Also, adding PHEVs utilizing V2G to a radial distribution system that typically sees only unidirectional power flows may create bidirectional power flows on the system. Both the additional communication network and bidirectional power flows lead to a high cost associated with V2G [47]. Furthermore, PHEVs are only capable of supplying a small amount of power in comparison to the overall system load of a large utility. Due to these factors, using PHEVs for peak shaving through V2G will likely face many challenges. Some existing studies attempt to conduct an economic analysis of V2G, however they either do not consider actual vehicle driving cycle data, fail to include the costs of negative impacts on the battery, or are conducted on large scale systems where the implementation of V2G is expected to be slow to gain traction [47]-[49]. Also, studies fail to show the breakeven point for PHEV owners in terms of TOU rates.

This research aims to implement V2G on a university campus system or other large commercial building. This type of system will alleviate some of these concerns while still allowing the potential for both the consumer and utility to benefit. In the system being studied, which is the Clemson University distribution system, the campus is seen as a large net consumer by the electric utility, similar to a large commercial building. Therefore, a large number of vehicles can be connected before all of the campus loads would be supplied by sources other than the electric utility. This would eliminate the issue of two way power flows on the electric utility system caused by the campus or other large commercial building supplying power back to the electric utility. Also, by using TOU rates, a decentralized method of control is used to command vehicle charging and discharging in order to greatly reduce or eliminate the need for communication. The electric utility also benefits through a reduction of load power drawn by the university campus during peak energy usage times.

PHEV Spatial and Distributions [45]

In order to complete an accurate economic analysis of V2C, the locations of PHEVs during different times of the day are needed. Both temporal and spatial distributions of PHEVs must be determined. The spatial distribution is used to determine how far a PHEV has traveled when it arrives on campus from home and how far it must travel to return home. The temporal distribution is used to determine what time PHEVs arrive on campus and what time they leave to return home. In order to develop distributions, data from the 2009 National Household Travel Survey is used along with the distribution fitting command in MATLAB [50]. For the spatial distribution, the

responses to how far a worker's job is from home are used. These responses correspond to the variable DISTTOWK in [50]. Based on the responses, an exponential distribution with the probability density function shown in Fig. 31 is chosen for the distance driven between work and home. It can be seen that a large number of drivers live very close to work, with the number of drivers decreasing exponentially as distance increased. The average distance driven between work and home is determined to be 14.1 miles.
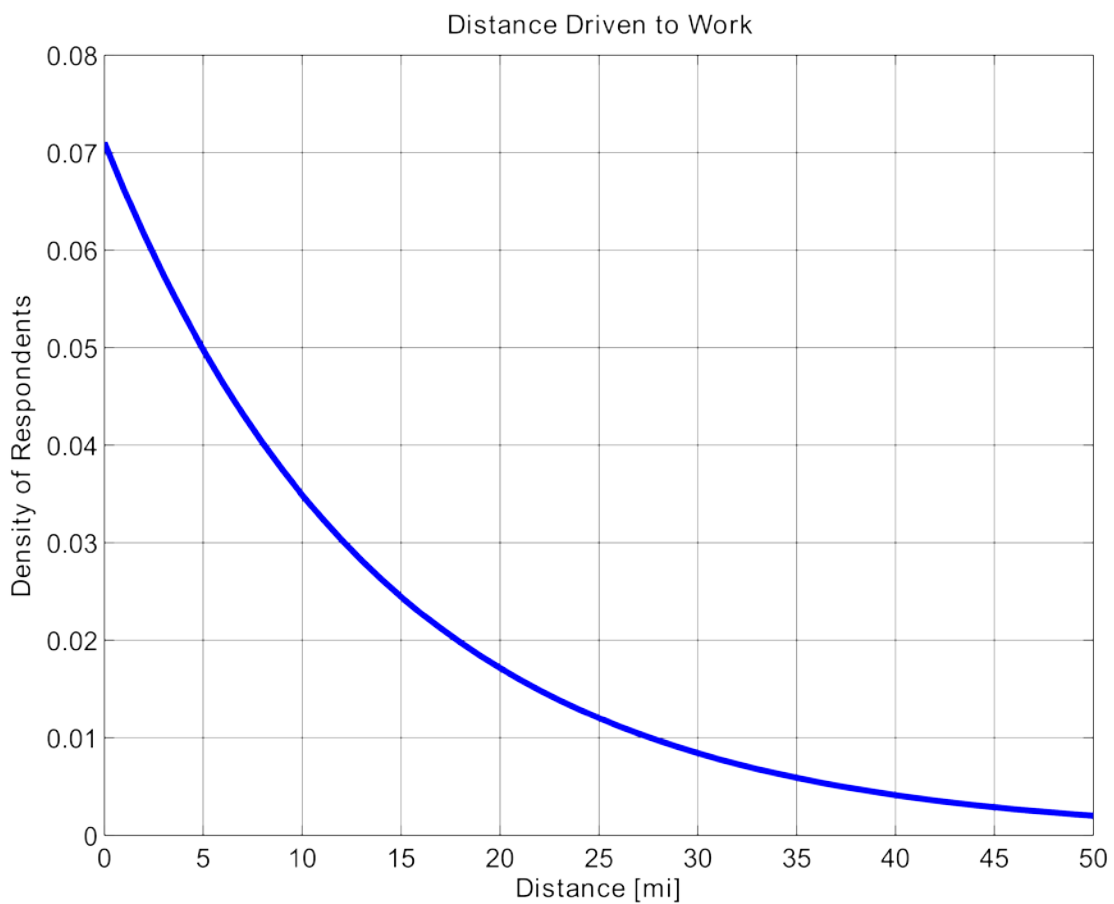

Fig. 31. PHEV Spatial Probability Density Function

The times PHEVs arrive on campus as well as when they leave must also be approximated. For the temporal distribution of when vehicles arrive on campus, the responses to the end time of all trips with the destination of work are used. For the temporal distribution of when vehicles leave campus to return home, the responses corresponding to the start time of all trips with the destination of home are used. These responses correspond to the variables ENDTIME, STRTTIME, and WHYTO for the arrival time, leaving time, and purpose of the trip, respectively. Based on the responses, normal distributions with the probability density functions shown in Fig. 32 are chosen for the arrival and departure times. The average arrival time of PHEVs on campus is determined to be 9:07 am and the average departure time of PHEVs from campus is determined to be 3:23 pm.
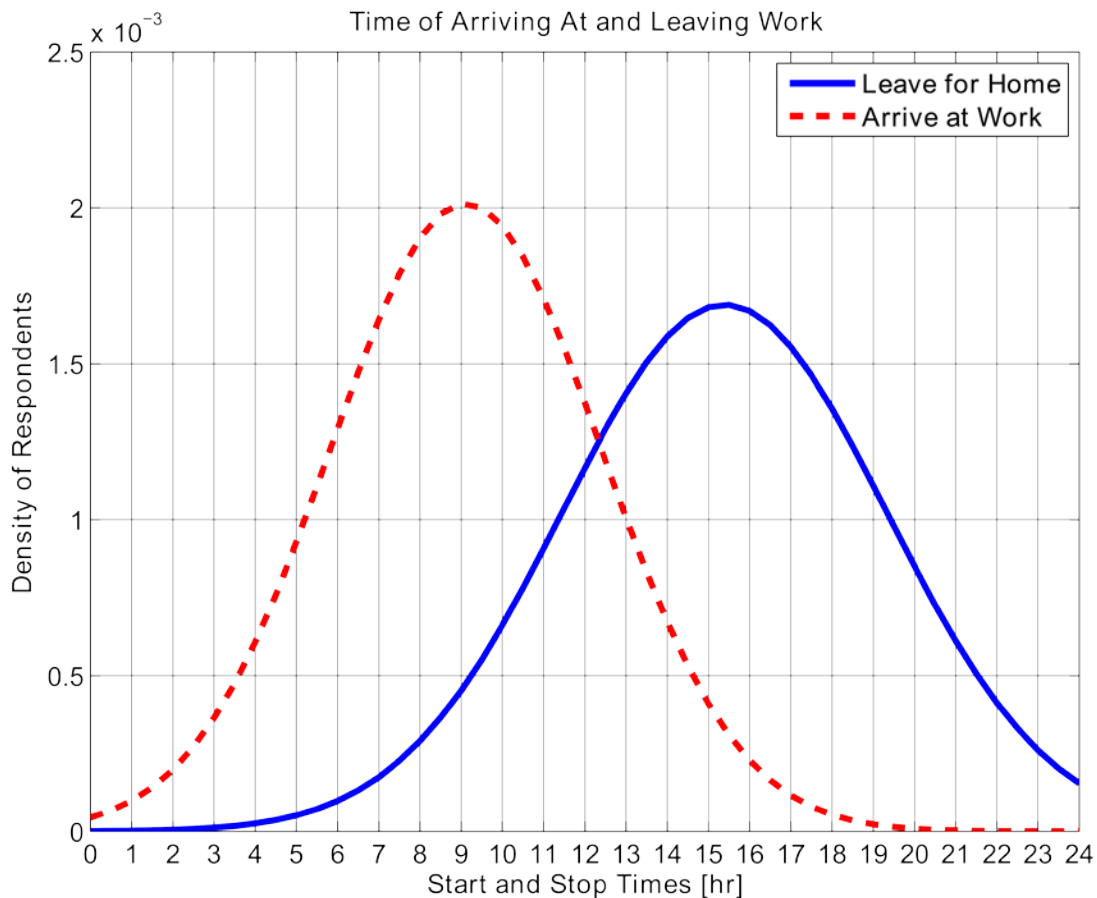
Fig. 32. Temporal Probability Density Function

Vehicle to Campus Algorithm [45]

In order to implement V2C, a decentralized algorithm is implemented. The algorithm requires the PHEV owner to estimate how far the vehicle will be driven after departure from campus and also input the time the PHEV will depart. The goal of the algorithm is to utilize V2C to supply as much energy as possible during the peak pricing period while also maintaining enough charge upon departure that the distance input by the PHEV owner can be traveled solely on electric power. The necessary SOC is calculated using the estimated distance input by the user as well as figures of 98 MPGe

and 16.5 kWh battery capacity based on [51]. Any charging necessary is performed during off peak pricing if possible. The only time on peak charging occurs is the case where a vehicle is not connected long enough during off peak times to reach the necessary SOC required by the PHEV owner.

The algorithm attempts to charge the PHEV as much as possible before the on peak period, limited by a maximum charging rate of 7 kW, which is chosen based on a level 2 charger [29]. The algorithm also attempts to discharge the PHEV as much as possible during on peak periods, limited by maintaining enough energy in the battery at the time of departure and a maximum discharging rate of 7 kW. If the PHEV remains connected after the peak period ends, off peak charging is also allowed during this time. An SOC operating range of 10-89.2% is chosen based on 98 MPGe, 38 mile all electric range, and 16.5 kWh battery capacity [51]. An efficiency of 90% is assumed for both charging and discharging operations [49]. Charging and discharging rates are reduced from 7 kW wherever possible such that the rate is the lowest that will allow completion of the energy transfer in the allotted time.

This is accomplished by first calculating how long the vehicle will be connected to the grid before, during, and after peak rates are in effect. Based on the maximum charge and discharge rates, as well as these calculated times, the theoretical maximum energy transfers that could occur to and from the battery, assuming the battery can supply an unlimited amount of energy are calculated. An example of this is shown in Fig. 33. The SOC point which will occur either at the end of peak rates or disconnection from the grid, whichever is first, is then found using the constraints of being able to meet the final

required SOC upon disconnection based on any available charging after peak rates end. The SOC at the beginning of peak rates is found using the constraints of the maximum energy that can be transferred to the battery above its initial SOC upon arriving to campus. An example of this is shown in Fig. 34. These points are then further constrained based on the minimum and maximum allowable range of the battery SOC, as shown in the blue profile found in Fig. 35. The SOC at the end of peak rates or disconnection from the charger, whichever is first, is then increased as necessary to ensure the maximum allowable discharge rate is not exceeded during peak rates and no more charging occurs than is necessary. Using these four points, the charging and discharging rates are then calculated such that they are the minimum possible that will still reach the desired SOC at a certain time, including losses due to inefficiencies, as shown in figure 35.
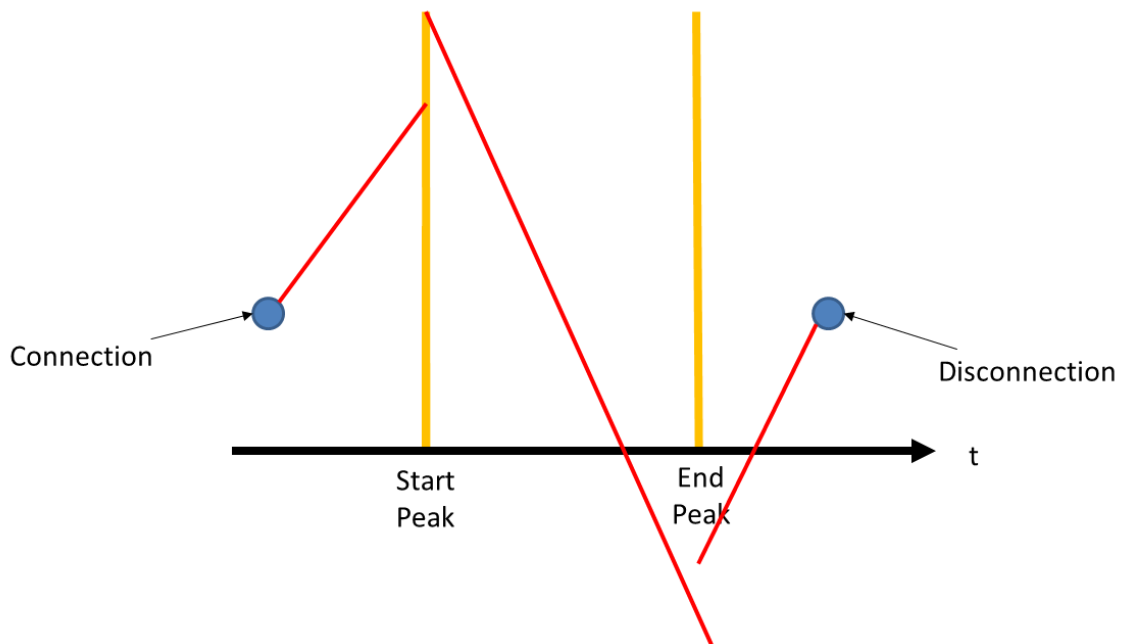

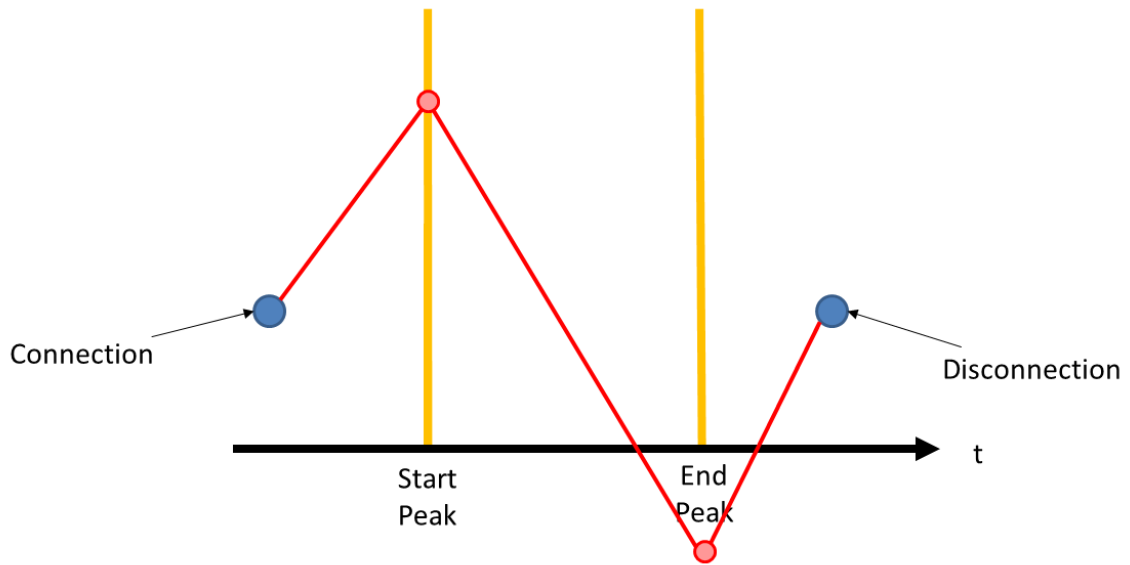Fig. 33. Maximum Energy Transfers during V2C

Fig. 34. Maximum Energy Transfers during V2C Constrained by Connection and Disconnection Times
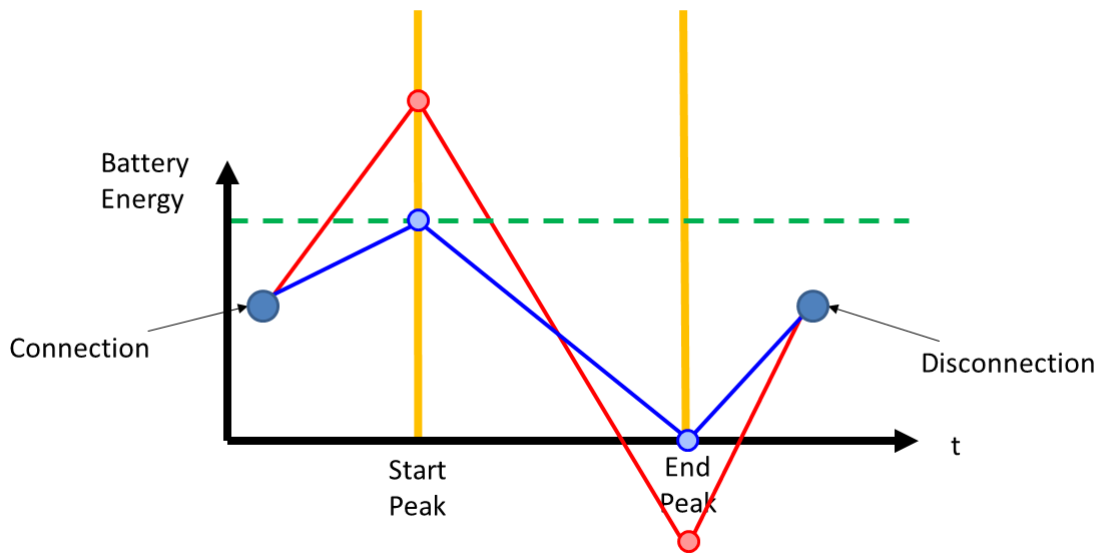

Fig. 35. Maximum Energy Transfers during V2C Constrained by Battery Operating Parameters

<u>Comprehensive Cost Analysis [45]</u>

For this economic analysis, it is assumed that the PHEV is driven the average of 14.1 miles to campus and arrives at the mean arrival time of 9:07 am. It is also assumed that the vehicle will be driven the average of 14.1 miles from campus to home upon leaving at the mean departure time of 3:23 pm. Using [52]-[58], on peak pricing is chosen to start at 2:00 pm and to end at 8:00 pm. Based on these parameters, the SOC profile of the PHEV battery while the vehicle is parked on campus is shown in Fig. 36. In the figure, the solid blue line represents the energy stored in the PHEV battery over time, starting at the arrival time and ending at the departure time. The vertical dashed red lines show the beginning and end of the on peak pricing period.

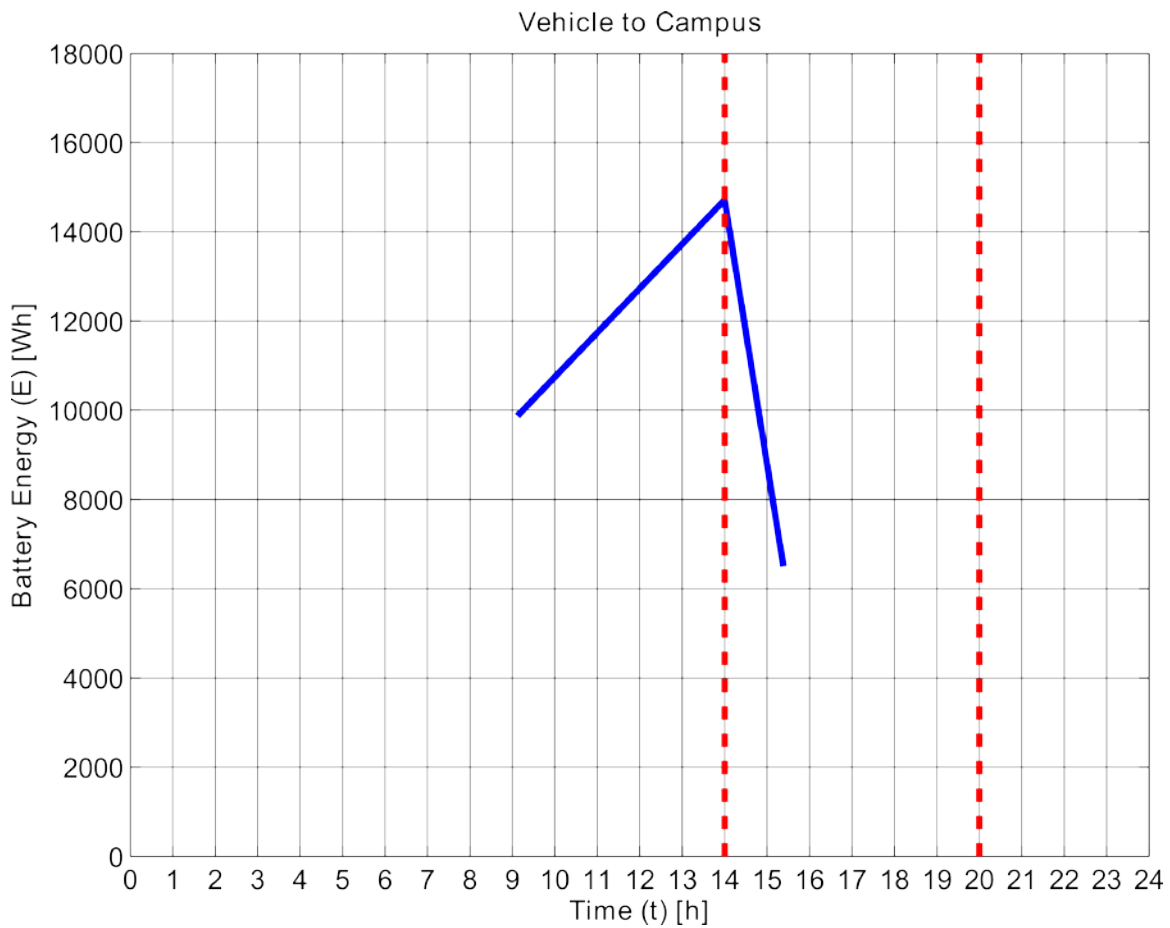Fig. 36. Energy Profile of the PHEV Battery during a Day While Parked on Campus

In order to fully examine the economic analysis of a V2C scheme, a comparison with a stationary battery that has the same capacity as the PHEV battery is conducted. The same SOC operating range and efficiency for the PHEV battery are also assumed for the stationary battery. Fig. 37 shows the energy stored in the stationary battery throughout the day.
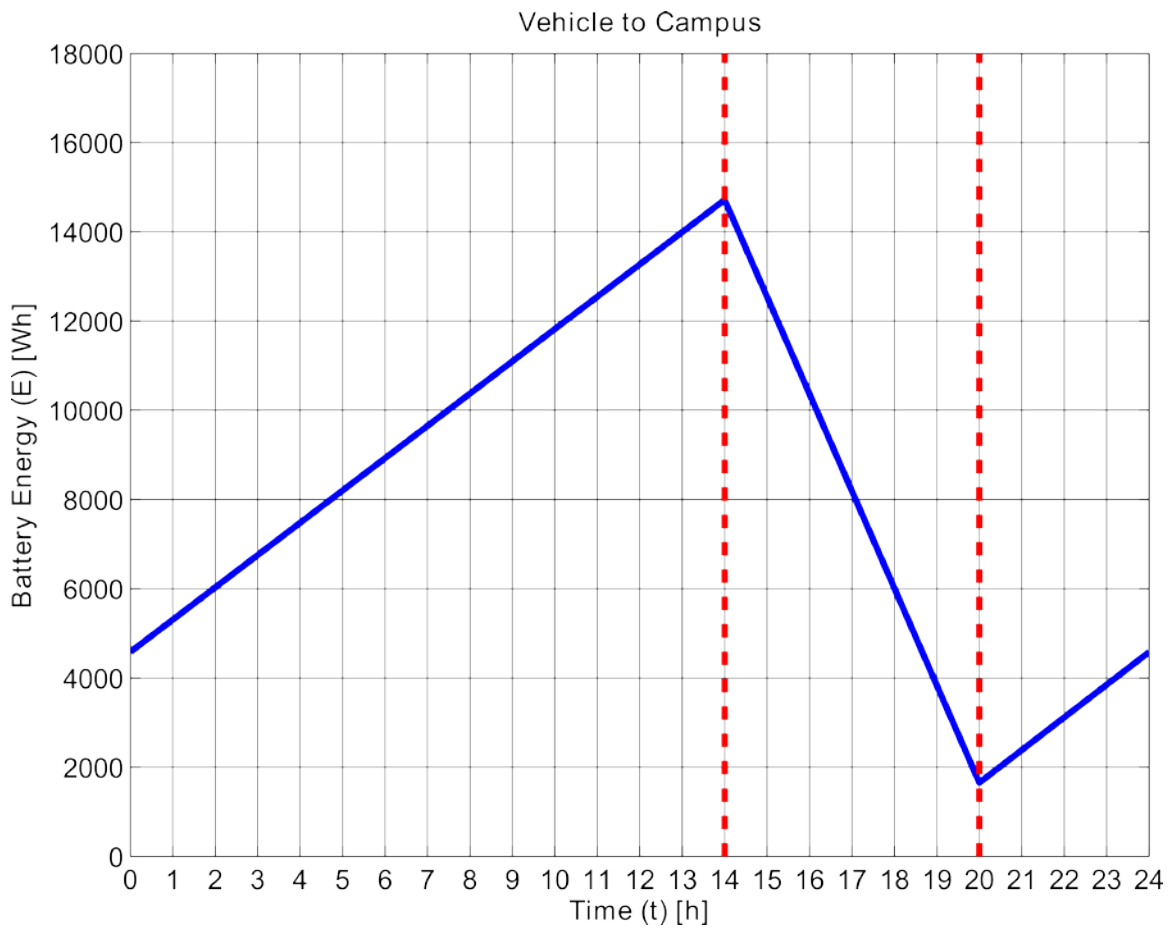
Fig. 37. Energy Profile of the Station Battery during a Day

To produce a meaningful comparison for V2C operation, a baseline cost for operating a PHEV without V2C must be considered. For the baseline, the cost of charging the PHEV only during off peak is considered. Also, only the energy necessary to drive to work and make the return trip home is necessary to consider as no other energy is depleted from the PHEV battery. Charging efficiency is also included in the calculation. The baseline cost is calculated using Eq. 5. For operation without V2C, there is no accelerated degradation of the battery, so no additional cost to compensate for that is necessary.

$$Cost_{BL} = (E_W + E_H) * Rate_{Off} \tag{5}$$

Whenever V2C is employed, an accelerated degradation of the PHEV battery occurs compared to without V2C due to the increased cycling of the battery. After repeated cycling, a battery loses some of its usable storage capacity. For this study, a cycle life of 2500 cycles was chosen based on [49], [51]. This must be accounted for in order to give PHEV owners an accurate estimate of whether or not it is economical to participate in V2C. This cost is accounted for using Eq. 6. This compensates the PHEV owner for a partial cycling of the battery based on how much energy is discharged from the battery for V2C operations [49].

$$Cost_C = \frac{Cost_B}{Cyc_R} * \frac{E_D}{E_B} \tag{6}$$

It is stated in [59] that the goal for battery price in PHEVs varies from \$150-\$500 per kWh. For this study, three different battery costs are studied including the two extremes and one halfway between these estimates. These costs include \$150 per kWh, which corresponds to a battery cost of \$2475, \$325 per kWh, which corresponds to a battery cost of \$5362.50, and \$500 per kWh, which corresponds to a battery cost of \$8250.

The total cost of energy exchange during V2C is given in Eq. 7. The total savings that are seen from using V2C are calculated using Eq. 8.

$$Cost_E = E_C * Rate_{Off} - E_D * Rate_{On} \tag{7}$$

$$Sav_{V2C} = Cost_{BL} - (Cost_C + Cost_E) \tag{8}$$

The results are shown in Figs. 38 – 43 for the three battery costs. The axes show the off peak price, the price difference between peak and off peak prices, and the total savings. In Figs. 38, 40, and 42 any points above the black surface represent an economic benefit from utilizing V2B while those below it represent a loss of money through utilizing V2C. Figures. 39, 41, and 43 give an overhead view of these surfaces, where the magenta line represents the intersection with the black surface. All points above the line represent an economic benefit from utilizing V2C while those below it represent a loss of money through utilizing V2C.
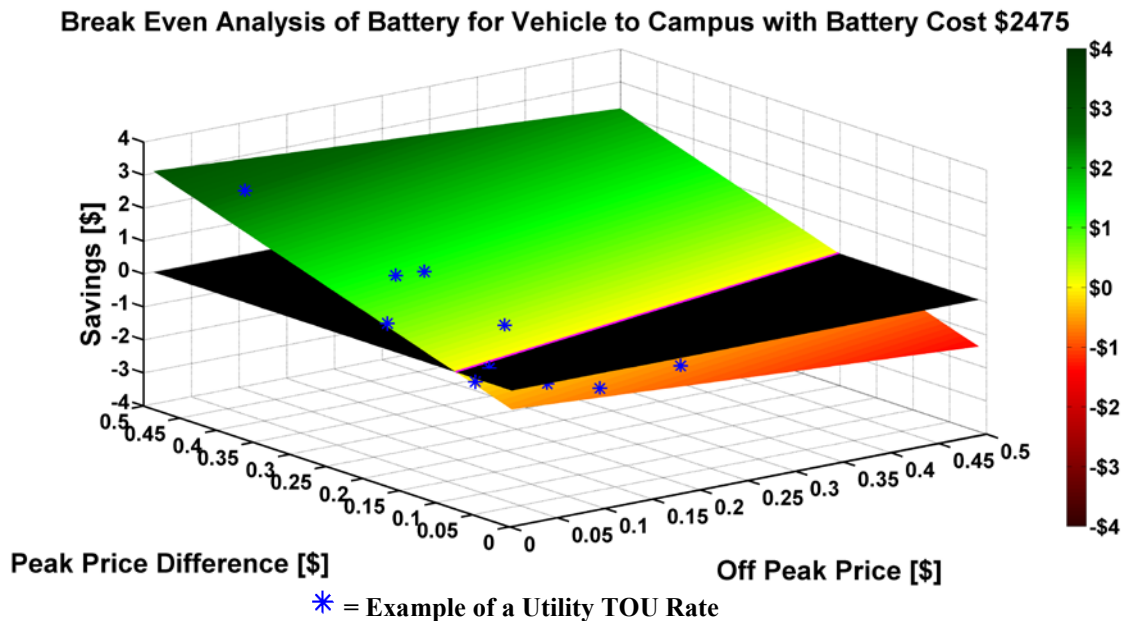

= Example of a Utility TOU Rate

Fig. 38. Break Even Analysis of Vehicle to Campus Using the Average Cycle – Battery

Cost $2475

Fig. 39. Break Even Analysis of Vehicle to Campus Using the Average Cycle – Battery

Cost $2475 – Overhead View

Fig. 40. Break Even Analysis of Vehicle to Campus Using the Average Cycle – Battery

Cost $5362.5

Fig. 41. Break Even Analysis of Vehicle to Campus Using the Average Cycle – Battery
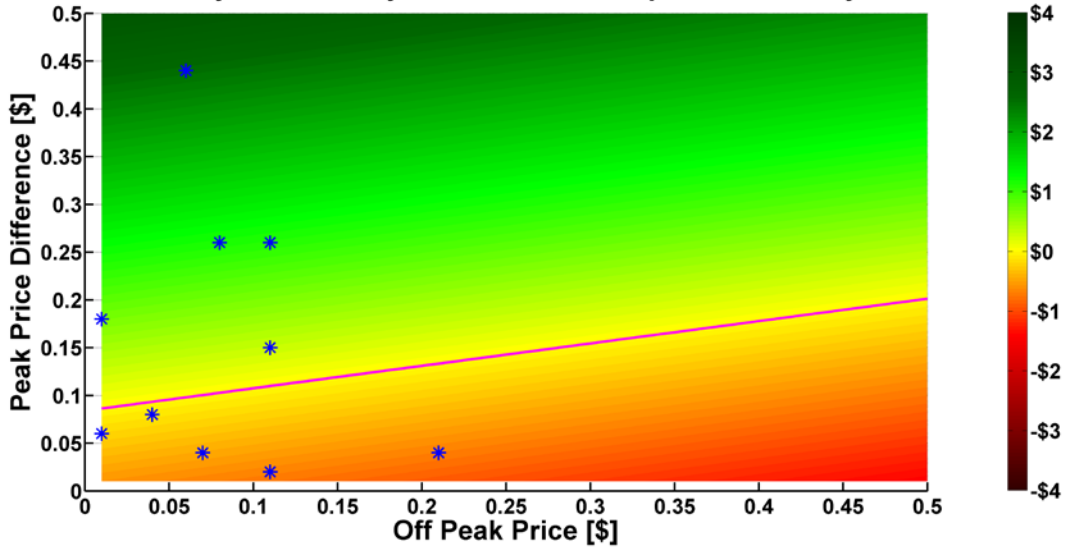
Cost $5362.5 – Overhead View

Fig. 42. Break Even Analysis of Vehicle to Campus Using the Average Cycle – Battery

Cost $8250

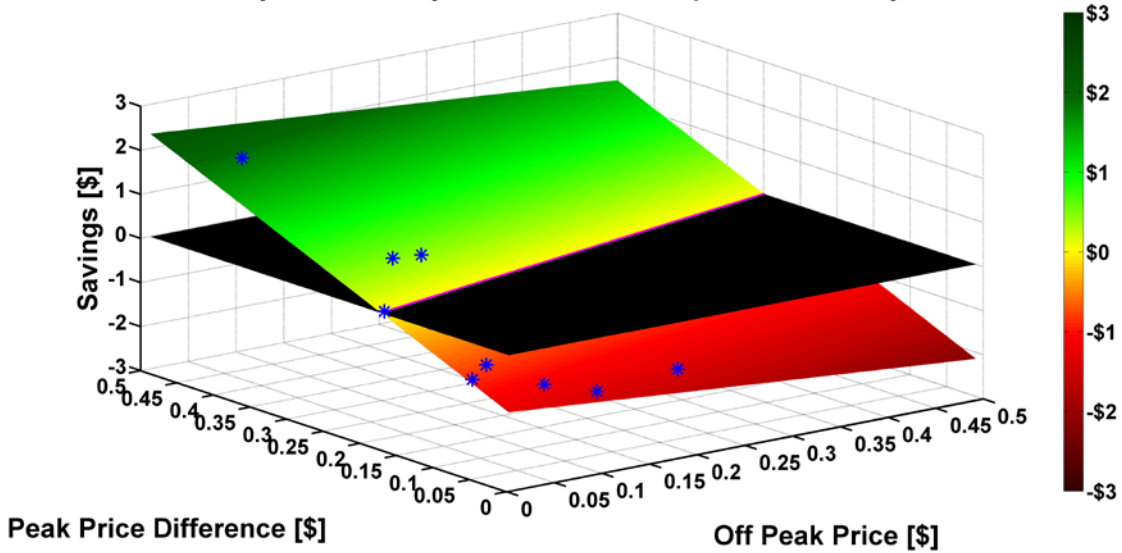**Break Even Analysis of Battery for Vehicle to Campus with Battery Cost $8250**
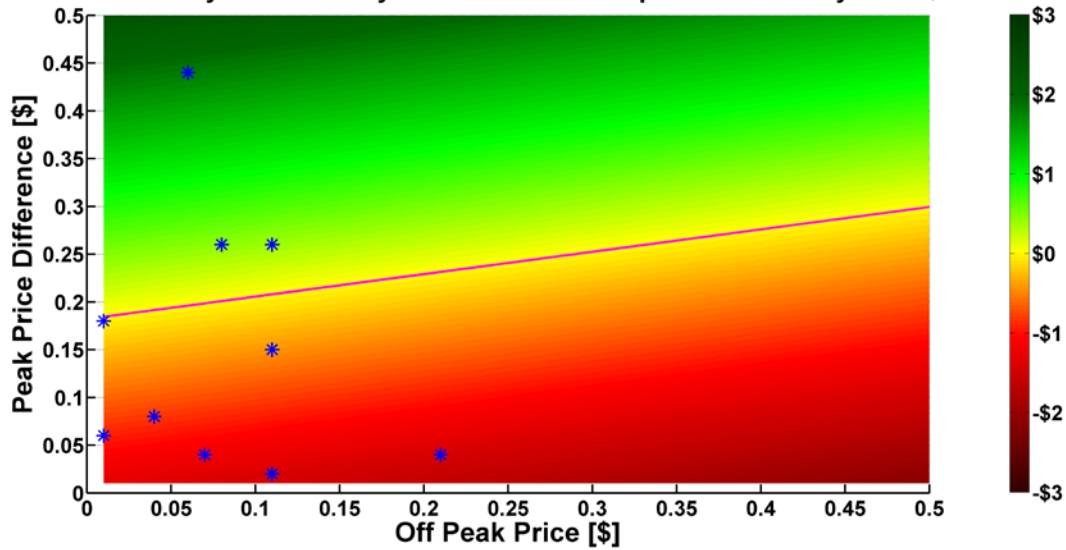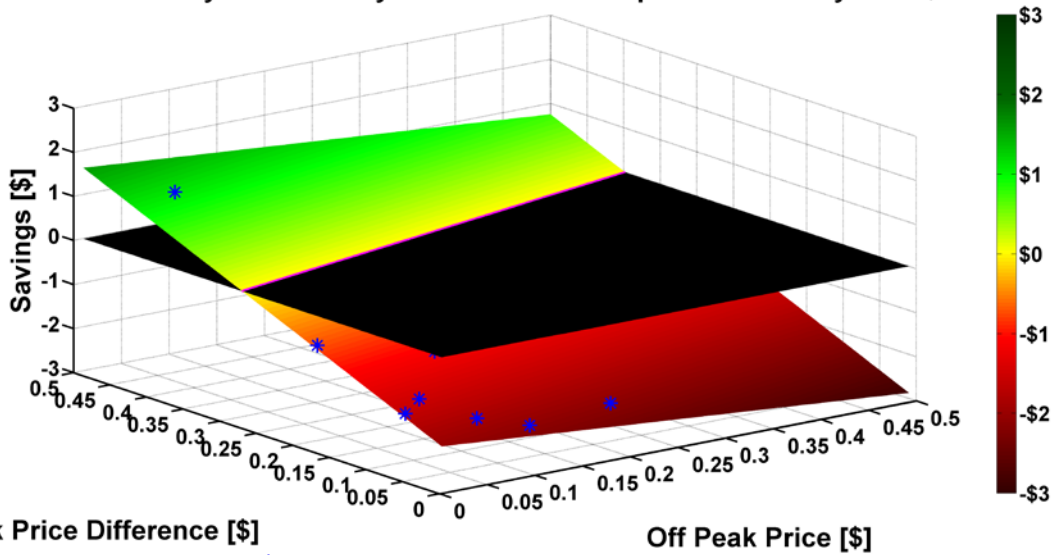
✳ = Example of a Utility TOU Rate
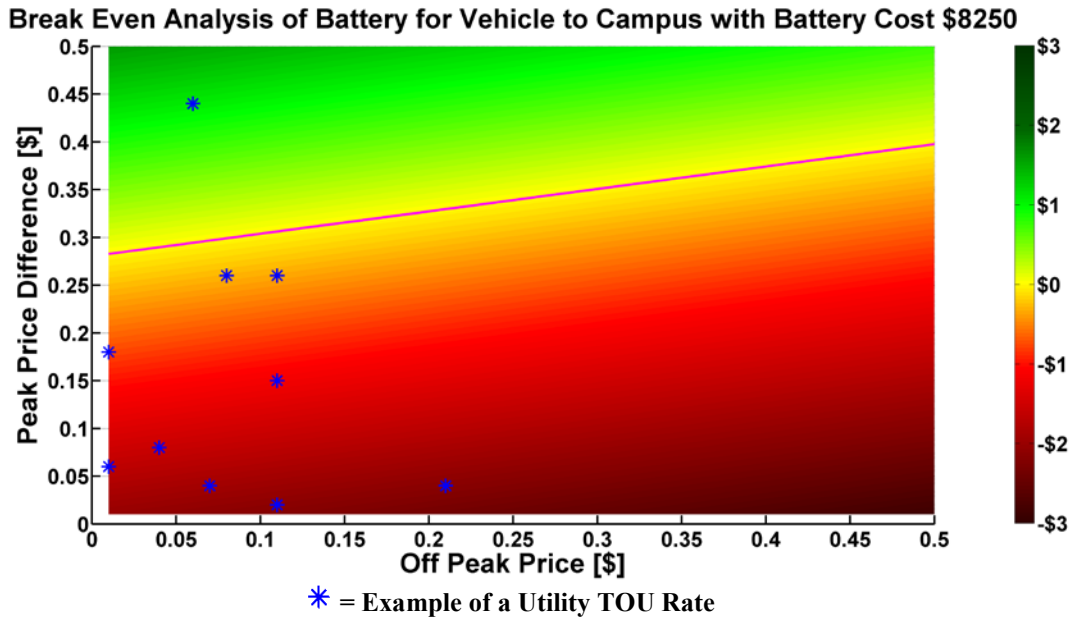
Fig. 43. Break Even Analysis of Vehicle to Campus Using the Average Cycle – Battery

Cost $8250 – Overhead View

It can be seen that as battery costs increase, the difference between peak and off peak price must increase in order to realize an economic benefit from V2C. In all cases however, an economic benefit is possible if the difference between peak price and off peak price is large enough. It can also be seen that at high off peak prices, the difference between peak and off peak prices must be larger than at low off peak prices in order to see an economic benefit. This is due to the charging and discharging efficiencies, both of which are below 100%. A PHEV owner may have to pay for energy losses, in which case this must be included in the analysis for accuracy. At high off peak prices, the cost of energy losses is higher than during low off peak prices. The blue asterisks on the graphs represent TOU rates offered by several different utilities [52]-[58]. Based on these rates, it is concluded that for the various battery costs, savings can be realized using some current utilities' TOU rates.

A similar economic analysis is conducted for a stationary battery. For a stationary battery with the SOC profile shown in Fig. 37, the cycle compensation is again given by Eq. 6. In this case however, E_D represents the full usable battery capacity, E_B. For the stationary battery, the savings are calculated using Eq. 9.

$$Sav_{SB} = -(Cost_C + Cost_E) \tag{9}$$

The results of the economic analysis for the stationary battery can be found in Figs. 44 – 49. Again, all points above the black surface or magenta line represent an economic benefit from utilizing stationary storage while those below represent a loss of money. It can be seen that the break even line for the PHEV battery and stationary battery is the same. This is due to using the same battery parameters for both comparisons. However, the amount of savings is different between the two analyses. This is due to the different charging and discharging profiles of the PHEV and stationary batteries.

Break Even Analysis of Stationary Battery to Campus with Battery Cost $2475

$*$ = Example of a Utility TOU Rate

Fig. 44. Break Even Analysis of Stationary Battery to Campus – Battery Cost $2475

Break Even Analysis of Stationary Battery to Campus with Battery Cost $2475

$*$ = Example of a Utility TOU Rate

Fig. 45. Break Even Analysis of Stationary Battery to Campus – Battery Cost $2475 –

Overhead View

Fig. 46. Break Even Analysis of Stationary Battery to Campus – Battery Cost $5362.5

Fig. 47. Break Even Analysis of Stationary Battery to Campus – Battery Cost $5362.5 –
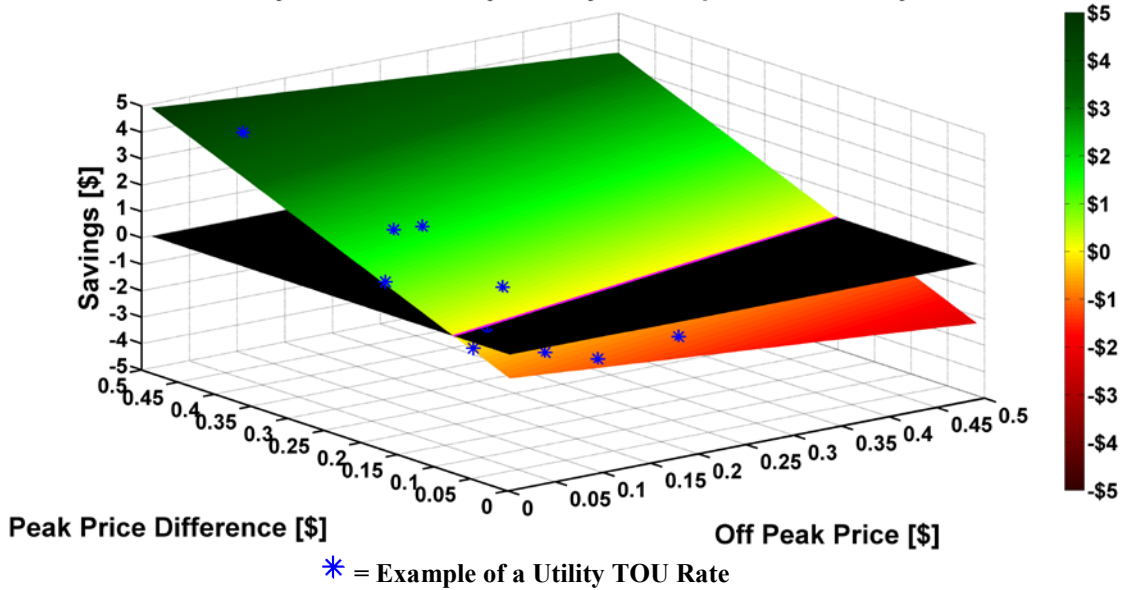
Overhead View

Fig. 48. Break Even Analysis of Stationary Battery to Campus – Battery Cost $8250

Fig. 49. Break Even Analysis of Stationary Battery to Campus – Battery Cost $8250 –
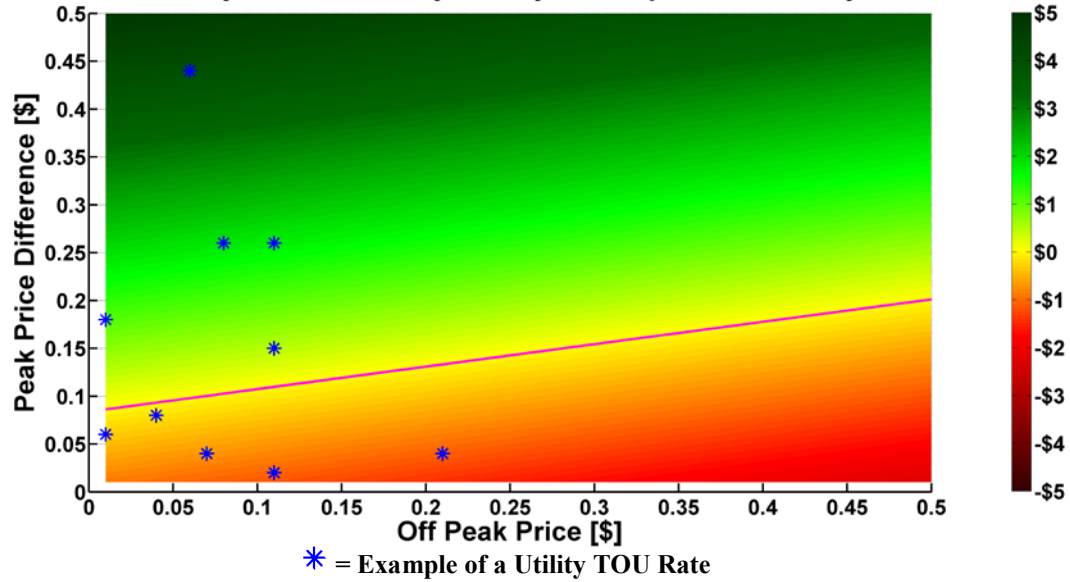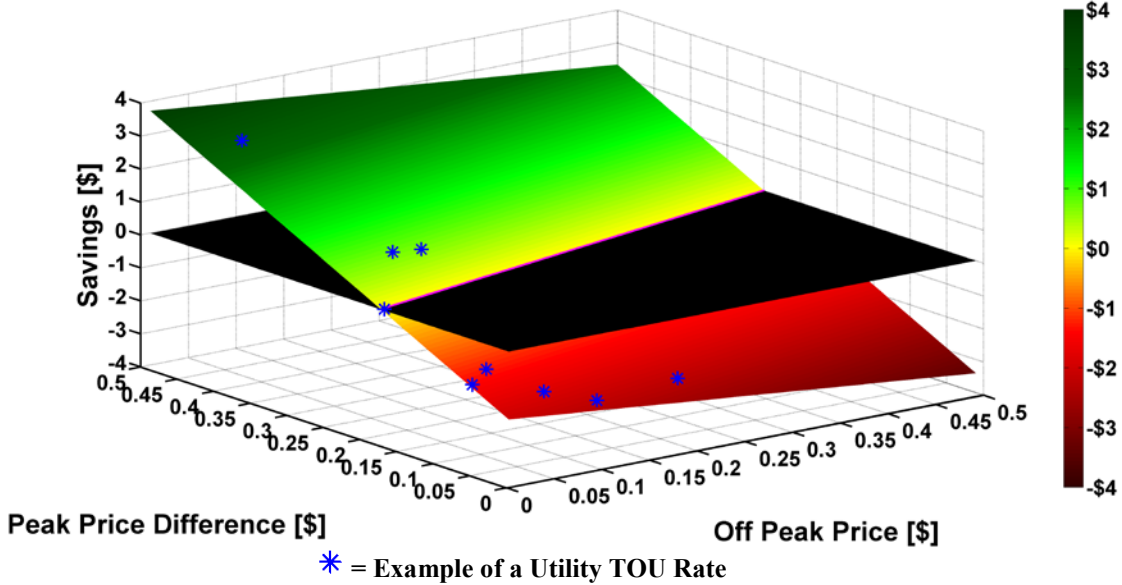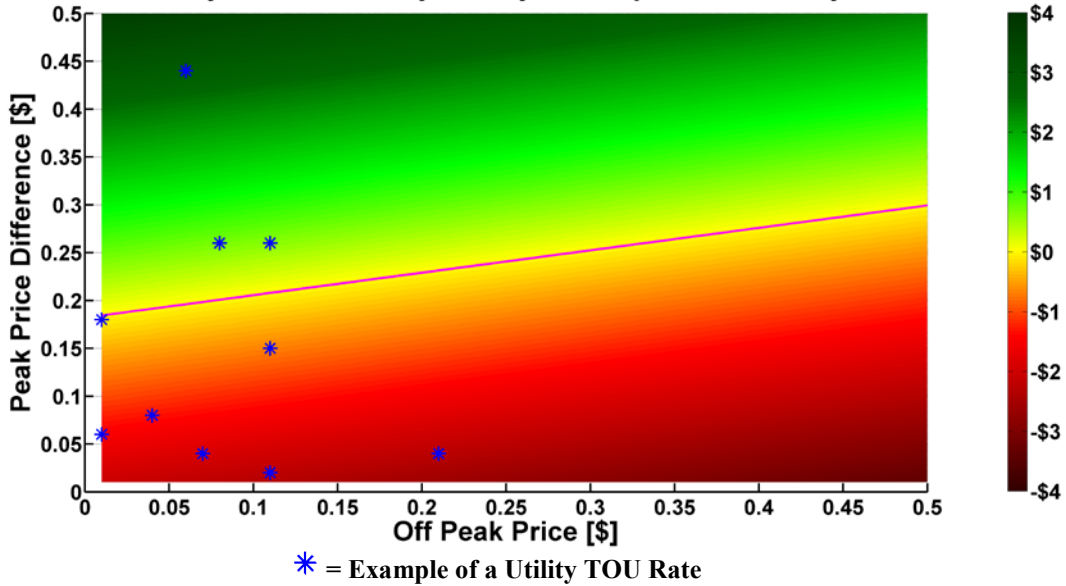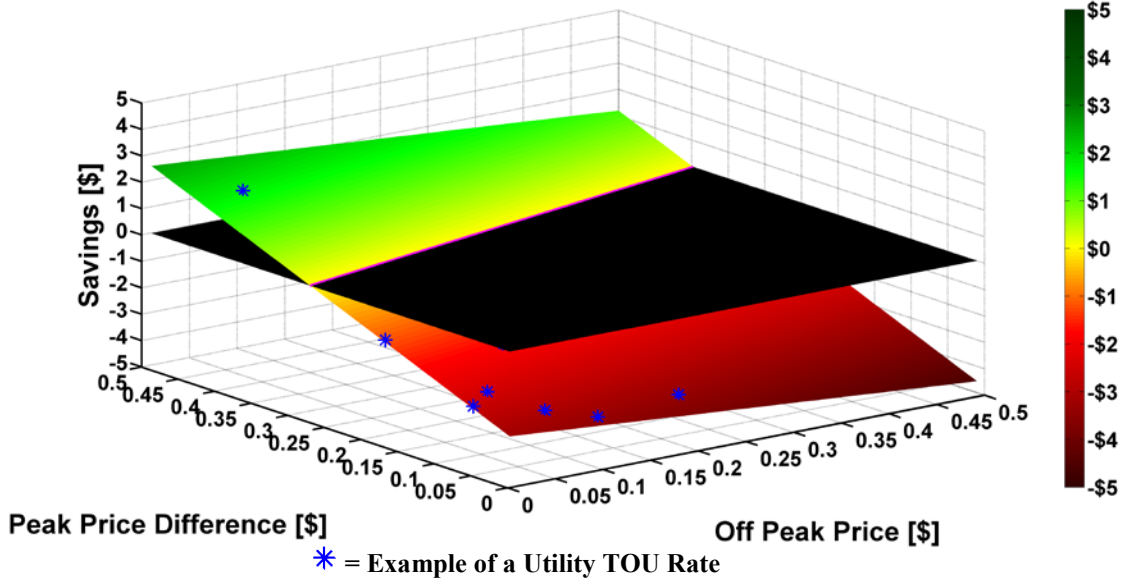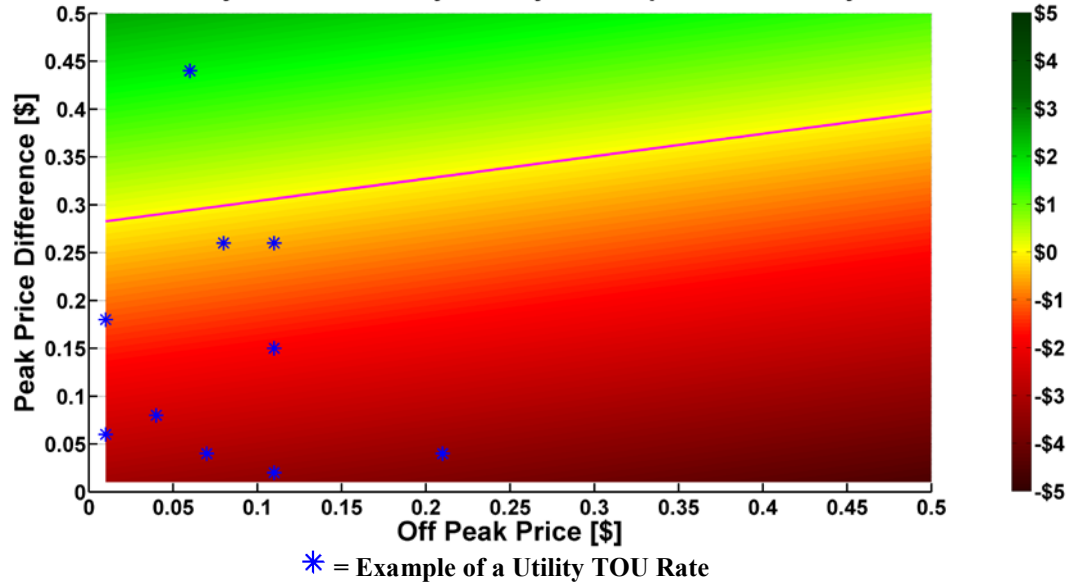
Overhead View

It is shown that V2B and stationary storage can both be cost effective on a

university campus. The cost effectiveness and the amount of savings are dependent on

the battery cost and electricity pricing during both on and off peak times. Under the V2C scenario, the PHEV owner is left with enough energy to travel a desired distance solely under electric power while still participating in V2C. While a stationary battery has the potential to save more than a PHEV battery, the break even point between the two is the same. Thus, utilizing V2C will allow a university campus to achieve similar benefits without the initial high cost and space requirements of a stationary battery.

Peak Shaving Impacts [45]

Based on the ability of V2C to prove profitable, it has been shown that V2C has the potential to benefit consumers without impacting required driving behavior. This section focuses on showing the benefit of V2C to the electric utility feeding campus. The V2C algorithm previously described works by charging PHEVs during off peak rate times and discharging them during peak rate times. The peak rate times correspond to the peak load values seen from campus loads. Figures 50, 51, and 52 show the campus load profile on the 12.47kV circuit for a spring, summer, and winter day based on a base case simulation, respectively. These load profiles do not include V2C or stationary battery energy storage. It can be seen that the peak load for the spring day occurs between 2 and 3 pm. For the summer day, the peak load also occurs between 2 and 3 pm. The winter day's peak occurs between 12 and 1 pm. It can also be seen that the highest peak load occurs during the spring season.

Fig. 50. Clemson University 12.47kV System Load – Spring – Base Case

Fig. 51. Clemson University 12.47kV System Load – Summer – Base Case

Fig. 52. Clemson University 12.47kV System Load – Winter – Base Case

In order to examine the impacts of adding PHEVs to the campus system while utilizing V2C, a total of 300 PHEVs are added in a total of 8 car parks around campus. The car parks are located based on currently available parking lots on campus. Six of the car parks contain thirty PHEV charging stations each, while the other two contain sixty PHEV charging stations each. The distance driven to campus, arrival time, and departure times are all chosen using random variables corresponding to the distributions described previously, with the constraint that departure time must be later than arrival time. Arrival and departure times are rounded to the nearest minute. Based on these parameters, the V2C algorithm is applied to each vehicle to determine the charge and discharge rates. In order to examine the maximum effects of peak shaving due to PHEVs, it is assumed for this section that the difference between on peak and off peak rates is high enough that

V2C proves profitable. The charge and discharge rates from the V2C algorithm are then applied to the 300 PHEVs. Due to the arrival and departure times, not all PHEVs are present on campus during the peak rate period, meaning not all PHEVs participate in peak shaving. Based on the temporal distributions however, it can be seen that the majority of PHEVs that park on campus regularly will be present during the beginning of the peak rate period, with the availability decreasing as the time gets later.

Figures 53, 54, and 55 show the campus 12.47kV system load with PHEVs participating in V2C for a spring, summer, and winter day, respectively. It can be seen that the peak system load is reduced for both the spring and summer cases. For the winter case, the load is reduced during the utility peak pricing period, however this does not overlap with the system peak load, so the peak is not reduced. Due to the use of PHEVs in a V2C campus scenario, the electric utility providing electric power to campus can expect a significant reduction of campus load during the peak pricing periods. By drawing less energy during peak rate periods, the campus will also save money on the purchase of electricity.
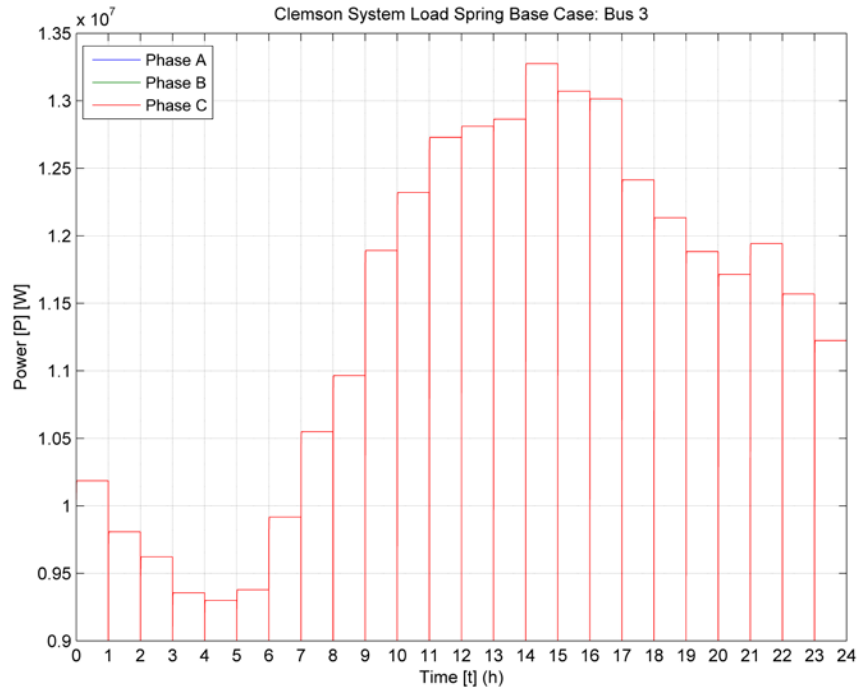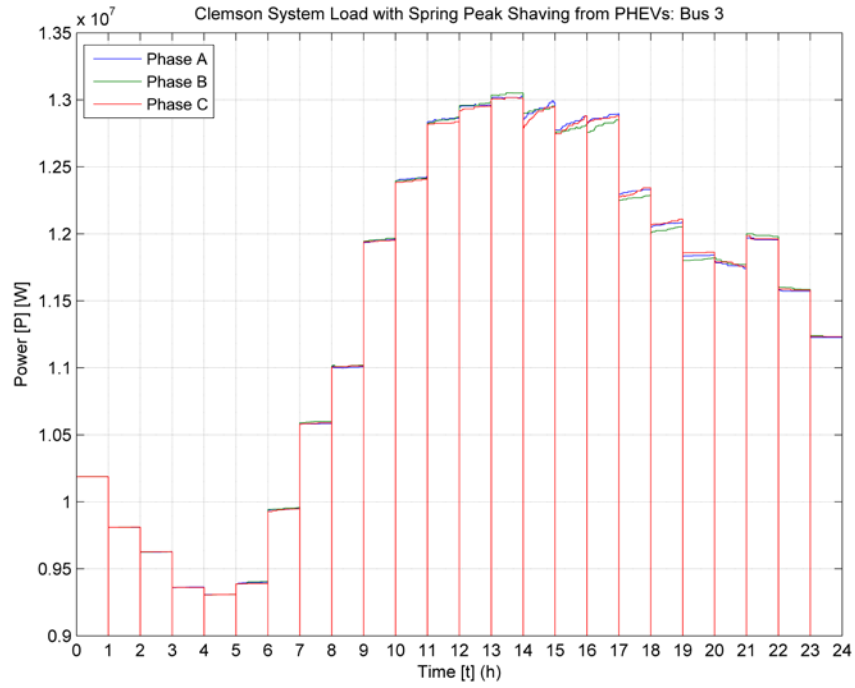
Fig. 53. Clemson University 12.47kV System Load – Spring – V2C
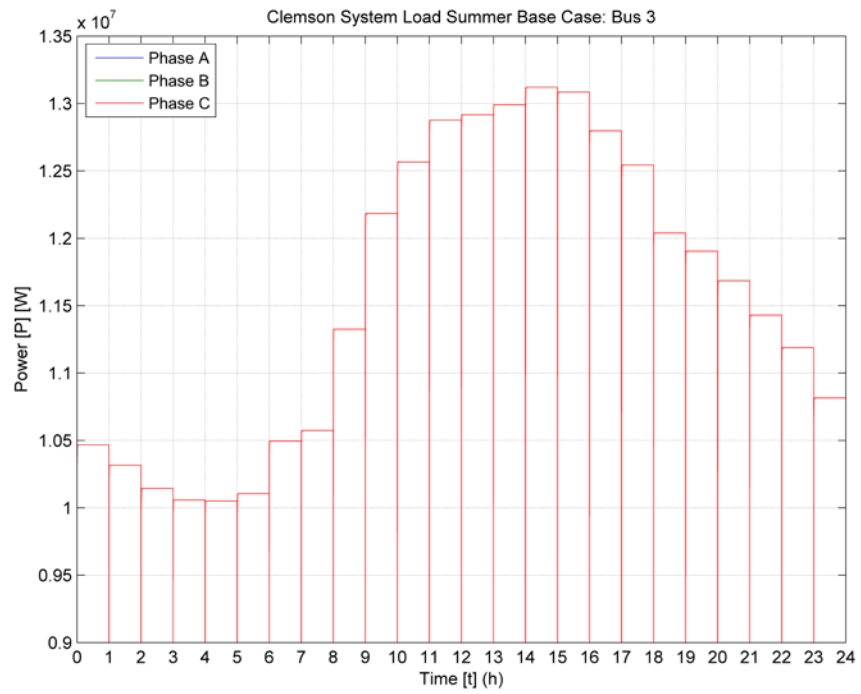

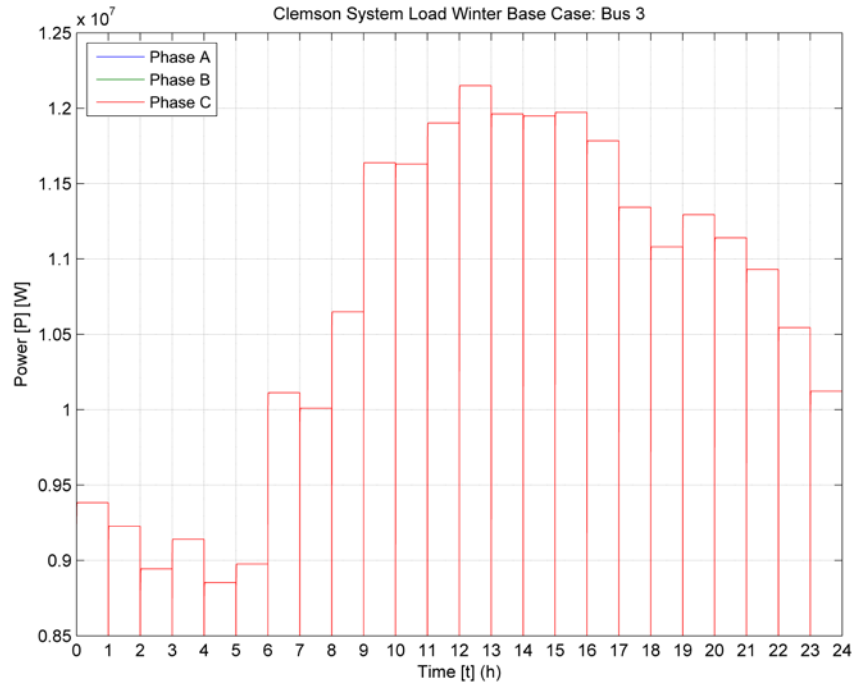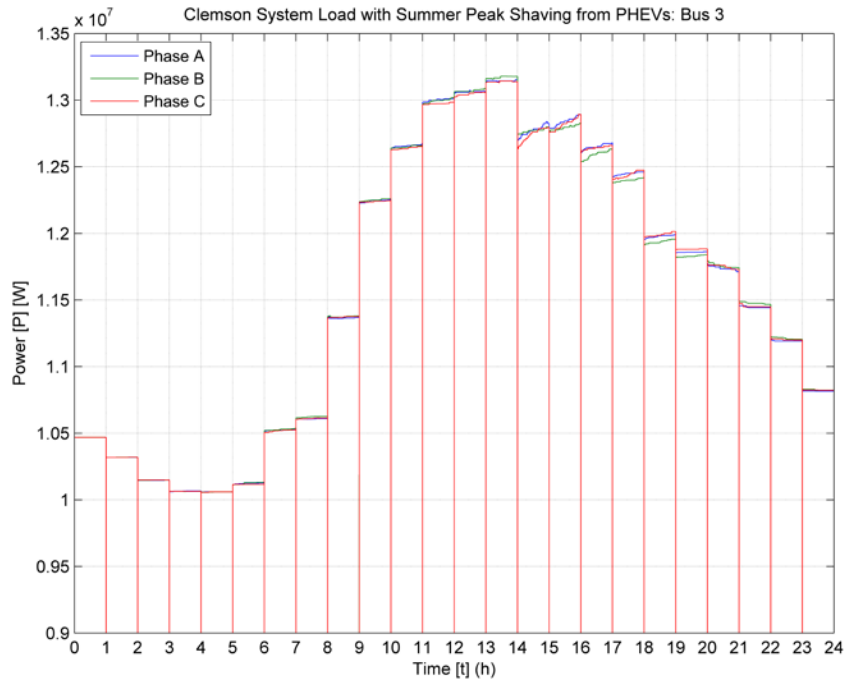Fig. 54. Clemson University 12.47kV System Load – Summer – V2C
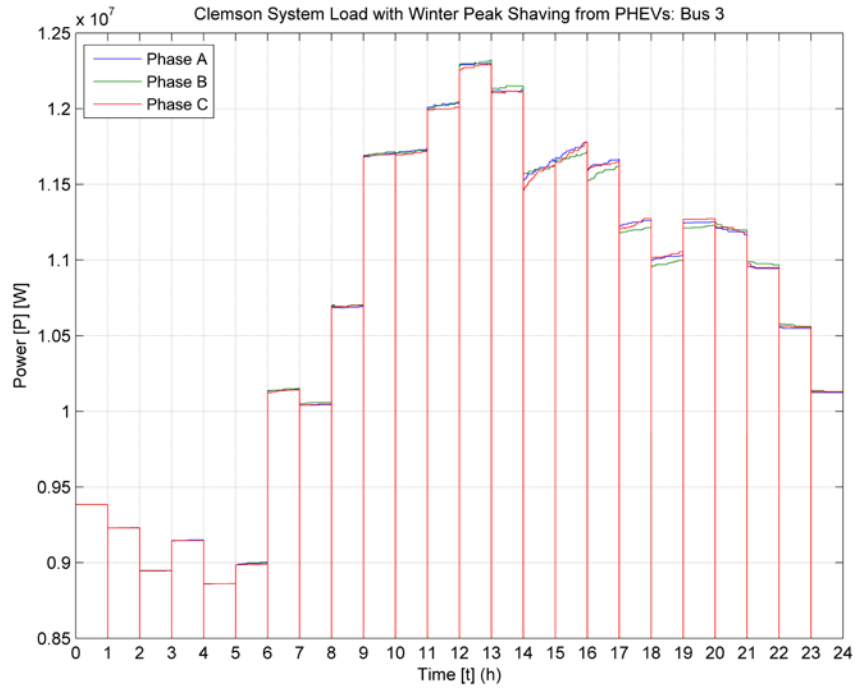
Fig. 55. Clemson University 12.47kV System Load – Winter – V2C

In order to show the viability of using V2C as an acceptable source for peak shaving, a comparison with stationary battery energy storage is again conducted. In order to draw a meaningful comparison, each PHEV is replaced with an equivalent sized stationary battery of the same capacity at the same location. The profile of the stationary battery energy is shown in Fig. 37. The load profile for the campus with stationary energy storage is shown in Figs. 56, 57, and 58 for a spring, summer, and winter day, respectively.
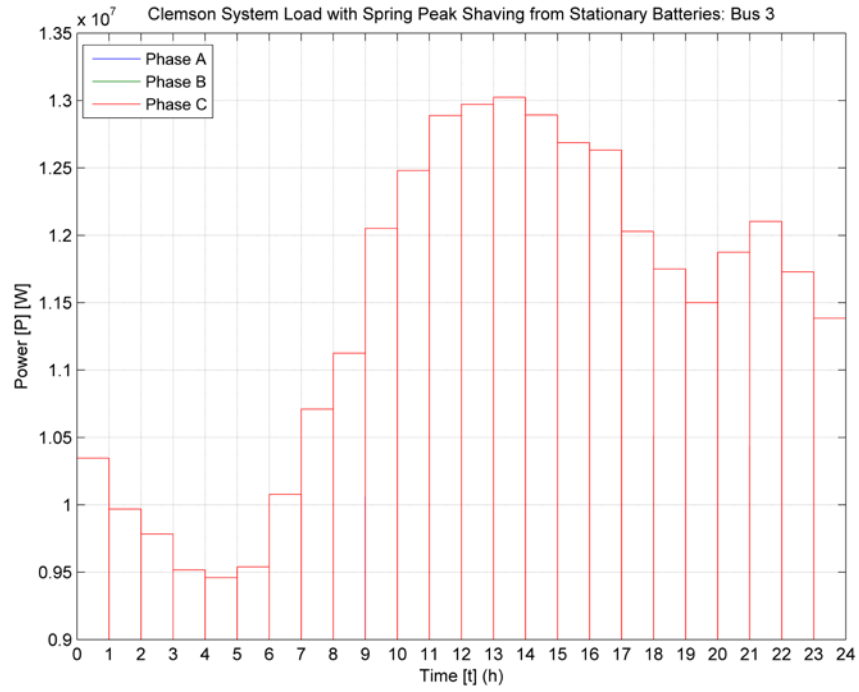
Fig. 56. Clemson University 12.47kV System Load – Spring – Stationary Battery
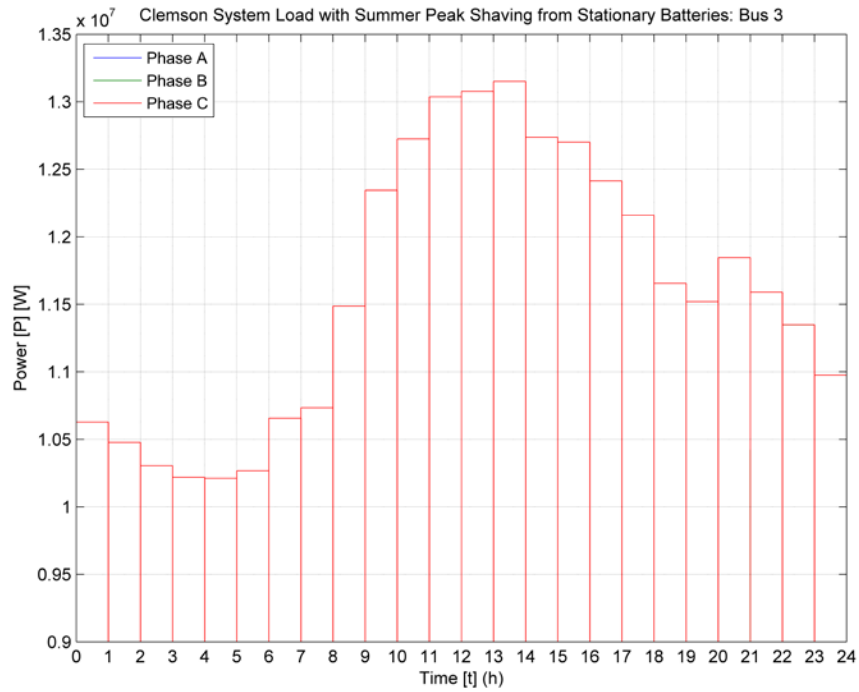
Fig. 57. Clemson University 12.47kV System Load – Summer – Stationary Battery
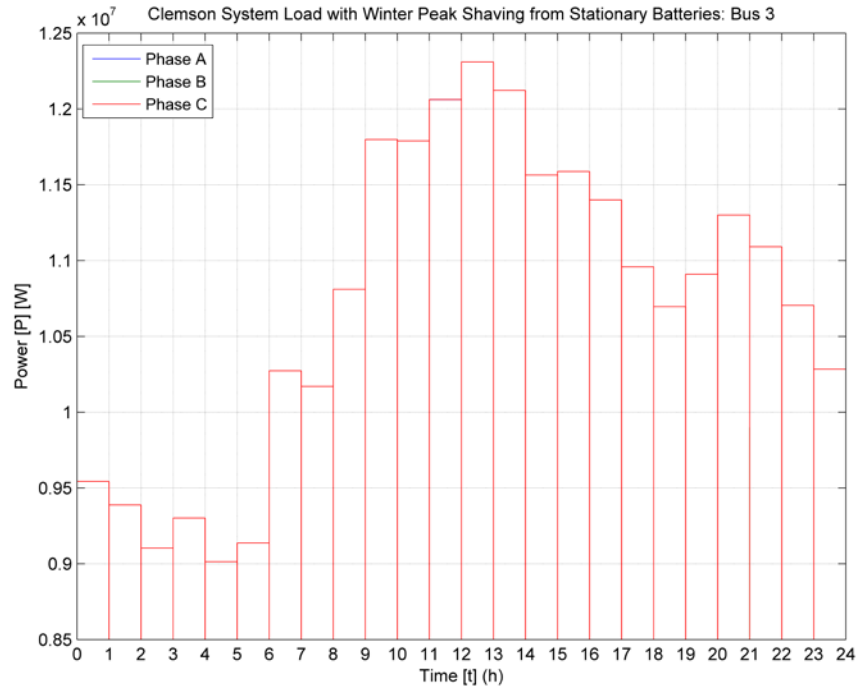
Fig. 58. Clemson University 12.47kV System Load – Winter – Stationary Battery

It can be seen that the peak shaving impacts of the stationary battery energy storage are similar to that of the PHEVs using V2C. The main difference is that more peak shaving occurs with the stationary battery energy storage than with PHEVs using V2C. This is especially apparent during the latter portion of the peak rate time. This is due to the disconnection of PHEVs based on the temporal distributions and the minimum SOC requirement placed on individual PHEVs by the spatial distribution.

CHAPTER SIX

CONCLUSION

It has been shown that PHEVs can be added to a campus system without presenting a significant threat to system operations during disturbances, provided appropriate control is included to stop charger switching during these periods. Different charger control schemes were developed in order to examine possible impacts from multiple charger types. The topology of the charger is found to play a major role in the behavior of the charger during disturbances. The addition of renewable generation to the system also plays an important role in the behavior, but does not necessarily exacerbate the problems. Again, in this case, fault control logic was able to significantly mitigate the negative impacts of adding PHEVs to the system.

If infrastructure is available for V2C or balancing operations to occur, PHEVs have the potential to benefit a distribution system. An algorithm is developed that can be used to balance real power by switching PHEVs between phases. By moving PHEVs from heavily loaded phases to lightly loaded phases, real power is balanced at the target point. This target can be either the real power drawn by the car park or somewhere on the feeder where the PHEV charging park draws it real power from, in which case the feeder real power is balanced by unbalancing the car park real power. It is shown using this algorithm that the overall system is pushed towards a balanced state of operation, even under changing system loads or changing vehicle charging and discharging rates. This service can be provided by PHEV charging parks without significant impacts on

PHEV charging and with no user interaction, allowing the campus to benefit from the connection of PHEVs.

A decentralized V2C algorithm is also developed. This algorithm requires knowledge of off peak and on peak electricity rates and their subsequent timings, driving distances, arrival time, and departure time in order to calculate charging and discharging rates and whether it is cost effective to participate in V2C. Battery degradation due to the increased cycling associated with V2C is accounted for in the savings calculation. It is found that as battery costs continue to decrease, the difference between off peak and peak electricity rates in order to be economically viable will also decrease. Finally, the benefit to the campus electric distribution system and the electric utility providing power to campus is shown through peak shaving. A random driving profile is provided for each vehicle based on distributions developed from driver reported data. The data is then used to calculate charging and discharging rates using the V2C algorithm. A total of 300 PHEVs are spread around campus in 8 car parks. It is found that the system load is significantly reduced during peak shaving operations. This will result in costs savings for the university as well as providing environmental benefits by lessening the amount of peak generation required.

REFERENCES

[1] Anumolu, P.; Banhazl, G.; Hilgeman, T.; Pirich, R., "Plug-in hybrid vehicles: An overview and performance analysis," *Systems, Applications and Technology Conference, 2008 IEEE Long Island* , vol., no., pp.1,4, 2-2 May 2008 doi: 10.1109/LISAT.2008.4638946

[2] Wirasingha, S.G.; Schofield, N.; Emadi, A., "Plug-in hybrid electric vehicle developments in the US: Trends, barriers, and economic feasibility," *Vehicle Power ,and Propulsion Conference, 2008. VPPC '08. IEEE* , vol., no., pp.1,8, 3-5 Sept. 2008 doi: 10.1109/VPPC.2008.4677702

[3] Mohseni, P.; Stevie, R. G., "Electric vehicles: Holy grail or fool's gold," *Power and Energy Society General Meeting, 2010 IEEE* , vol., no., pp.1,5, 25-29 July 2010 doi: 10.1109/PES.2010.5588159

[4] Taylor, J.; Maitra, A.; Alexander, M.; Brooks, D.; Duvall, M., "Evaluations of plug-in electric vehicle distribution system impacts," *Power and Energy Society General Meeting, 2010 IEEE* , vol., no., pp.1,6, 25-29 July 2010 doi: 10.1109/PES.2010.5589538

[5] Jenkins, S.D.; Rossmaier, J.R.; Ferdowsi, M., "Utilization and effect of plug-in hybrid electric vehicles in the United States power grid," *Vehicle Power and Propulsion Conference, 2008. VPPC '08. IEEE* , vol., no., pp.1,5, 3-5 Sept. 2008 doi: 10.1109/VPPC.2008.4677501

[6] Madawala, U.K.; Schweizer, P.; Haerri, V.V., ""Living and mobility"- a novel multipurpose in-house grid interface with plug in hybrid BlueAngle," *Sustainable Energy Technologies, 2008. ICSET 2008. IEEE International Conference on* , vol., no., pp.531,536, 24-27 Nov. 2008 doi: 10.1109/ICSET.2008.4747065

[7] Clement, K.; Haesen, E.; Driesen, J., "Coordinated charging of multiple plug-in hybrid electric vehicles in residential distribution grids," *Power Systems Conference and Exposition, 2009. PSCE '09. IEEE/PES* , vol., no., pp.1,7, 15-18 March 2009 doi: 10.1109/PSCE.2009.4839973

[8] Dow, L.; Marshall, M.; Le Xu; Aguero, J.R.; Willis, H.L., "A novel approach for evaluating the impact of electric vehicles on the power distribution system," *Power and Energy Society General Meeting, 2010 IEEE* , vol., no., pp.1,6, 25-29 July 2010 doi: 10.1109/PES.2010.5589507

[9] Bevis, T.; Hacker, B.; Edrington, C.S.; Azongha, S., "A review of PHEV grid impacts," *North American Power Symposium (NAPS), 2009* , vol., no., pp.1,6, 4-6 Oct. 2009 doi: 10.1109/NAPS.2009.5483995

[10] Shengnan Shao; Pipattanasomporn, M.; Rahman, S., "Challenges of PHEV penetration to the residential distribution network," *Power & Energy Society General Meeting, 2009. PES '09. IEEE* , vol., no., pp.1,8, 26-30 July 2009 doi: 10.1109/PES.2009.5275806

[11] Lukic, S.M.; Saunders, M.; Pantic, Z.; Hung, S.; Taiber, J., "Use of inductive power transfer for electric vehicles," *Power and Energy Society General Meeting, 2010 IEEE* , vol., no., pp.1,6, 25-29 July 2010 doi: 10.1109/PES.2010.5589673

[12] Mitra, P.; Venayagamoorthy, G.K.; Corzine, K., "Real-time study of a current controlled plug-in vehicle for vehicle-to-grid transaction," *Power Electronics Conference (IPEC), 2010 International* , vol., no., pp.796,800, 21-24 June 2010 doi: 10.1109/IPEC.2010.5543308

[13] Yang C-J.; Jackson, R. "Opportunities and barriers to pumped-hydro energy storage in the United States." *Renewable and Sustainable Energy Reviews*, vol. 15, no. 1, pp. 839,844, doi: 10.1016/j.rser.2010.09.020

[14] Boyes, J.D.; Clark, N.H., "Technologies for energy storage. Flywheels and super conducting magnetic energy storage," *Power Engineering Society Summer Meeting, 2000. IEEE* , vol.3, no., pp.1548,1550 vol. 3, 2000 doi: 10.1109/PESS.2000.868760

[15] Tokuda, N.; Furuya, M.; Kikuoko, Y.; Tsutui, Y.; Kumamoto, T.; Kanno, T., "Development of a redox flow (RF) battery for energy storage," *Power Conversion Conference, 2002. PCC-Osaka 2002. Proceedings of the* , vol.3, no., pp.1144,1149 vol.3, 2002 doi: 10.1109/PCC.2002.998133

[16] Shuang Yu; Mays, T.J.; Dunn, R.W., "A new methodology for designing hydrogen energy storage in wind power systems to balance generation and demand," *Sustainable Power Generation and Supply, 2009. SUPERGEN '09. International Conference on* , vol., no., pp.1,6, 6-7 April 2009 doi: 10.1109/SUPERGEN.2009.5348061

[17] Garimella, N.; Nair, N.C., "Assessment of battery energy storage systems for small-scale renewable energy integration," *TENCON 2009 - 2009 IEEE Region 10 Conference* , vol., no., pp.1,6, 23-26 Jan. 2009 doi: 10.1109/TENCON.2009.5395831

[18] Huang Wei; Wang Xin; Guo Jiahuan; Zhang Jianhua; Yang Jingyan, "Discussion on application of super capacitor energy storage system in microgrid," *Sustainable Power Generation and Supply, 2009. SUPERGEN '09. International Conference on* , vol., no., pp.1,4, 6-7 April 2009 doi: 10.1109/SUPERGEN.2009.5348079

[19] Clarke, A., Makram, E., "A Novel Idea for Self-Balancing Car Parks for Plug In Electric Vehicle Charging." *Journal of Power and Energy Engineering*, vol.2, no.10, pp. 34-40, 2014. doi: 10.4236/jpee.2014.210005

[20] Bosch. "Charging Stations," *Bosch Electric Vehicle Solutions*. 2014. Web. Available: <http://www.pluginnow.com/charging stations>

[21] Hilshey, AD.; Hines, P.D.H.; Rezaei, P.; Dowds, J.R., "Estimating the Impact of Electric Vehicle Smart Charging on Distribution Transformer Aging," Smart Grid, IEEE Transactions on , vol.4, no.2, pp.905,913, June 2013 doi: 10.1109/TSG.2012.2217385

[22] Sortomme, E.; Hindi, M.M.; MacPherson, S.D.J.; Venkata, S.S., "Coordinated Charging of Plug-In Hybrid Electric Vehicles to Minimize Distribution System Losses," Smart Grid, IEEE Transactions on , vol.2, no.1, pp.198,205, March 2011 doi: 10.1109/TSG.2010.2090913

[23] Pieltain Fernández, L.; Román, T.G.S.; Cossent, R.; Domingo, C.M.; Frías, P., "Assessment of the Impact of Plug-in Electric Vehicles on Distribution Networks," Power Systems, IEEE Transactions on , vol.26, no.1, pp.206,213, Feb. 2011 doi: 10.1109/TPWRS.2010.2049133

[24] Sekyung Han; Soohee Han; Sezaki, K., "Development of an Optimal Vehicle-to-Grid Aggregator for Frequency Regulation," Smart Grid, IEEE Transactions on , vol.1, no.1, pp.65,72, June 2010 doi: 10.1109/TSG.2010.2045163

[25] Sortomme, E.; El-Sharkawi, M.A, "Optimal Scheduling of Vehicle-to-Grid Energy and Ancillary Services," Smart Grid, IEEE Transactions on , vol.3, no.1, pp.351,359, March 2012 doi: 10.1109/TSG.2011.2164099

[26] Chindris, M.; Cziker, A; Miron, A; Balan, H.; Iacob, A; Sudria, A, "Propagation of unbalance in electric power systems," Electrical Power Quality and Utilisation, 2007. EPQU 2007. 9th International Conference on , vol., no., pp.1,5, 9-11 Oct. 2007 doi: 10.1109/EPQU.2007.4424221

[27] Makram, E.B.; Zambrano, V.O.; Harley, R.G.; Balda, J.C., "Three-phase modeling for transient stability of large scale unbalanced distribution systems," Power Systems, IEEE Transactions on , vol.4, no.2, pp.487,493, May 1989 doi: 10.1109/59.193820

[28] Bihani, H. A. (2014). "Analysis and mitigation of impacts of plug-in electric vehicles on distribution system during faults." *ProQuest Dissertations and Theses,*72. Available: <http://search.proquest.com/docview/1551514588>

[29] Kisacikoglu, M.C.; Ozpineci, B.; Tolbert, L.M., "Examination of a PHEV bidirectional charger system for V2G reactive power compensation," *Applied Power Electronics Conference and Exposition (APEC), 2010 Twenty-Fifth Annual IEEE* , vol., no., pp.458,465, 21-25 Feb. 2010 doi: 10.1109/APEC.2010.5433629

[30] Kisacikoglu, M.C.; Ozpineci, B.; Tolbert, L.M., "Reactive power operation analysis of a single-phase EV/PHEV bidirectional battery charger," *Power Electronics and ECCE Asia (ICPE & ECCE), 2011 IEEE 8th International Conference on* , vol., no., pp.585,592, May 30 2011-June 3 2011 doi: 10.1109/ICPE.2011.5944614

[31] Sung-Hun Ko; Lee, S.R.; Dehbonei, H.; Nayar, C.V., "Application of voltage- and current-controlled voltage source inverters for distributed generation systems," *Energy Conversion, IEEE Transactions on* , vol.21, no.3, pp.782,792, Sept. 2006 doi: 10.1109/TEC.2006.877371

[32] Lettl, J.; Bauer, J., Linhart, L., "Comparison of Different Filter Types for Grid Connected Inverter," *Progress In Electromagnetics Research Symposium*., pp. 1426-1429, 20-23, Mar. 2011

[33] Verma, A.K.; Singh, B.; Shahani, D. T., "Grid to vehicle and vehicle to grid energy transfer using single-phase bidirectional AC-DC converter and bidirectional DC-DC converter," *Energy, Automation, and Signal (ICEAS), 2011 International Conference on,* vol., no., pp.1,5, 28-30 Dec. 2011 doi: 10.1109/ICEAS.2011.6147084

[34] Fain, D., "A Dual Input Bidirectional Power Converter for Charging and Discharging a PHEV Battery," *Master's thesis, Dept. of Elec. and Comp. Eng., Clemson Univ.,* Clemson, 2009. Available: <http://etd.lib.clemson.edu/documents/1252424759/Fain_clemson_0050M_103 21.pdf>

[35] Clarke, A.; Bihani, H.;Makram, E.;Corzine, K.; "Fault Analysis on an Unbalanced Distribution System in the Presence of Plug-In Hybrid Electric Vehicles," *Clemson Power System Conference, 2013*

[36] Monfared, M.; Sanatkar, M.; Golestan, S., "Direct active and reactive power control of single-   phase grid-tie converters," *Power Electronics, IET* , vol.5, no.8, pp.1544,1550, September 2012, doi: 10.1049/iet-pel.2012.0131

[37] Clarke, A.D., Bihani, H.A., Makram, E.B. and Corzine, K.A., "Analysis of the Impact of Different PEV Battery Chargers during Faults," *Journal of Power and Energy Engineering,* vol.2, no.8, pp.31-44, 2014. doi:10.4236/jpee.2014.28004

[38] "IEEE 13 Node Test Feeder," *IEEE PES Distribution System Analysis Subcommittee.* Available: <http://ewh.ieee.org/soc/pes/dsacom/testfeeders/feeder13.zip>

[39] "Radial Distribution Test Feeders," *IEEE PES Distribution System Analysis Subcommittee.* Available: <http://ewh.ieee.org/soc/pes/dsacom/testfeeders/testfeeders.pdf>

[40] Clarke, A. D. and Makram, E. B., "An Innovative Approach in Balancing Real Power Using Plug In Hybrid Electric Vehicles," *Journal of Power and Energy Engineering*, vol.2, no.10, pp.1-8, 2014. doi:10.4236/jpee.2014.210001

[41] Kersting, William H. *Distribution System Modeling and Analysis.* CRC Press, 2002. Web. Available: <http://www.crcnetbase.com/isbn/978-0-8493-0812-3>

[42] Okonite. "Okoguard Okoseal Type MV-105," *Product Data.* Web. Available: <http://okonite.com/Product_Catalog/section2/section2-pdfs/2-19.pdf>

[43] Gonen, Turan. *Electric Power Distribution System Engineering, Second Edition*. CRC Press, 2007. Print.

[44] Rajapakse, A.D.; Muthumuni, D., "Simulation tools for photovoltaic system grid integration studies," Electrical Power & Energy Conference (EPEC), 2009 IEEE , vol., no., pp.1,5, 22-23 Oct. 2009 doi: 10.1109/EPEC.2009.5420370

[45] Clarke, A., Makram, E. "A Comprehensive Analysis of Plug In Hybrid Electric Vehicles to Commercial Campus (V2C)," *Electric Power Systems Research.* Under Review.

[46] Davis, B.M.; Bradley, T.H., "The Efficacy of Electric Vehicle Time-of-Use Rates in Guiding Plug-in Hybrid Electric Vehicle Charging Behavior," Smart Grid, IEEE Transactions on , vol.3, no.4, pp.1679,1686, Dec. 2012 doi: 10.1109/TSG.2012.2205951

[47] Yilmaz, M.; Krein, P.T., "Review of the Impact of Vehicle-to-Grid Technologies on Distribution Systems and Utility Interfaces," Power Electronics, IEEE Transactions on , vol.28, no.12, pp.5673,5689, Dec. 2013 doi: 10.1109/TPEL.2012.2227500

[48] Pang, C.; Dutta, P.; Kezunovic, M., "BEVs/PHEVs as Dispersed Energy Storage for V2B Uses in the Smart Grid," Smart Grid, IEEE Transactions on , vol.3, no.1, pp.473,482, March 2012 doi: 10.1109/TSG.2011.2172228

[49] Das, R.; Thirugnanam, K.; Kumar, P.; Lavudiya, R.; Singh, M., "Mathematical Modeling for Economic Evaluation of Electric Vehicle to Smart Grid Interaction," Smart Grid, IEEE Transactions on , vol.5, no.2, pp.712,721, March 2014 doi: 10.1109/TSG.2013.2275979

[50] U.S. Department of Transportation, Federal Highway Administration, *2009 National Household Travel Survey*. Web. Available: <http://nhts.ornl.gov>

[51] Chevrolet. "2014 Volt: Electric Car - Hybrid Car", *Chevrolet*, 2014. Web. Available: <http://www.chevrolet.com/volt-electric-car.html>

[52] PG&E. "Time-of-Use," *PG&E*. 2014. Web. Available: <http://www.pge.com/en/mybusiness/rates/tvp/toupricing.page?WT.mc_id=Vanity_tou>

[53] PPL Electric Utilities. "Time-of-Use Rate Option," *PPL Electric Utilities*. 2014. Web. Available: <https://www.pplelectric.com/at-your-service/electric-rates-and-rules/time-of-use-option.aspx>

[54] Southern California Edison. "Residential Rate Plans," *Southern California Edison*. 2014. Web. Available: <https://www.sce.com/wps/portal/home/residential/rates/residential-plan/tou/>

[55] Portland General Electric. "Time Of Use: Pricing," *PGE*. 2014. Web. Available: <http://www.portlandgeneral.com/residential/your_account/billing_payment/time_of_use/pricing.aspx>

[56] Con Edison. "Voluntary Time-of-Use," *Con Edison*. 2014. Web. Available: <http://www.coned.com/customercentral/energyresvoluntary.asp>

[57] NV Energy. "Residential Time of Use for Southern Service Territory," *Time of Use Rate for Home*. 2014. Web. Available: <https://www.nvenergy.com/home/paymentbilling/timeofuse.cfm>

[58] BGE. "Time of Use Pricing," *BGE*. 2014. Web. Available: <http://www.bge.com/waystosave/manageyourusage/pages/time-of-use-pricing.aspx>

[59] Anderson, D., "An Evaluation of Current and Future Costs for Lithium-Ion Batteries for Use in Electrified Vehicle Powertrains," M.S. thesis, Environ. Manage., Duke Univ., Durham, NC, 2009